

Studies Towards the Total Synthesis of Atropurpuran and the Arcutines

by

Ahlam M. Armaly

A dissertation submitted in partial fulfillment
of the requirements for the degree of
Doctor of Philosophy
(Chemistry)
in the University of Michigan
2019

Doctoral Committee:

Professor Corinna S. Schindler, Chair
Professor Corey R. J. Stephenson
Professor John Montgomery
Professor David H. Sherman

Ahlan M. Armaly

amarmaly@umich.edu

ORCID iD: 0000-0001-5340-3039

© Ahlan M. Armaly 2019

Dedication

To my family and friends

Table of Contents

| | |
|---|------|
| Dedication | ii |
| List of Figures | v |
| Abstract | viii |
| Chapter 1 The Diterpene Alkaloid Natural Products | 1 |
| 1.1 Introduction | 1 |
| 1.2 Biosynthesis of Diterpene Alkaloids | 3 |
| 1.3 References | 5 |
| Chapter 2 Aluminum Chloride-Mediated Dieckmann Cyclization for the Synthesis of Cyclic 2-Alkyl- and 2-Acyl-1,3-diones | 7 |
| 2.1 Introduction | 7 |
| 2.2 Results and Discussion | 9 |
| 2.3 Synthesis of the Chiloglottones | 14 |
| 2.4 Conclusion | 15 |
| 2.5 Experimental Details | 15 |
| 2.5.1 General Information | 15 |
| 2.5.2 Reaction Optimization | 16 |
| 2.5.3 Additives Screen | 18 |
| 2.5.4 Synthesis of 2-alkyl-1,3-diones | 18 |
| 2.6 References | 31 |
| Chapter 3 Acid Chlorides as Formal Carbon Dianion Linchpin Reagents in the Aluminum Chloride-Mediated Dieckmann Cyclization of Dicarboxylic Acids | 33 |
| 3.1 Introduction | 33 |

| | |
|--|----|
| 3.2 Results and Discussion | 34 |
| 3.3 Mechanistic Investigations | 34 |
| 3.4 Conclusion | 39 |
| 3.5 Experimental Details | 39 |
| 3.5.1 General Information | 39 |
| 3.5.2 Isolation of 2-(3,3-dimethylbutanoyl)cyclohexane-1,3-dione (9) | 40 |
| 3.5.3 ¹³ C-Labeling Experiments | 41 |
| 3.5.4 Sacrificial Acylating Agent | 43 |
| 3.6 References | 45 |
| Chapter 4 Enantioselective Total Synthesis of Atropurpuran and the Arcutines | 46 |
| 4.1 Introduction | 46 |
| 4.2 Proposed Biogenesis | 47 |
| 4.3 Previous Synthetic Approaches | 49 |
| 4.4 Results and Discussion | 52 |
| 4.5 Conclusion | 72 |
| 4.6 Experimental Details | 73 |
| 4.6.1 General Information | 73 |
| 4.6.2. Base-Mediated Dieckmann Cyclization in Model Systems | 73 |
| 4.6.3. Synthesis of Racemic Vinyl Ketone | 75 |
| 4.6.4 Synthesis of Enantioenriched Vinyl Ketone | 76 |
| 4.6.5. Synthesis of Key Dieckmann Cyclization Product in the Synthesis of Atropurpuran and the Arcutines | 79 |
| 4.6.6 Investigation of Tetracycle Formation | 82 |
| 4.7 References | 84 |

List of Figures

| | |
|--|----|
| Figure 1.1 Biological activity of select diterpene alkaloids and diterpene natural products | 2 |
| Figure 1.2 Retrosynthetic strategy towards atropurpuran (5) and the arcutines (6) relying on a Dieckmann cyclization strategy | 3 |
| Figure 1.3 Biosynthesis of diterpene natural products | 4 |
| Figure 1.4 Proposed biogenesis of the diterpene alkaloids from diterpene precursors | 4 |
| Figure 2.1 Strategies towards cyclic 2-alkyl-1,3-diones (3) | 8 |
| Figure 5.2 Substrates previously accessed by Matoba and Schick demonstrate a decrease in yield and complexity increases | 8 |
| Figure 2.6 A) Our desired AlCl ₃ -mediated Dieckmann cyclization for the synthesis of atropurpuran; B) Natural products and building blocks derived from cyclic-1,3-diones | 9 |
| Figure 2.7 Evaluation of various Lewis acids for the Dieckmann Cyclization | 10 |
| Figure 2.8 A) Optimization of AlCl ₃ -mediated Dieckmann cyclization; B) Competing Lewis acid-mediated self-condensation of acid chlorides | 11 |
| Figure 2.9 Substrate scope for the synthesis of 2-alkyl-1,3-diones | 12 |
| Figure 2.10 Substrate scope for the synthesis of 2-acetyl-1,3-diones | 13 |
| Figure 2.11 Attempts to incorporate functionality into the dicarboxylic acid substrate | 13 |
| Figure 2.12 Attempts to incorporate functionality into the acid chloride substrate | 14 |
| Figure 2.13 A) Previous route by Barrow et al. towards chiloglottone 3 (78); B) Our one-step strategy to chiloglottone 3 (78) based on our AlCl ₃ -mediated Dieckmann Cyclization | 15 |
| Figure 3.1 Divergent reactivity leading to 2-alkyl-1,3-diones or 2-acyl-1,3-diones based on choice of acid chloride | 33 |
| Figure 3.2 Unexpected isolation of 2-acyl-1,3-dione with 3,3-dimethyl butyryl chloride (7) | 34 |
| Figure 3.3 Previously proposed mechanism by Schick et al. | 34 |
| Figure 3.4 ¹³ C-labelling studies of 2-alkyl-1,3-diones | 35 |
| Figure 3.5 ¹³ C-labelling studies of 2-acetyl-1,3-diones | 36 |
| Figure 3.6 Our revised reaction mechanism for the AlCl ₃ -mediated Dieckmann cyclization of dicarboxylic acids | 37 |

| | |
|--|----|
| Figure 3.6 A) The use of a sacrificial acylating agent to induce cyclization after linchpin incorporation; B) Experimental probe of dual role of acid chlorides as linchpin reagents and acylating agents | 38 |
| Figure 3.7 Our mechanistic hypothesis that accounts for the formation of 2-acyl-1,3-diones with β -substituted acid chlorides | 39 |
| Figure 4.1 The diterpene atropurpuran (1) and related diterpene alkaloids the arcutines (2-4) | 46 |
| Figure 4.2 Members of the atisane class of diterpene alkaloids and atropurpuran and the arcutines | 47 |
| Figure 4.3 Wang's proposed biosynthesis of atropurpuran from hetidane (11) | 48 |
| Figure 4.4 Sarpong's proposed biosynthesis of atropurpuran (1) and arcutines (2-4) from terpene precursor <i>ent</i> -atisir-16-ene (19) | 48 |
| Figure 4.5 Sarpong's proposed biosynthesis of atropurpuran (1) and arcutines (2-4) from hetidine core (25) | 49 |
| Figure 4.6 Key step in Kobayashi's synthesis of core of atropurpuran | 50 |
| Figure 4.7 Key steps in Qin's total synthesis of atropurpuran (1) | 50 |
| Figure 4.8 Key steps in Xu's total synthesis of atropurpuran (1) | 51 |
| Figure 4.9 Key steps in Qin's total synthesis of arctunidine (2) | 51 |
| Figure 4.10 Key steps in Sarpong's total synthesis of arctunidine (2) relying on network guided analysis | 52 |
| Figure 4.11 Key steps in Li's total synthesis of arctunidine (2) via biomimetic cation cascade | 52 |
| Figure 4.12 Our unique strategy towards atropurpuran (1) and the arcutines (2-4) that takes advantage of their inherent symmetry and relies on a key cyclic 1,3-dione (66) | 53 |
| Figure 4.13 Our original approach to the key cyclic 1,3-dione 66 via the AlCl ₃ -mediated Dieckmann cyclization (left) and our revised strategy relying on a base-mediated Dieckmann cyclization approach (right) | 54 |
| Figure 4.14 Investigation of key base-mediated Dieckmann cyclization in racemic model system | 55 |
| Figure 4.15 Model studies of base-mediated Dieckmann cyclization | 56 |
| Figure 4.16 Our revised strategy for the base-mediated Dieckmann cyclization (top) and synthesis of a model substrate for preliminary investigations (bottom) | 57 |

| | |
|---|----|
| Figure 4.17 A) Preliminary investigations of base-mediated Dieckmann cyclization in acetate-protected substrate 94 ; B) Possible path leading to acetate cleavage via direct deprotection; C) Alternative path for acetate cleavage that occurs after Dieckmann cyclization | 58 |
| Figure 4.18 Evaluation of suitable protecting group for the Dieckmann cyclization | 59 |
| Figure 4.19 Synthesis of saturated substrate to evaluate the Dieckmann cyclization for the synthesis of atropurpuran and the arcutines | 59 |
| Figure 4.20 Evaluation of various bases for the Dieckmann cyclization of 109 | 60 |
| Figure 4.21 Optimization of conjugate reduction | 61 |
| Figure 4.22 Evaluation of various bases for the Dieckmann cyclization of 112 | 61 |
| Figure 4.23 Asymmetric synthesis of chiral vinyl ketone 118 via a Johnson-Claisen strategy | 62 |
| Figure 4.24 Asymmetric synthesis of chiral vinyl ketone 118 via an Ireland-Claisen strategy | 62 |
| Figure 4.25 Synthesis of the key cyclic 1,3-dione 125 required for the synthesis of atropurpuran via NaHMDS-mediated Dieckmann cyclization | 63 |
| Figure 4.26 Acid-mediated approach to tetracycle formation | 64 |
| Figure 4.27 Base-mediated approach to tetracycle formation | 64 |
| Figure 4.28 Study of enolate formation in base-mediated approach for tetracycle formation | 65 |
| Figure 4.29 Organocatalytic approach to tetracycle formation | 66 |
| Figure 4.30 Functional group conversion of methyl ether into a good leaving group | 66 |
| Figure 4.31 Conversion of methyl ether to iodidene using TMSCl/NaI in model systems and actual system for the synthesis | 67 |
| Figure 4.32 Ozonolysis of cyclic 1,3-dione | 68 |
| Figure 4.33 Strategy towards tetracycle formation relying on initial ozonolysis | 68 |
| Figure 4.34 Alternative strategy for tetracycle formation | 69 |
| Figure 4.35 Synthesis of common intermediate (159) for the synthesis of atropurpuran and the arcutines | 70 |
| Figure 4.36 Preliminary investigations of selective C-H oxidation in model system | 70 |
| Figure 4.37 DFT energy calculations for selective acetal formation | 71 |
| Figure 4.38 Synthesis of atropurpuran (1) and the arcutines (2-4) from the common intermediate 159 | 72 |

Abstract

Compounds isolated from natural sources serve as an inspiration for current drug design and development due to their broad biological activities. However, these desirable compounds are often isolated in minute quantities that often limit extensive biological evaluation and further medicinal applications. The diterpene atropurpuran and its diterpene alkaloid analogs, the arcutines, are isolated from the plant roots of various *Aconitum* plants that are used in the traditional Chinese medicine “Cao-Wu” for the treatment of diseases associated with pain and inflammation. However, the biological activity of atropurpuran and the arcutines has yet to be elucidated. These compounds pose a synthetic challenge as they bear an intriguing tetracyclic carbon core that has never been observed in any other diterpene or diterpene alkaloid natural products. We describe a unique approach to atropurpuran and the arcutines that takes advantage of their inherent symmetry and relies on a key pseudo-symmetric cyclic 1,3-dione intermediate. This approach exploits the inherent reactivity of the compounds and will enable an efficient synthesis of atropurpuran and the arcutines when coupled with an aluminum chloride-mediated Dieckmann cyclization strategy that will provide rapid access to the cyclic 1,3-dione. Chapter 1 provides a brief overview of the historical use of diterpene alkaloids and their recent development as therapeutic agents. This chapter also includes the proposed biosynthesis of these compounds that relates them to their diterpene precursors. Chapter 2 describes the development of an aluminum chloride-mediated Dieckmann cyclization of dicarboxylic acids and acid chlorides that provides direct access to cyclic 2-alkyl-1,3-diones from acyclic starting materials. This strategy is showcased in the one-step synthesis of chiloglottone 3. These studies also revealed the unique properties of an aluminum chloride – nitromethane complex that is better suited for this transformation than individual Lewis acids. Chapter 3 describes our efforts to expand the scope of this transformation to include more substituted acid chloride substrates but instead observed the formation of 2-acetyl-1,3-diones. This led us to conduct ^{13}C -labelling studies that established acid

chlorides as formal carbon dianion linchpin reagents and led us to propose a revised mechanistic proposal for this transformation. Chapter 4 describes the evolution of our Dieckmann cyclization for the synthesis of atropurpuran and the arcutines. This chapter describes the synthetic design that enabled access to our key cyclic 1,3-dione intermediate and our ongoing efforts regarding the transformation of this advanced intermediate to the natural products.

Chapter 1 The Diterpene Alkaloid Natural Products

1.1 Introduction

Biologically active natural products serve as an essential source and inspiration for current drug design and development. An extensive analysis conducted by Newmann and Cragg¹ from 1981-2014 found that 40% of drugs that were approved by the United States Food and Drug Administration or comparable foreign entities were derived or inspired by natural products. Such statistics are not surprising when considering the historical value of natural products. Records of the use of herbs in traditional Chinese medicine for the treatment of various maladies date back as early as 2700 B.C.² The traditional Chinese medicine “Cao-Wu” obtained from the tubers of *Aconitum* species was traditionally employed for the treatment of pain and diseases associated with inflammation.³ These desirable pharmacological properties exhibited by the *Aconitum* plants are attributed to the presence of characteristic C₁₈-, C₁₉- and C₂₀-diterpene alkaloids isolated from the plant roots.^{4,5,6} These compounds exhibit a broad range of biological activity including analgesic, de-addictive, antiarrhythmic, anti-inflammatory, anticancer, anti-epileptiform, anti-parasite, antibacterial, antiviral, and antioxidant activities.⁶ These compounds are particularly attractive in the area of pain management as they are non-narcotic, inducing neither morphine-like tolerance nor physical dependence, and therefore may serve as better alternatives to current analgesics, such as morphine and methadone.⁶ These desirable pharmacological properties have led to the development of three alkaloids,^{7,8,9} which are currently employed as analgesic drugs in China and four additional diterpenes that are currently undergoing clinical trials in Japan.¹⁰

The primary challenge, however, when considering *Aconitum*-derived remedies is that balance between these beneficial bioactivities and toxicity.^{11,12} For example, despite being a potent analgesic, aconitine (**1**), one of the primary compounds produced by various *Aconitum* plants, is highly toxic (Figure 1.1). As such, the historical use of *Aconitum* plants also encompasses their usage as poisons for spears and arrows as well as homicide, both accidental and intentional.⁶ The toxicity of a related compound, methylaconitine, still poses a problem to this day. According to

the FDA Poisonous Plant Database,¹³ the larkspur plant is responsible for the most cattle deaths in the western United States. One of primary compounds found in larkspurs that is responsible for up to 15% of cattle deaths is the diterpene alkaloid methylaconitine (2), which is also called mesaconitine (2).^{13,14,15} The paradoxical relationship between remedy and poison can be reconciled when considering the biological activity of the individual compounds. For example, while aconitine (1) and mesaconitine (2) are highly toxic compounds that cause arrhythmias, there are far less toxic compounds such as lappaconitine (3), heteratisine, and napelline, that have demonstrated anti-arrhythmic activity¹¹ and may be responsible have detoxification properties towards their toxic analogs.¹² One of the most potent and non-toxic anti-arrhythmic alkaloid diterpenes is Guan Fu base A (4), which has been developed for the therapeutic treatment of arrhythmia in China.¹⁶ Another caveat added to the narrative of the diterpene alkaloids is the presence of other non-alkaloid constituents that have recently been isolated from *Aconitum* plants.¹⁷ These compounds similarly exhibit promising biological activities but are less toxic than their alkaloid counterparts. Only a handful of non-alkaloid diterpenes have been reported including methyl atisenoate,¹⁸ campylopin,¹⁹ and atropurpuran (5).²⁰ However, the biological activity of atropurpuran and its arcutines analogs (6) has not yet been elucidated. Beyond their potential medicinal application, these non-alkaloid diterpenes are of particular interest to the scientific community as they may help elucidate that biogenesis of the diterpene alkaloids.

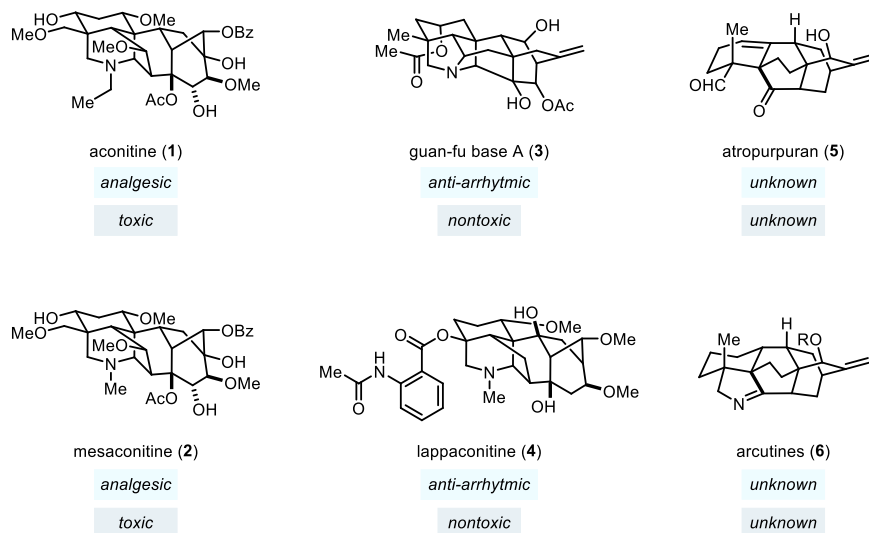


Figure 1.1 Biological activity of select diterpene alkaloids and diterpene natural products

The research described herein details our efforts towards three structurally intriguing diterpene alkaloids the arcutines (**6**) and their diterpene analog, atropurpuran (**5**), all of which have not been studied for their therapeutic use. Initial retrosynthetic analysis of these compounds revealed cleavage of the A-ring unveiled a pseudo-symmetric cyclic 1,3-dione intermediate **7** that had an external chiral center (Figure 1.2). The single chiral center highlighted in **7** would play a crucial role in our enantioselective approach towards atropurpuran (**5**) and the arcutines (**6**) as it would set all the subsequent stereocenters required for the synthesis. Our strategy towards atropurpuran and the arcutines relies on the efficient access of the key intermediate cyclic 1,3-dione **7**. As such, Chapters 1 and 2 describe our efforts in the development of a unique AlCl₃-mediated Dieckmann cyclization strategy^{21,22} to enable the direct one-step access to cyclic 2-alkyl-1,3-diones from acyclic materials. Chapter 3 describes the evolution of this Dieckmann cyclization strategy in our efforts towards the total synthesis of atropurpuran (**5**) and the arcutines (**6**).

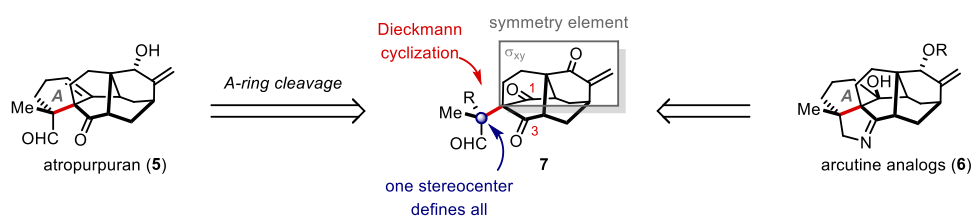


Figure 1.2 Retrosynthetic strategy towards atropurpuran (**5**) and the arcutines (**6**) relying on a Dieckmann cyclization strategy

1.2 Biosynthesis of Diterpene Alkaloids

Although these natural products are termed diterpene alkaloids, they are not derived from amino acid precursors and ultimately do not qualify as *true alkaloids*. Rather, these nitrogen-containing compounds are more accurately defined as *pseudo- or crypto-alkaloids*.⁵ This is due to the fact that these compounds are biogenetically derived from terpene precursors that then incorporate a nitrogen that is sourced from methylamine, ethylamine, or β -aminoethanol. The biogenesis of these compounds is similar to that of tetracyclic diterpenes (Figure 1.3).⁵ The biosynthesis of the tetracyclic diterpenes is well-studied and commences with cyclization of geranylgeranyl pyrophosphate **8** by *ent*-copalyl diphosphate synthase and *ent*-kaurane synthase to generate the *ent*-primarenyl cation **12**. Recent quantum chemical investigations by Tantillo et al. propose a route that is devoid of secondary carbocations but rather proceeds via a concerted-asynchronous

cation-alkene cyclization and 1,2-alkyl shift leads to tertiary carbocation **11**.²³ Quenching of **11** leads to the *ent*-beyerenes (**14**) or the *ent*-kauranes (**15**) upon a conformational change of **11**. Alternatively, tertiary carbocation **11** can undergo another series of concerted-asynchronous shifts to provide a new tertiary carbocation **13**, which leads *ent*-atisir-16-ene, **16**. *Ent*-atisir-16-ene **16** leads to the class of compounds to which atropurpuran (**5**) and the arcutines (**6**) belong to. Furthermore, the generation of *ent*-atisir-16-ene (**16**) marks the first phase and the most well-studied phase of the biosynthesis of the diterpene alkaloids.

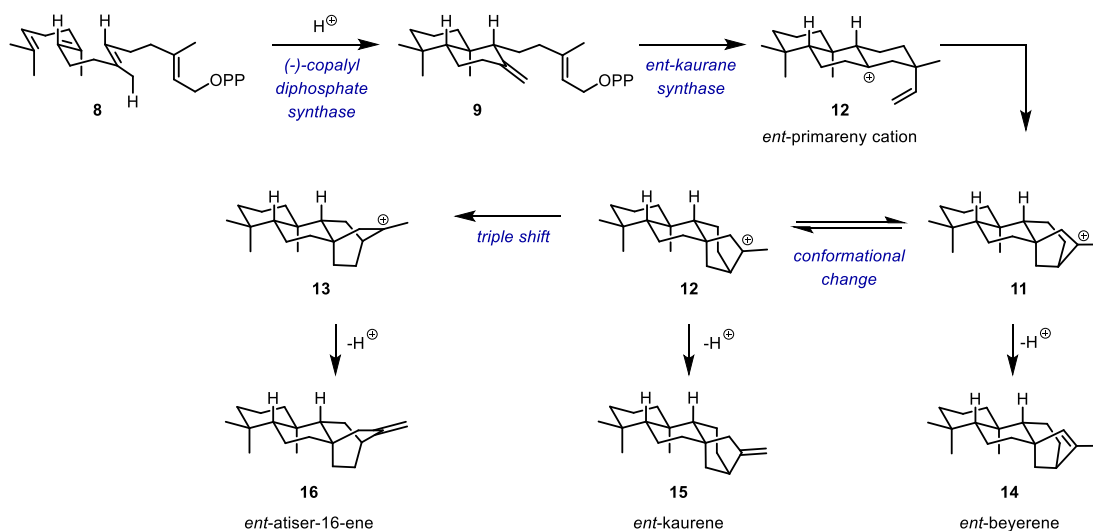


Figure 1.3 Biosynthesis of diterpene natural products

The subsequent phase regarding nitrogen atom incorporation is not as well-understood (Figure 1.4). It is postulated that *ent*-atisir-16-ene (**16**) is oxidized to dialdehyde **17**. Incorporation of a nitrogen source via double reductive amination provides the atisine skeleton **18**. The hetidine core is (**19**) thought to arise from a Mannich reaction of **18**. This biosynthesis towards the atisine and hetisine cores serves as the basis of the biogenesis of atropurpuran (**5**) and the arcutines (**6**).²⁴

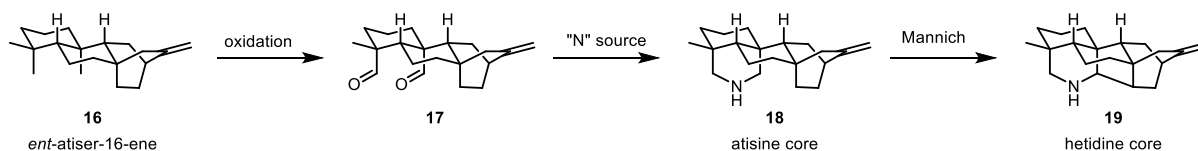


Figure 1.4 Proposed biogenesis of the diterpene alkaloids from diterpene precursors

1.3 References

- (1) Newman, D.J.; Cragg, G.M. *J. Nat. Prod.* **2016**, *79*, 629-661.
- (2) Deng, Q. S. *Trends Pharmacol. Sci.* **1985**, *6*, 453-455
- (3) Mori, T.; Ohsawa, T.; Murayama, M.; Bando, H.; Wada, K.; Amiya, T. *Heterocycles* **1989**, *29*, 873-885.
- (4) Zheng, P.; Yang, Y.R.; Zhang, W.P.; Wang, H.C.; Lao, A.N. *Acta Pharmacol. Sin.* **1994**, *15*, 239-243.
- (5) F.-P. Wang, X.-T. Liiang in *The Alkaloids, Chemistry and Biology*, Vol 59 (Ed.: G. A. Cordell), Elsevier, Amsterdam, 2002, pp. 1–280.
- (6) Wang, F.-P.; Chen, Q.-H.; Liu, X.-Y. *Nat. Prod. Rep.* **2010**, *27*, 529-570.
- (7) Tang, X.C.; Liu, X.J.; Zhang, W.P.; Wang, H.C.; Lao, A.N. *Acta. Pharm. Sin.* **1986**, *21*, 886
- (8) a) Liu, J.H.; Zhu, Y.X.; Tang, X.C. *Acta Pharmacol. Sin.* **1987**, *8*, 301-305; b) Guo, X.; Tang, X.C. *Acta Pharmacol. Sin.* **1989**, *10*, 504-507; c) Guo, X.; Tang, X.C. *Acta Pharmacol. Sin.* **1990**, *11*, 107-112.
- (9) Tang, X.C. *New Drug Clin.* **1986**, *5*, 120
- (10) Cordell, G.A. *The Alkaloids: Chemistry and Biology* (Volume 69), Elsevier 2010.
- (11) Ameri, A. *Prog. Neurobiol.* **1998**, *56*, 211-235.
- (12) Yan, Y.; Zhang, A.; Dong, H.; Yan, G.; Sun, H.; Wu, X.; Han, Y.; Wang, X. *Pharmacogn. Mag.* **2017**, *13*, 683-692.
- (13) Reducing Livestock Losses From Larkspur Poisoning in the Western States. *U.S. Dep. Agric. Pamphlet, PA* [Online], U.S. Food & Drug Administration. <https://www.accessdata.fda.gov/scripts/plantox/detail.cfm?id=1342> (accessed July 15, 2019).
- (14) Manners, G.D.; Panter, K.E.; Pelletier, S.W. *J. Nat. Prod.* **1995**, *58*, 863-869.
- (15) Knight, A.P.; Pfister, J.A. *Rangelands* **1997**, *19*, 10-13.
- (16) Yang, X. J.; Wang, G. J.; Ling, S. S.; Qiu, N. Y.; Wang, G. G.; Zhu, J.; Liu, J. H. *J. Chromatogr., B: Biomed. Sci. Appl.*, **2000**, *740*, 273; See also the announcement: *Chin. J. Nat. Med.*, **2006**, *4*, 1.
- (17) Yin, T.; Zhou, H.; Cai, L.; Ding, Z. *RSC Adv.* **2019**, *9*, 10184-10194.
- (18) Bohlman, F.; Abraham, W.; Sherdlick, W. S. *Phytochemistry* **1980**, *19*, 869-871
- (19) Wang, F.-P.; Yan, L.-P. *Tetrahedron* **2007**, *63*, 1417-1420.
- (20) P. Tang, Q.-H. Chen, F.-P. Wang, *Tet. Lett.* **2009**, *50*, 460-462.

- (21) Armaly, A.M.; Bar, S.; Schindler, C.S.; *Org. Lett.* **2017**, *19*, 3958-3961.
- (22) Armaly, A.M.; Bar, S.; Schindler, C.S.; *Org. Lett.* **2017**, *19*, 3962-3965.
- (23) (a) Hong, Y. J.; Tantillo, D. J. *J. Am. Chem. Soc.* **2010**, *132*, 5375-5386; (b) Tantillo, D. J. *Nat. Prod. Rep.* **2011**, *28*, 1035-1053.
- (24) Weber, M.; Owens, K.; Sarpong, R. *Tetrahedron Lett.* **2015**, *56*, 3600-3603.

Chapter 2 Aluminum Chloride-Mediated Dieckmann Cyclization for the Synthesis of Cyclic 2-Alkyl- and 2-Acyl-1,3-diones

2.1 Introduction

Our synthesis of atropurpuran and the arcutines relies on an essential cyclic 2-alkyl-1,3-dione intermediate (**3**), which led us to consider a route to efficiently access this key structural motif but found that the vast majority of reported methods relied on multi-step sequences (Figure 2.1).¹ This is primarily due to the fact that the desired motif, *cyclic 2-alkyl-1,3-dione* (**3**), requires at least two distinct steps – one to introduce the alkyl component (*cyclic 2-alkyl-1,3-dione*) and another step to cyclize the material or gain access to cyclic material (*cyclic 2-alkyl-1,3-dione*) – that can be carried out in any order. For example, introduction of the alkyl component via Grignard addition to a cyclic anhydride **1** could give rise to β -ketoester **2** that could undergo base-mediated Dieckmann cyclization. However, the Dieckmann cyclization is reversible, and these reactions are known to suffer from the competing retro-Dieckmann ring-cleavage reaction. Alternatively, if one can gain access to the cyclic 1,3-dione such as **4** the alkyl component can be introduced using traditional base-mediated alkylation chemistry. However, these methods suffer from *O*-alkylation, over-alkylation, and ring-cleavage reactions. The problems associated with base-mediated approaches have resulted in the development of alternative alkylation strategies,² however, this approach is similar to the alkylation approach in that it requires access to the cyclic precursor and prohibits incorporation of quaternary carbon at the 3'-position. We were attracted to a direct, one-step approach to cyclic 2-alkyl-1,3-diones (**3**) that was reported by Schick et. al.³ In this work, dicarboxylic acids **6** and acid chlorides **7** were converted to 2-alkyl-1,3-diones (**3**) using superstoichiometric amounts of Lewis acid.

B. Current multi-step approaches to cyclic 2-alkyl-1,3-diones (left) and our direct, one-step approach from readily available materials (right)

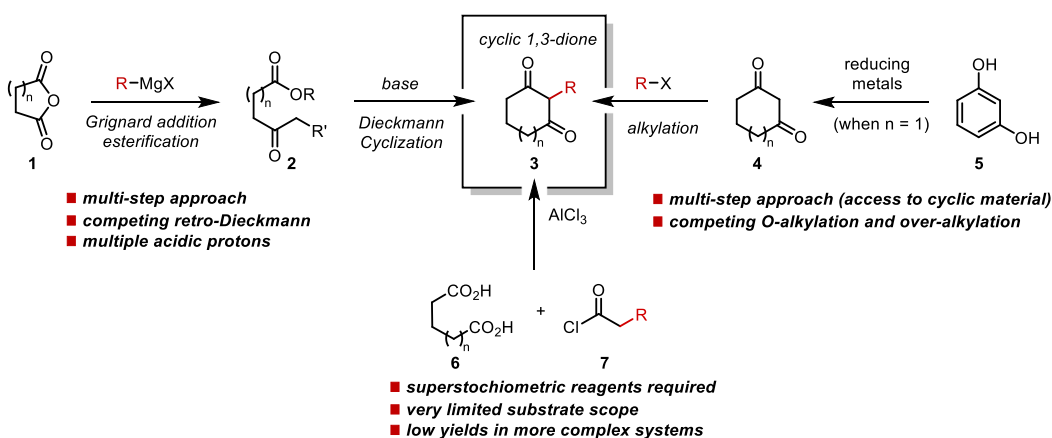


Figure 2.1 Strategies towards cyclic 2-alkyl-1,3-diones (3)

However, this approach suffered from limitations in the complexity of both the dicarboxylic acid and acid chloride starting materials (Figure 2.2). This is evidenced by the significant decrease in yield with the addition of a single carbon into the length of the acid chloride when comparing the accessibility of the 2-methyl-1,3-cyclopentanedione (8) and 2-ethyl-1,3-cyclopentanedione (9).³ Furthermore, Schick et. al were only able to access simple cyclopentane- and cyclohexane-1,3-diones in conjunction with lower order acid chloride homologs (e.g. propionyl chloride and butyryl chloride). It was not until the work of Matoba et al. in 1986 that advances in the scope and capabilities of this transformation were reported.⁴ Specifically, more complex bicyclic scaffolds and some higher order acid chlorides were tolerated (see 10-14).⁴ Matoba was able to expand this scope to access bicyclic 2-alkyl-1,3-diones, but saw the same trend as Schick – the yields of the desired 1,3-dione products decreased with increasing complexity of the dicarboxylic acid or acid chloride starting materials.

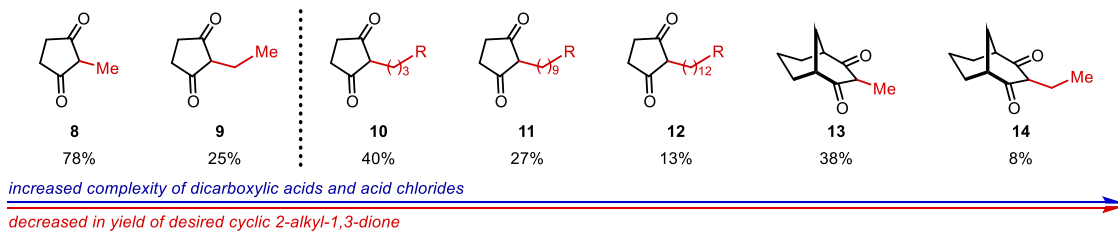


Figure 5.2 Substrates previously accessed by Matoba and Schick demonstrate a decrease in yield and complexity increases

Despite these limitations, this transformation was advantageous due to the fact that acyclic starting dicarboxylic acids and acid chlorides are combined in a convergent approach to provide

the desired cyclic 2-alkyl-1,3-diones (**3**). Importantly, this approach would allow us to readily incorporate the chiral quaternary center at the 3'-position required for our synthesis of atropurpuran and the arcutines (Figure 2.3A). Beyond our own synthesis, cyclic 2-alkyl-1,3-alkanediones (**3**) constitute key synthetic building blocks for the construction of other natural products,⁵ complex molecules, and heterocycles (Figure 2.3B).⁶ Two of the most prominent examples derived from these structural motifs are the Wieland-Miescher⁷ and Hajos-Parrish ketones,⁸ which represent crucial synthetic intermediates in established strategies towards steroid and terpene natural products.⁹ Furthermore, cyclic 2,2-dialkyl-1,3-alkanediones have been successfully transformed in desymmetrization approaches to give rise to essential chiral building blocks for the synthesis of biologically active compounds.¹⁰ Recognizing the synthetic potential of a general approach for the Dieckmann cyclization of dicarboxylic acids not only for our synthetic efforts but also as an alternative strategy towards cyclic-1,3-diones **3**, we initiated investigations into this reaction.

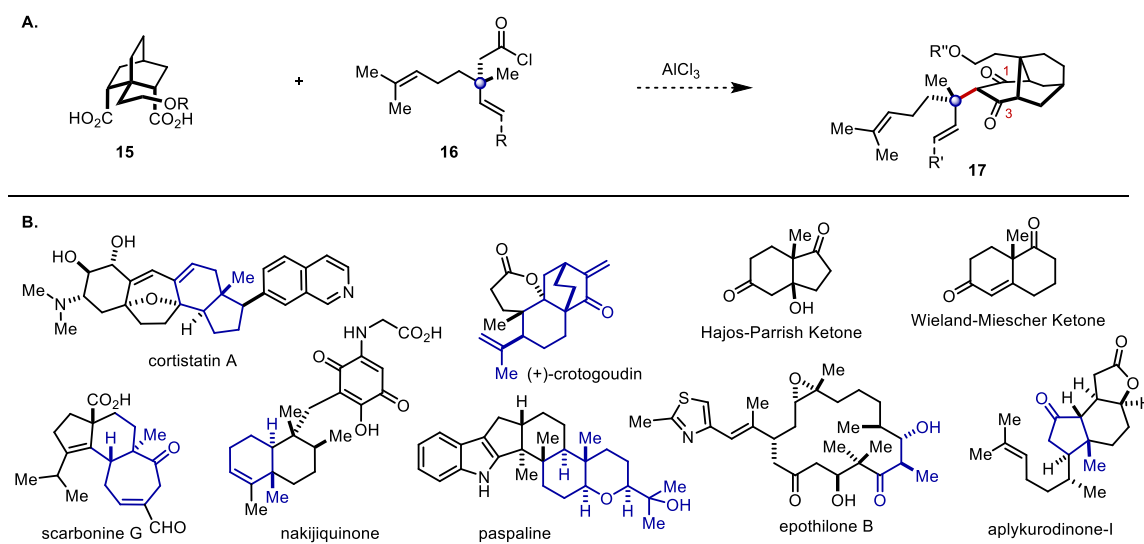
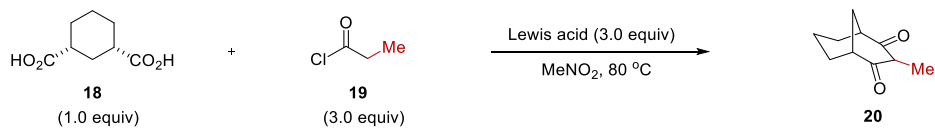


Figure 2.6 **A)** Our desired AlCl₃-mediated Dieckmann cyclization for the synthesis of atropurpuran; **B)** Natural products and building blocks derived from cyclic-1,3-diones

2.2 Results and Discussion

Initial efforts focused on evaluating various Lewis acids in the conversion of dicarboxylic acid **18** and propionyl chloride **19** to the desired cyclic 2-alkyl-1,3-dione **20** (Figure 2.4). Specifically, we evaluated Lewis acids that had a range of established strengths in Friedel-Crafts

reactions.¹¹ Among these, ZrCl₄, GaCl₃, and FeCl₃ provided the desired 2-alkyl-1,3-dione **20** in less than 10% yield. AlCl₃ proved uniquely effective and gave the desired product **20** in 55% yield. We also found similar trends in those reported previously – optimal yields required 3 equivalents of both acid chloride and Lewis acid.^{3,4}



| entry | Lewis acid | concentration (M) | time (h) | yield 20 (%) |
|-------|------------------------------------|-------------------|----------|---------------------|
| 1 | AlBr ₃ | 5 | 3 | - |
| 2 | BF ₃ · OEt ₂ | 5 | 3 | - |
| 3 | FeCl ₂ | 5 | 3 | - |
| 4 | SnCl ₄ | 5 | 3 | - |
| 5 | GaCl ₃ | 5 | 3 | <5 |
| 6 | FeCl ₃ | 5 | 3 | <5 |
| 7 | SbCl ₅ | 5 | 3 | <5 |
| 8 | TiCl ₄ | 5 | 3 | <5 |
| 9 | ZrCl ₄ | 5 | 3 | 15 |
| 10 | AlCl ₃ | 5 | 3 | 55 |

Conditions: *cis*-1,3-cyclohexanedicarboxylic acid **18** (1.0 equiv), propionyl chloride **19** (3.0 equiv), and Lewis acid (3.0 equiv) in MeNO₂ (5 M) were heated at 80 °C for 3 h. All yields were obtained by GC using dodecane as an internal standard.

Figure 2.7 Evaluation of various Lewis acids for the Dieckmann Cyclization

With the optimal Lewis acid in hand, we sought to develop a general strategy for the synthesis of complex cyclic 2-alkyl-1,3-diones using dicarboxylic acid **21** and propionyl chloride **19**. We started our efforts with the optimal conditions reported by Schick and Matoba.^{3,4} Employing AlCl₃ in nitromethane (MeNO₂) provided the desired product **12** in 36% yield (Entry 1, Figure 2.5A). Conducting the reaction in 1,2-dichloroethane (DCE) under otherwise identical conditions resulted in the formation of **22** in 28% yield (Entry 2). We suspected that the low mass recovery could be attributed to undesired side-reactivity of the acid chlorides. It is known that AlCl₃ enables the self-condensation of acid chlorides to give 4-hydroxy-2-pyrones **25**,¹² which isolated during our optimization efforts of this transformation (Figure 2.5B). This prompted us to consider tuning the reactivity of AlCl₃. Nitromethane is known to moderate the activity of AlCl₃ by forming an AlCl₃·MeNO₂ complex. This complex has been studied in Friedel-Crafts reactions and is considered to be a significantly milder alternative to AlCl₃ alone.¹³ As such, we focused our efforts on overcoming this self-condensation of the acid chloride by accessing this AlCl₃·MeNO₂ complex *in situ*. We found that pre-stirring the dicarboxylic acid **21** and AlCl₃ in MeNO₂ for one hour prior to addition of propionyl chloride **19** resulted in an increased yield of **22** in 59% (Entry

3). Ultimately, formation of the $\text{AlCl}_3 \cdot \text{MeNO}_2$ complex in DCE was identified as optimal, resulting in the formation **22** in 90% yield (Entry 4).

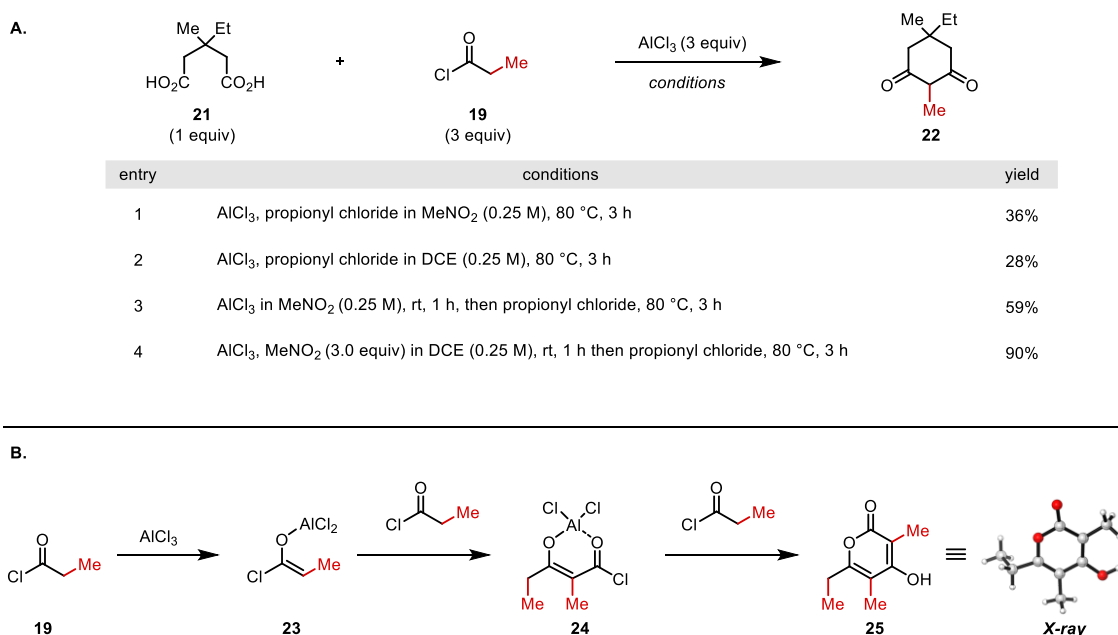


Figure 2.8 A) Optimization of AlCl_3 -mediated Dieckmann cyclization; B) Competing Lewis acid-mediated self-condensation of acid chlorides

With these optimal conditions in hand, we evaluated the scope of this transformation. When propionyl chloride was converted with dicarboxylic acids bearing distinct substitution patterns, the corresponding 2-methyl-1,3-alkanediones were obtained in up to 96% yield (**20**, **22**, **26-32**, Figure 2.6). It is important to note that rapid keto–enol and enol–enol tautomerization prohibits identification of the major diastereoisomers formed. Good to excellent yields of the desired 2-ethyl-1,3-diones were obtained with butyryl chloride, resulting in the formation of the desired products in up to 73% yield (**33-38**, Table 2). Higher order acid chlorides such as heptanoyl chloride and dodecanoyl chloride proved viable substrates, resulting in the formation of the desired products in up to 71% yield (**39-50**, Table 2). Importantly, previously reported literature procedures were limited by low yields of products such as **20** and **38** (38% yield and 8% yield, respectively) and proved unsuitable for higher order acid chloride substrates such as heptanoyl and dodecanoyl chloride, resulting exclusively in the formation of polymeric byproducts.⁴ The ability

to access these more complex carbocyclic scaffolds and do so with higher yield demonstrates the power of the $\text{AlCl}_3 \cdot \text{MeNO}_2$ complex in this transformation.

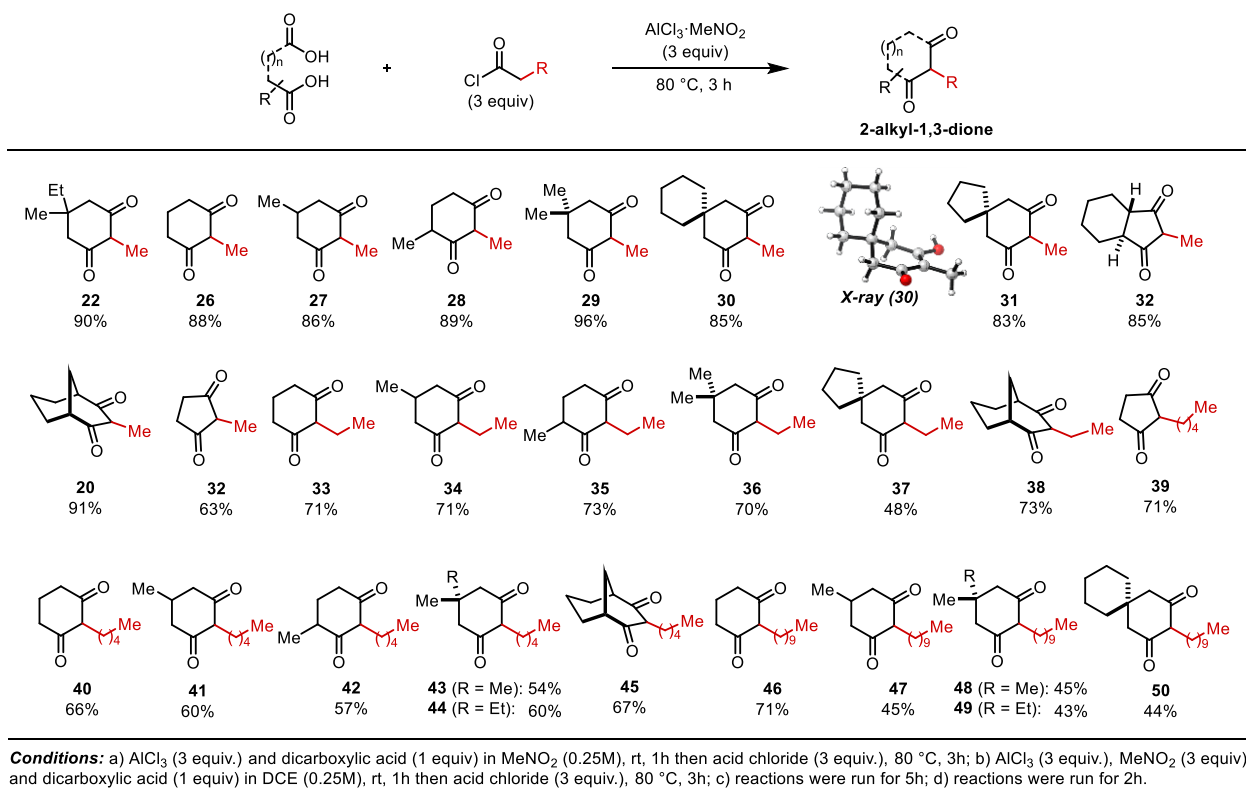
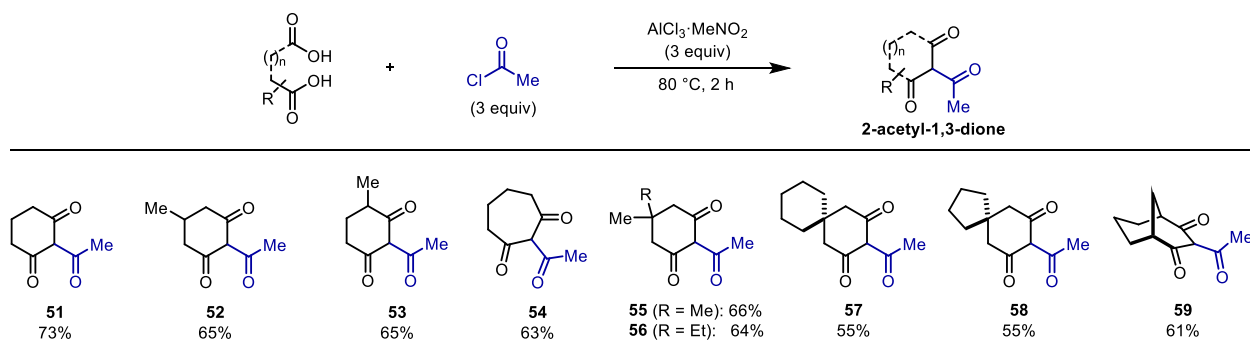


Figure 2.9 Substrate scope for the synthesis of 2-alkyl-1,3-diones

We were also able to apply this approach to the synthesis of 2-acetyl-1,3-diones (Figure 2.7). These products arose from the Dieckmann cyclization of dicarboxylic acids with acetyl chloride, which had previously been reported to give rise to the 2-acetyl-1,3-diones by Matoba et al. but proceeded in low yield (up to 15% yield of **59**).⁴ Similar to their alkyl counterparts, the structurally related cyclic 2-acyl-1,3-alkanediones represent common motifs in many complex molecules of biological importance¹⁴ but require multi-step approaches¹⁵ or harsh reaction conditions.¹⁶ We were able to employ our one-step Dieckmann cyclization strategy relying on an $\text{AlCl}_3 \cdot \text{MeNO}_2$ complex to access various cyclic 2-acetyl-1,3-diones that arose from the reaction of dicarboxylic acids with acetyl chloride (**51-59**).



Conditions: AlCl₃ (3 equiv) and dicarboxylic acid (1 equiv) in MeNO₂ (0.25 M) were stirred at rt for 1 h then acid chloride (3 equiv) was added and reaction was heated at 80 °C for 2 h.

Figure 2.10 Substrate scope for the synthesis of 2-acetyl-1,3-diones

Unfortunately, subsequent attempts to further incorporate functionality into either the dicarboxylic acid or acid chloride substrates were not successful (Figure 2.8). Attempts to expand the scope of the dicarboxylic acid substrate were conducted with propionyl chloride. However, we found that incorporation of heteroatoms into the dicarboxylic acid (**60**, **62**, **64**, **66**) scaffold did not give the functionalized cyclic 2-alkyl-1,3-diones (**61**, **63**, **65**, **67**) but rather 4-hydroxy-2-pyrones **25** (Figure 2.11) that resulted from the self-condensation of propionyl chloride.

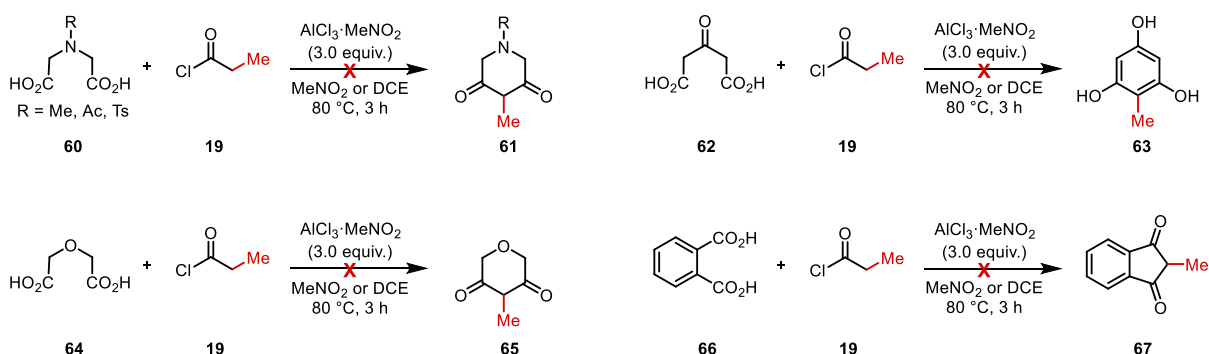


Figure 2.11 Attempts to incorporate functionality into the dicarboxylic acid substrate

Efforts to expand the scope of the acid chloride substrate were primarily investigated in conjunction with glutaric acid **68** as the dicarboxylic acid (Figure 2.9). However, any incorporation of heteroatoms or functional groups did not provide any of the desired products (**70**, **72**, **74**) but solely gave decomposition of the reaction mixtures.

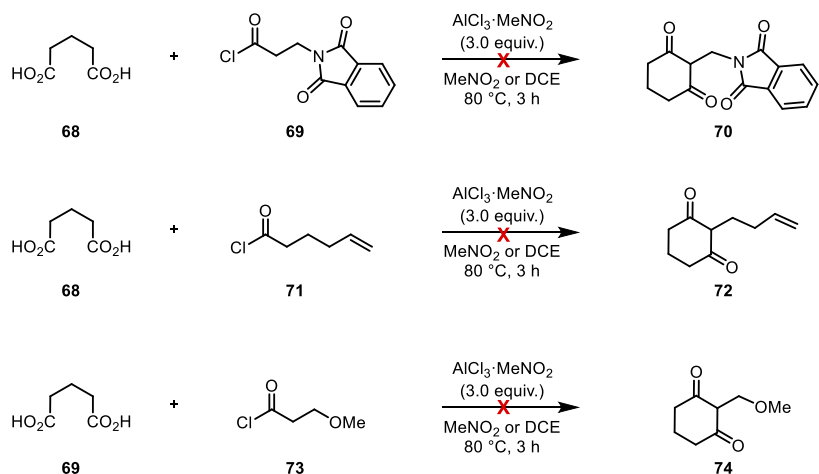


Figure 2.12 Attempts to incorporate functionality into the acid chloride substrate

2.3 Synthesis of the Chiloglottones

The chiloglottone natural products were isolated in 2003 by Francke et. al from the Australian orchid (*Chiloglottis trapeziformis*).¹⁷ These orchids are known to rely on mechanisms of sexual deception to induce pollination. Specifically, Francke et. al identified a compound that is produced by both *C. trapeziformis* and its pollinator, the thynnine wasp *Neozeleboria cryptoides*. The compound, chiloglottone 1, was the first 2,5-dialkylcyclohexane-1,3-dione found in nature and represents a new class of natural products.¹⁷ Access to various chiloglottone natural products is desirable and essential to gain further insight into the evolutionary dynamics of the plant-insect interaction. The first total synthesis of the chiloglottones was reported by Barrow et al., which proceeded in 9 steps and 14% yield overall¹⁸ and was followed by shorter sequences.¹⁹ Specifically, the second-generation strategy to the chiloglottones relies on two consecutive Birch reductions of 2,5-dimethoxybenzoic acid (**75**) to ultimately form chiloglottone 3 (**78**) in 22% overall yield (Figure 2.10). With our newly developed Dieckmann cyclization strategy relying on an $\text{AlCl}_3 \cdot \text{MeNO}_2$ complex we could access chiloglottone 3 (**78**) in 61% yield from commercially available dicarboxylic acid **79** and acid chloride **80**.

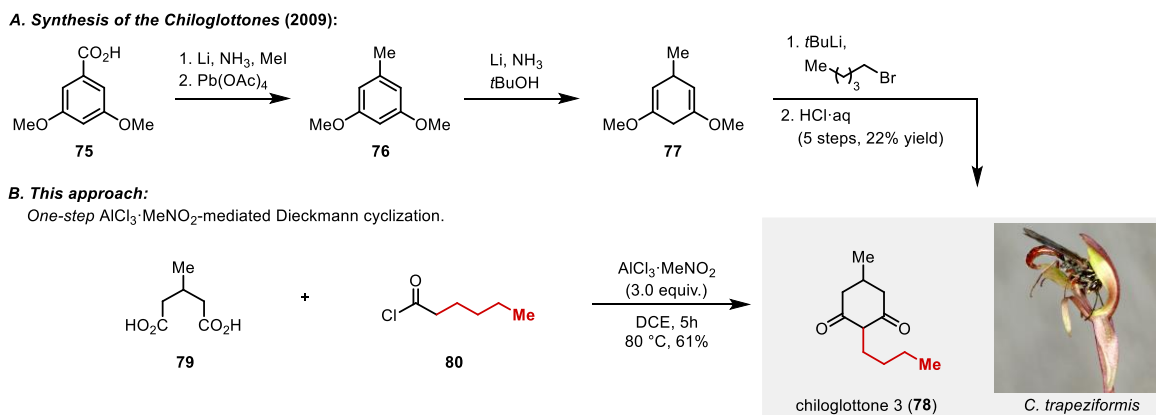


Figure 2.13 A) Previous route by Barrow et al. towards chiloglottone 3 (**78**); B) Our one-step strategy to chiloglottone 3 (**78**) based on our AlCl_3 -mediated Dieckmann Cyclization

2.4 Conclusion

This Dieckmann cyclization strategy of dicarboxylic acids described herein takes advantage of the attenuated reactivity of an $\text{AlCl}_3 \cdot \text{MeNO}_2$ complex to provide complex, cyclic 2-alkyl-1,3-diones in a single synthetic transformation from readily available dicarboxylic acid and acid chloride starting materials. Importantly, we found that attenuating the Lewis acidity of AlCl_3 by forming an $\text{AlCl}_3 \cdot \text{MeNO}_2$ complex enabled the development of this approach into a general protocol that was the first to tolerate higher order acid chlorides and dicarboxylic acid substrates. The synthetic potential of this new reaction protocol was demonstrated in a one-step synthesis of chiloglottone 3 (**78**) in 61% yield from commercial material.

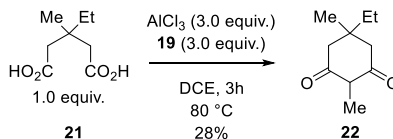
2.5 Experimental Details

2.5.1 General Information

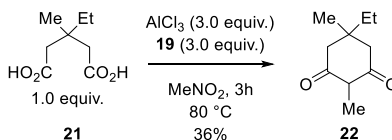
Unless otherwise noted, all reactions were performed in oven-dried glassware under an atmosphere of nitrogen. All chemicals were purchased from commercial suppliers and were used without further purification. Anhydrous nitromethane (MeNO_2) and anhydrous 1,2-dichloroethane (DCE) were obtained from Acros Organics and were used as received. Flash chromatography was performed using Biotage Isolera One ACI™ Accelerated Chromatography Isolation system on Silicycle Silia Flash® 40-63 micron (230-400 mesh). Gas chromatography (GC) was conducted on a Shimadzu GC-2010 Plus system using a Shimadzu SHRXI-5MS column. Proton Nuclear Magnetic Resonance NMR (^1H NMR) spectra and carbon nuclear magnetic resonance (^{13}C NMR) spectra were recorded on a Varian Unity Plus 400, Varian MR400, Varian vnmrs 500, Varian

Inova 500, Varian Mercury 500, and Varian vnmrs 700 spectrometers. Chemical shifts for protons are reported in parts per million and are referenced to the NMR solvent peak (CDCl_3 : δ 7.26; CD_3OD : δ 4.87). Chemical shifts for carbons are reported in parts per million and are referenced to the carbon resonances of the NMR solvent (CDCl_3 : δ 77.16; CD_3OD : δ 49.00). Data are represented as follows: chemical shift, integration, multiplicity (br = broad, s = singlet, d = doublet, t = triplet, q = quartet, p = pentet, m = multiplet), and coupling constants in Hertz (Hz). Mass spectroscopic (MS) data was recorded at the Mass Spectrometry Facility at the Department of Chemistry of the University of Michigan in Ann Arbor, MI on an Agilent Q-TOF HPLC-MS with ESI high resolution mass spectrometer. Infrared (IR) spectra were obtained using either an Avatar 360 FT-IR or Perkin Elmer Spectrum BX FT-IR spectrometer. IR data are represented as frequency of absorption (cm^{-1}).

2.5.2 Reaction Optimization



Conditions A: To a 25 mL round bottom flask equipped with magnetic stir bar and reflux condenser was added AlCl_3 (6 mmol, 3 equiv) and 1,2-DCE (0.25 M). Once AlCl_3 had dissolved, 3-ethyl-3-methylglutaric acid **22** (2 mmol, 1 equiv) and propionyl chloride **20** (6 mmol, 3 equiv) were introduced at room temperature. Flask was heated to $80\text{ }^\circ\text{C}$ in an aluminum heating block for three hours. After cooling to room temperature, the reaction was poured into an Erlenmeyer flask containing 1:1 mixture saturated solution of Rochelle's salt and DCM. After stirring for one hour, the layers were separated. The organic layer was dried over sodium sulfate, filtered, and concentrated to give the crude product, which was purified by flash chromatography (EtOAc/hexanes).

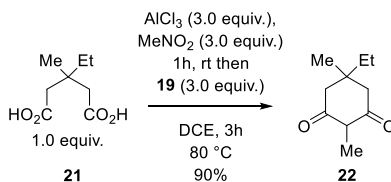


Conditions B: To a 25 mL round bottom flask equipped with magnetic stir bar and reflux condenser was added AlCl_3 (6 mmol, 3 equiv) and MeNO_2 (0.25 M). Once AlCl_3 had dissolved, 3-ethyl-3-methylglutaric acid **22** (2 mmol, 1 equiv) and propionyl chloride **20** (6 mmol, 3 equiv) were introduced at room temperature. Flask was heated to $80\text{ }^\circ\text{C}$ in an aluminum heating block for

three hours. After cooling to room temperature, the reaction was poured into and Erlenmeyer flask containing 1:1 mixture saturated solution of Rochelle's salt and DCM. After stirring for one hour, the layers were separated. The organic layer was dried over sodium sulfate, filtered, and concentrated to give the crude product, which was purified by flash chromatography (EtOAc/hexanes).

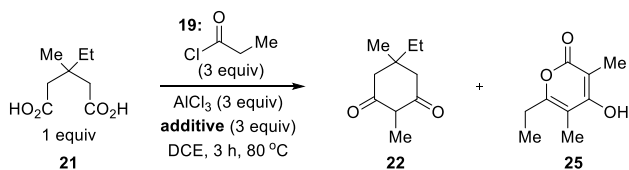


Conditions C: To a 25 mL round bottom flask equipped with magnetic stir bar and reflux condenser was added AlCl_3 (6 mmol, 3 equiv) and MeNO_2 (0.25 M). Once AlCl_3 had dissolved, 3-ethyl-3-methylglutaric acid **22** (2 mmol, 1 equiv) was added and the solution was left to stir at room temperature for one hour. Then propionyl chloride **20** (6 mmol, 3 equiv) was introduced at room temperature. Flask was heated to 80 °C in an aluminum heating block for three hours. After cooling to room temperature, the reaction was poured into and Erlenmeyer flask containing 1:1 mixture saturated solution of Rochelle's salt and DCM (100 mL). After stirring for one hour, the layers were separated. The organic layer was dried over sodium sulfate, filtered, and concentrated to give the crude product, which was purified by flash chromatography (EtOAc/hexanes).



Conditions D: To a 25 mL round bottom flask equipped with magnetic stir bar and reflux condenser was added AlCl_3 (6 mmol, 3 eq.), MeNO_2 (9 mmol, 3 eq.) and 1,2-DCE (0.25 M). To this solution was then added 3-ethyl-3-methylglutaric acid **22** (2 mmol, 1 eq.) and left to stir at room temperature for one hour. Then propionyl chloride **20** (6 mmol, 3 eq.) was introduced at room temperature. Flask was heated to 80 °C in an aluminum heating block for three hours. After cooling to room temperature, the reaction was poured into and Erlenmeyer flask containing 1:1 mixture saturated solution of Rochelle's salt and DCM. After stirring for one hour, the layers were separated. The organic layer was dried over sodium sulfate, filtered, and concentrated to give the crude product, which was purified by flash chromatography (EtOAc/hexanes).

2.5.3 Additives Screen

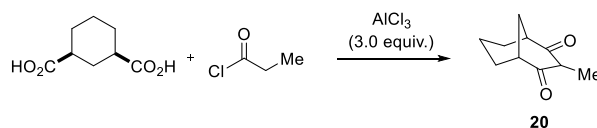


| entry | additive | yield 22 (%) | yield 25 (%) |
|-------|--|---------------------|---------------------|
| 1 | Al ₂ O ₃ (basic) | 10 | - |
| 2 | Al ₂ O ₃ (neutral) | 33 | - |
| 3 | MeSO ₃ H | - | - |
| 4 | DMF | - | 64 |
| 5 | DME | - | 66 |
| 6 | MeCN | - | 56 |
| 7 | DMSO | - | 40 |

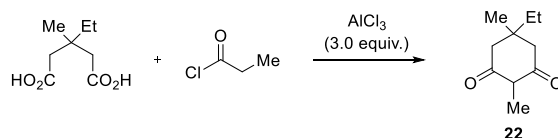
Conditions: AlCl₃ (3.45 mmol, 3.0 equiv), MeNO₂ (3.45 mmol, 3.0 equiv) and dicarboxylic acid **22** (1.15 mmol, 1.0 equiv) in DCE (0.25 M) were stirred at rt for 1 h then acid chloride **19** (3.45 mmol, 3.0 equiv) was added and reaction was heated at 80 °C for 3 h.

2.5.4 Synthesis of 2-alkyl-1,3-diones

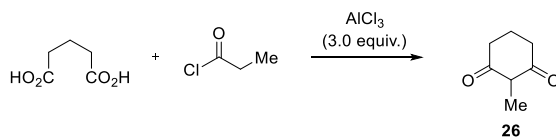
General procedure for synthesis of cyclic 2-alkyl-1,3-alkanediones: Cyclic 2-alkyl-1,3-alkanediones were prepared using a 3 mmol scale of dicarboxylic acid via the optimized conditions in MeNO₂ (**conditions C**, Supporting Information) and/or DCE (**conditions D**, Supporting Information). For reactions that were run in both MeNO₂ and DCE, both yields are listed. All reactions were run for 3h unless otherwise noted. Products were purified by flash chromatography eluting with hexanes/EtOAc.



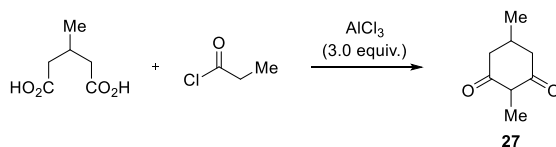
3-methylbicyclo[3.3.1]nonane-2,4-dione (20) was obtained as a white solid (0.423 g, 85% yield in MeNO₂, 0.453 g, 91% yield in DCE). ¹H NMR (400 MHz, CD₃OD) δ 2.50 (s, 2H), 2.19 (d, *J* = 12.3 Hz, 1H), 1.77 (dd, *J* = 12.4, 2.0 Hz, 1H), 1.70 (s, 3H), 1.70 – 1.51 (m, 5H), 1.51 – 1.41 (m, 1H); ¹³C NMR (100 MHz, CD₃OD) δ 114.0, 34.4, 27.4, 19.4, 6.9; IR (Neat): ν 2933, 2861, 1706, 1569, 1448, 1388, 1256, 1062. 900, 836 cm⁻¹; HRMS-ESI (*m/z*) [M+H] calcd for C₁₀H₁₄O₂, 167.1067; found: 167.1066.



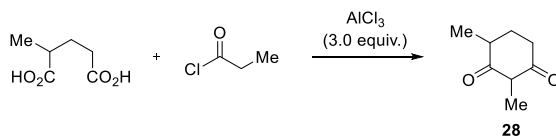
2-methyl-5-ethyl-5-methylcyclohexane-1,3-dione (22) was obtained as a white solid (0.297 g, 59% yield in MeNO₂, 0.454 g, 90% yield in DCE). ¹H NMR (400 MHz, CD₃OD) δ 2.33 (d, *J* = 16.7 Hz, 2H), 2.20 (d, *J* = 16.7 Hz, 2H), 1.63 (s, 3H), 1.40 (q, *J* = 7.5 Hz, 2H), 0.98 (s, 3H), 0.87 (t, *J* = 7.5 Hz, 3H); ¹³C NMR (100 MHz, CD₃OD) δ 110.7, 45.6, 35.7, 34.7, 24.7, 8.4, 7.0; IR (Neat): ν 2965, 1741, 1708, 1600, 1459, 1386, 1091 cm⁻¹; HRMS-ESI (*m/z*) [M+H] calcd for C₁₀H₁₆O₂, 169.1223; found: 169.1222.



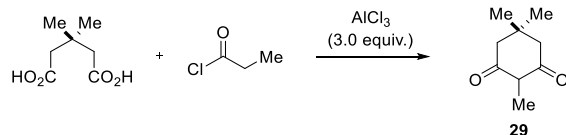
2-methylcyclohexane-1,3-dione (26) was obtained as a white solid (0.332 g, 88% yield in MeNO₂, 0.321 g, 85% yield in DCE). ¹H NMR (400 MHz, CD₃OD) δ 2.38 (t, *J* = 6.3 Hz, 4H), 1.97 – 1.86 (m, 2H), 1.63 (s, 3H); ¹³C NMR (100 MHz, CD₃OD) δ 111.9, 22.0, 7.1; IR (Neat): ν 2932, 1566, 1338, 1262, 1080, 916, 853 cm⁻¹; HRMS-ESI (*m/z*) [M+H]⁺ calcd for C₇H₁₀O₂, 127.0754; found: 127.0754.



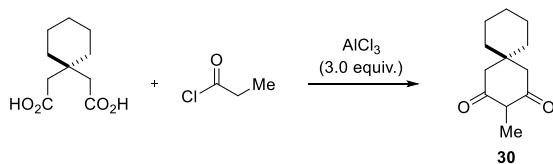
2,5-dimethylcyclohexane-1,3-dione (27) was obtained as a white solid (0.327 g, 78% yield in MeNO₂, 0.361 g, 86% yield in DCE). ¹H NMR (400 MHz, CD₃OD) δ 2.42 (d, *J* = 12.7 Hz, 2H), 2.12 (d, *J* = 11.9 Hz, 3H), 1.62 (s, 3H), 1.05 (d, *J* = 4.1 Hz, 3H); ¹³C NMR (100 MHz, CD₃OD) δ 110.0, 40.0, 28.4, 19.8, 5.7; IR (Neat): ν 2945, 1564, 1241, 1080 cm⁻¹; HRMS-ESI (*m/z*) [M+H]⁺ calcd for C₈H₁₂O₂, 141.0910; found: 141.0909.



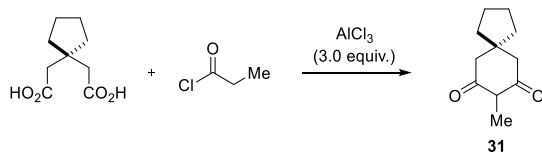
2,4-dimethylcyclohexane-1,3-dione (28) was obtained as a white solid (0.344 g, 82% yield in MeNO₂, 0.374 g, 89% yield in DCE). ¹H NMR (400 MHz, CD₃OD) δ 2.47 (t, *J* = 5.4 Hz, 2H), 2.34 (d, *J* = 4.4 Hz, 1H), 2.04 (dt, *J* = 18.3, 5.6 Hz, 1H), 1.68 (dd, *J* = 14.3, 7.9 Hz, 1H), 1.63 (s, 3H), 1.14 (d, *J* = 6.9 Hz, 3H); ¹³C NMR (100 MHz, CD₃OD) δ 109.6, 28.3, 15.1, 6.1; IR (Neat): ν 2933, 2670, 1565, 1455, 1355, 1260, 1084, 834 cm⁻¹; HRMS-ESI (*m/z*) [M+H] calcd for C₈H₁₂O₂, 141.0910; found: 141.0909.



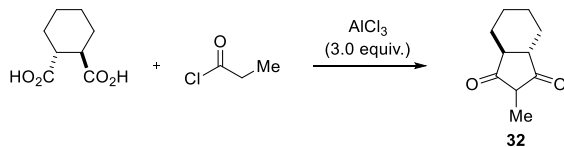
2,5,5-trimethylcyclohexane-1,3-dione (29) was obtained as a white solid (0.272 g, 0.59% yield in MeNO₂, 0.444 g, 96% yield in DCE). ¹H NMR (400 MHz, CD₃OD) δ 4.87, 3.31, 2.28, 1.65, 1.05; ¹³C NMR (100 MHz, CD₃OD) δ 109.2, 31.5, 27.1, 5.5; IR (Neat): ν 2955, 2644, 1646, 1569, 1446, 1343, 1306, 1248, 1084, 890 cm⁻¹; HRMS-ESI (*m/z*) [M+H] calcd for C₉H₁₄O₂, 155.1067; found: 155.1067.



3-methylspiro[5.5]undecane-2,4-dione (30) was obtained as a white solid (0.453 g, 78% yield in MeNO₂, 0.494 g, 85% yield in DCE). ¹H NMR (400 MHz, CD₃OD) δ 2.36 (s, 4H), 1.63 (s, 3H), 1.46 (d, *J* = 10.6 Hz, 10H); ¹³C NMR (100 MHz, CD₃OD) δ 109.2, 36.1, 34.4, 25.9, 21.3, 5.5; IR (Neat): ν 2927, 1574, 1452, 1384, 1255, 1091 cm⁻¹; HRMS-ESI (*m/z*) [M+H] calcd for C₁₂H₁₈O₂, 195.1380; found: 195.1382.

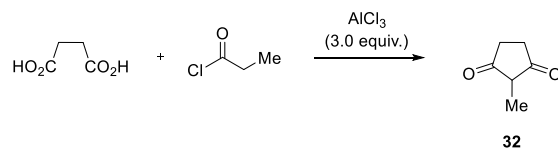


8-methylspiro[4.5]decane-7,9-dione (31) was obtained as a white solid (0.324 g, 60% yield in MeNO₂, 0.448 g, 83% yield in DCE). ¹H NMR (400 MHz, CD₃OD) δ 2.39 (s, 4H), 1.70 – 1.67 (m, 4H), 1.64 (s, 3H), 1.50 (t, *J* = 7.1 Hz, 4H); ¹³C NMR (100 MHz, CD₃OD) δ 111.3, 44.0, 39.2, 25.1, 7.0; IR (Neat): ν 2925, 1652, 1557, 1372, 1247, 1090, 895 cm⁻¹; HRMS-ESI (*m/z*) [M+H] calcd for C₁₁H₁₆O₂, 181.1223; found: 181.1221.

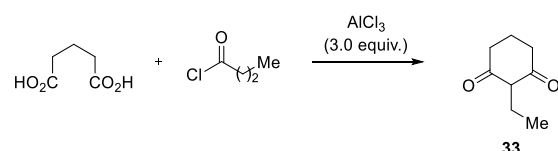


2-methylhexahydro-1H-indene-1,3(2H)-dione (32) was obtained as a white solid (0.274 g, 55% yield in MeNO₂, 0.423 g, 85% yield in DCE). ¹H NMR (400 MHz, CD₃OD) δ 2.20 (d, *J* = 8.5 Hz, 2H), 2.12 (d, *J* = 8.6 Hz, 2H), 1.89 (d, *J* = 6.4 Hz, 2H), 1.53 (s, 3H), 1.32 (dd, *J* = 14.2, 5.4 Hz, 4H); ¹³C NMR (100 MHz, CD₃OD) δ 110.9, 27.5, 26.7, 5.4; IR (Neat): ν 2930, 2859, 1734, 1667,

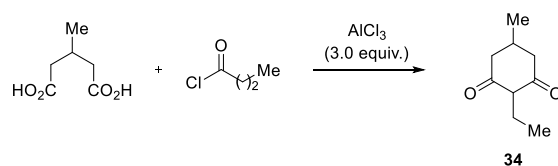
1560, 1360, 1269, 1028, 901 cm^{-1} ; **HRMS-ESI** (m/z) [$M+H$] calcd for $\text{C}_{10}\text{H}_{14}\text{O}_2$, 167.1067; found: 167.1066.



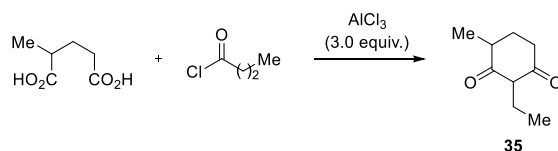
2-methylcyclopentane-1,3-dione (32) was obtained as a white solid (0.211 g, 63% yield in MeNO_2). **$^1\text{H NMR}$** (400 MHz, CD_3OD) δ 2.46 (s, 4H), 1.55 (s, 3H); **$^{13}\text{C NMR}$** (100 MHz, CD_3OD) δ 112.6, 29.8, 4.1; **IR** (Neat): ν 1573, 1381, 1347, 1256, 1094, 818 cm^{-1} ; **HRMS-ESI** (m/z) [$M+H$] calcd for $\text{C}_6\text{H}_8\text{O}_2$, 113.0597; found: 113.0599.



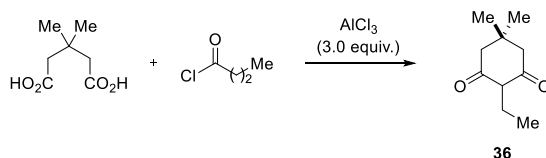
2-ethylcyclohexane-1,3-dione (33) was obtained as a white solid (0.298 g, 71% yield in MeNO_2 , 0.294 g, 70% yield in DCE). **$^1\text{H NMR}$** (400 MHz, CD_3OD) δ 11.66 (s, 1H), 2.57 (dt, $J = 8.0, 4.5$ Hz, 4H), 2.31 (q, $J = 7.4$ Hz, 2H), 2.02 – 1.92 (m, 2H), 0.99 – 0.90 (m, 3H); **$^{13}\text{C NMR}$** (100 MHz, CD_3OD) δ 205.5, 190.3, 118.0, 69.0, 39.9, 32.5, 20.8, 18.3, 17.2, 15.2, 13.2, 12.1, 9.2; **IR** (Neat): ν 2943, 1564, 1359, 1268, 1197, 1101, 943 cm^{-1} ; **HRMS-ESI** (m/z) [$M+H$] calcd for $\text{C}_8\text{H}_{12}\text{O}_2$, 141.0911; found: 141.0911.



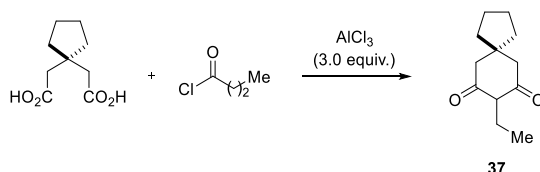
2-ethyl-5-methylcyclohexane-1,3-dione (34) was obtained as a white solid (0.328 g, 71% yield in MeNO_2 , 0.328 g, 71% yield in DCE). **$^1\text{H NMR}$** (400 MHz, CD_3OD) δ 2.46 – 2.35 (m, 2H), 2.22 (tt, $J = 7.3, 3.7$ Hz, 2H), 2.17 – 2.07 (m, 3H), 1.04 (d, $J = 3.8$ Hz, 3H), 0.88 (td, $J = 7.4, 1.7$ Hz, 3H); **$^{13}\text{C NMR}$** (100 MHz, CD_3OD) δ 116.6, 40.7, 28.4, 19.7, 14.5, 12.1; **IR** (Neat): ν 2959, 1632, 1561, 1377, 1330, 1258, 1102, 885 cm^{-1} ; **HRMS-ESI** (m/z) [$M+H$] calcd for $\text{C}_9\text{H}_{14}\text{O}_2$, 155.1067; found: 155.1065.



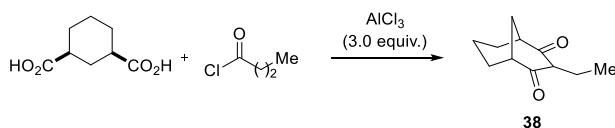
2-ethyl-4-methylcyclohexane-1,3-dione (35) was obtained as a white solid (0.300 g, 65% yield in MeNO₂, 0.337 g, 73% yield in DCE). ¹H NMR (400 MHz, CD₃OD) δ 2.48 (s, 2H), 2.34 (s, 1H), 2.30 – 2.16 (m, 2H), 2.12 – 1.97 (m, 1H), 1.67 (dd, *J* = 13.0, 6.8 Hz, 1H), 1.15 (d, *J* = 6.3 Hz, 3H), 0.90 (t, *J* = 7.3 Hz, 3H); ¹³C NMR (100 MHz, CD₃OD) δ 116.2, 28.2, 15.1, 14.7, 12.2; IR (Neat): ν 2934, 1710, 1570, 1456, 1378, 1266, 1205, 1106, 919 cm⁻¹; HRMS-ESI (*m/z*) [M+H] calcd for C₉H₁₄O₂, 155.1067; found: 155.1065.



2-ethyl-5,5-dimethylcyclohexane-1,3-dione (36) was obtained as a white solid (0.302 g, 60% yield in MeNO₂, 0.352 g, 70% yield in DCE). ¹H NMR (400 MHz, CD₃OD) δ 2.65 (d, *J* = 1.8 Hz, 1H), 2.37 – 2.12 (m, 5H), 1.06 (dd, *J* = 20.0, 1.7 Hz, 7H), 0.89 (td, *J* = 7.4, 1.7 Hz, 3H); ¹³C NMR (100 MHz, CD₃OD) δ 167.1, 115.8, 42.6, 31.5, 27.0, 26.1, 14.4, 12.1; IR (Neat): ν 2966, 1809, 1773, 1707, 1566, 1379, 1184, 1072, 963, 805 cm⁻¹; HRMS-ESI (*m/z*) [M+H] calcd for C₁₀H₁₆O₂, 169.1223; found: 169.1223.

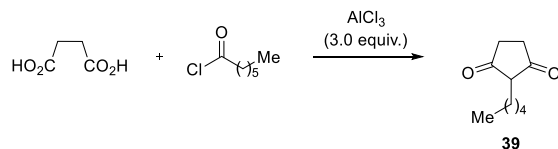


8-ethylspiro[4.5]decane-7,9-dione (37) was obtained as a white solid (0.194 g, 33% yield in MeNO₂, 0.279 g, 48% yield in DCE). ¹H NMR (700 MHz, CDCl₃) δ 6.76 (s, 1H), 3.19 (s, .63H), 2.68 (d, *J* = 13.9 Hz, 1H), 2.57 (d, *J* = 13.9 Hz, 1H), 2.40 (s, 3H), 2.28 (q, *J* = 7.3 Hz, 2H), 1.88 – 1.81 (m, 1H), 1.67 (d, *J* = 20.9 Hz, 6H), 1.52 (d, *J* = 29.0 Hz, 5H), 1.30 (s, 1H), 0.96 (t, *J* = 7.3 Hz, 3H), 0.92 (t, *J* = 7.4 Hz, 2H). ¹³C NMR (176 MHz, CDCl₃) δ 205.1, 117.0, 68.2, 52.3, 42.9, 39.3, 38.3, 36.3, 24.5, 24.2, 24.2, 17.7, 15.1, 13.3, 12.0. IR (Neat): ν 2924, 1636, 1553, 1412, 1386, 1362, 1327, 1236, 1063, 957, 891 cm⁻¹; HRMS-ESI (*m/z*) [M+H] calcd for C₁₂H₁₈O₂, 195.1380; found: 195.1376.

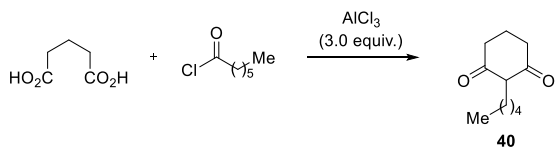


3-ethylbicyclo[3.3.1]nonane-2,4-dione (38) was obtained as a white solid (0.394 g, 73% yield in MeNO₂, 0.351 g, 65% yield in DCE). ¹H NMR (400 MHz, CD₃OD) δ 2.38 (s, 2H), 2.19 (q, *J* =

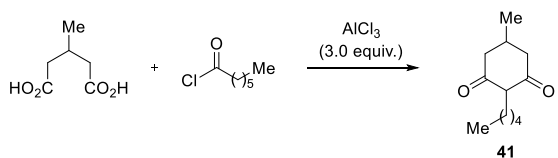
7.4 Hz, 2H), 2.07 (dd, $J = 12.4, 1.7$ Hz, 1H), 1.70 – 1.35 (m, 7H), 0.84 (t, $J = 7.4$ Hz, 3H); ^{13}C NMR (100 MHz, CD_3OD) δ 190.3, 120.8, 40.0, 34.4, 27.4, 19.3, 16.0, 13.7; IR (Neat): ν 2934, 1562, 1370, 1347, 1259, 1194, 1088, 845 cm^{-1} ; HRMS-ESI (m/z) [$\text{M}+\text{H}$] calcd for $\text{C}_{10}\text{H}_{14}\text{O}_2$, 181.1225; found: 181.1223.



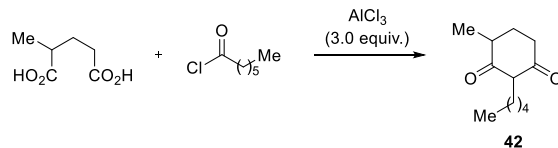
2-pentylcyclopentane-1,3-dione (39) was obtained as a white solid (0.357 g, 71% yield in MeNO_2). ^1H NMR (400 MHz, CD_3OD) δ 2.45 (s, 4H), 2.08 (t, $J = 7.5$ Hz, 2H), 1.46 – 1.18 (m, 6H), 0.87 (t, $J = 7.0$ Hz, 3H); ^{13}C NMR (100 MHz, CD_3OD) δ 118.9, 32.8, 31.3, 28.7, 23.6, 21.7, 14.4; IR (Neat): ν 2928, 1539, 1342, 1265, 1121 cm^{-1} ; HRMS-ESI (m/z) [$\text{M}+\text{H}$] calcd for $\text{C}_{10}\text{H}_{16}\text{O}_2$, 169.1223; found: 169.1222.



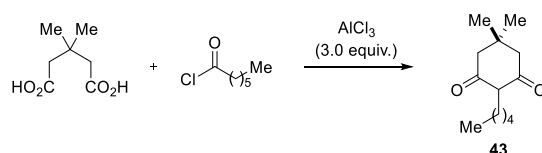
2-pentylcyclohexane-1,3-dione (40) was obtained as a white solid (0.360 g, 66% yield in MeNO_2). ^1H NMR (400 MHz, CD_3OD) δ 13.42 (s, 1H), 2.73 (s, 4H), 2.26 (s, 2H), 1.97 (s, 2H), 1.27 (dd, $J = 20.6, 10.1$ Hz, 6H), 0.81 (t, $J = 6.7$ Hz, 3H); ^{13}C NMR (100 MHz, CD_3OD) δ 194.3, 116.8, 77.5, 76.8, 31.8, 31.7, 28.0, 22.5, 21.6, 20.5, 14.1; IR (Neat): ν 2924, 1568, 1375, 1270, 1184, 1115, 1002 cm^{-1} ; HRMS-ESI (m/z) [$\text{M}+\text{H}$] calcd for $\text{C}_{11}\text{H}_{18}\text{O}_2$, 183.1380; found: 183.1382.



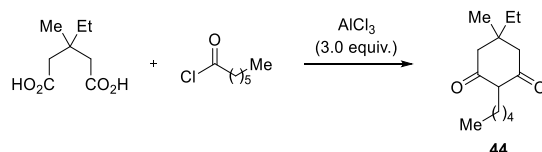
2-pentyl-5-methylcyclohexane-1,3-dione (41) was obtained as a white solid (0.352 g, 60% yield in MeNO_2). ^1H NMR (400 MHz, CD_3OD) δ 2.43 (d, $J = 12.5$ Hz, 2H), 2.26 – 2.06 (m, 5H), 1.29 (dt, $J = 16.5, 8.4$ Hz, 6H), 1.06 (d, $J = 3.5$ Hz, 3H), 0.88 (t, $J = 6.8$ Hz, 3H); ^{13}C NMR (100 MHz, CD_3OD) δ 115.3, 40.3, 31.6, 28.4, 27.9, 22.2, 21.2, 19.7, 13.0; IR (Neat): ν 2953, 2925, 1707, 1565, 1379, 1329, 1243, 1117 cm^{-1} ; HRMS-ESI (m/z) [$\text{M}+\text{H}$] calcd for $\text{C}_{12}\text{H}_{20}\text{O}_2$, 197.1536; found: 197.1533.



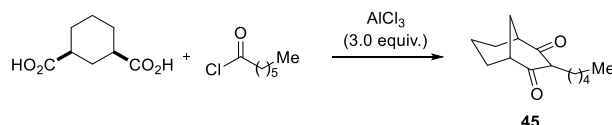
2-pentyl-4-methylcyclohexane-1,3-dione (42) was obtained as a white solid (0.335 g, 57% yield in MeNO₂). ¹H NMR (400 MHz, CD₃OD) δ 4.03 (d, *J* = 5.5 Hz, 2H), 3.89 (s, 1H), 3.79 (dd, *J* = 15.4, 8.5 Hz, 2H), 3.65 – 3.56 (m, 1H), 3.22 (ddd, *J* = 15.1, 13.6, 7.0 Hz, 1H), 2.92 – 2.78 (m, 6H), 2.69 (t, *J* = 9.0 Hz, 3H), 2.44 (t, *J* = 7.0 Hz, 3H); ¹³C NMR (100 MHz, CD₃OD) δ 116.3, 33.0, 29.7, 29.4, 23.7, 22.8, 16.6, 14.5; IR (Neat): ν 2933, 1711, 1575, 1457, 1381, 1268, 1106, 919 cm⁻¹; HRMS-ESI (*m/z*) [M+H] calcd for C₁₂H₂₀O₂, 197.1536; found: 197.1533.



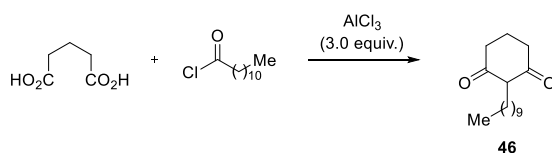
2-pentyl-5,5-dimethylcyclohexane-1,3-dione (43) was obtained as a white solid (0.340 g, 54% yield in MeNO₂). ¹H NMR (400 MHz, CD₃OD) δ 2.57 – 2.35 (m, 5H), 2.26 – 2.09 (m, 2H), 1.31 – 1.09 (m, 3H), 1.04 (d, *J* = 1.4 Hz, 6H), 0.98 (dd, *J* = 19.3, 1.2 Hz, 3H), 0.76 (dd, *J* = 9.5, 4.5 Hz, 3H); ¹³C NMR (100 MHz, CD₃OD) δ 205.3, 166.2, 115.0, 66.54, 53.8, 46.6, 43.7, 31.93, 31.87, 31.8, 30.9, 29.6, 29.4, 28.29, 28.26, 27.5, 27.0, 26.9, 24.2, 22.6, 22.3, 21.5, 14.1, 14.0; IR (Neat): ν 2956, 1775, 1705, 1184, 1075, 963 cm⁻¹; HRMS-ESI (*m/z*) [M+H] calcd for C₁₃H₂₂O₂, 211.1693; found: 211.1692.



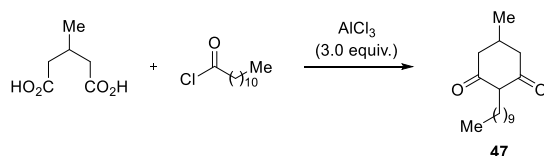
2-pentyl-5-ethyl-5-methylcyclohexane-1,3-dione (44) was obtained as a white solid (0.403 g, 60% yield in MeNO₂). ¹H NMR (400 MHz, CD₃OD) δ 2.76 – 2.61 (m, 4H), 2.40 – 2.19 (m, 5H), 1.66 – 1.59 (m, 1H), 1.46 (dd, *J* = 14.8, 7.4 Hz, 3H), 1.32 (ddd, *J* = 14.9, 12.0, 5.9 Hz, 7H), 1.08 (s, 3H), 1.03 (s, 1H), 0.97 – 0.88 (m, 8H); ¹³C NMR (100 MHz, CD₃OD) δ 177.6, 168.7, 116.0, 42.2, 35.7, 34.9, 34.7, 33.9, 33.2, 33.0, 32.7, 29.9, 29.3, 26.0, 24.6, 24.2, 23.7, 23.6, 22.5, 14.5, 14.4, 8.4, 8.2; IR (Neat): ν 2917, 1572, 1384, 1252, 1071 cm⁻¹; HRMS-ESI (*m/z*) [M+H] calcd for C₁₄H₂₄O₂, 225.1849; found: 225.1852.



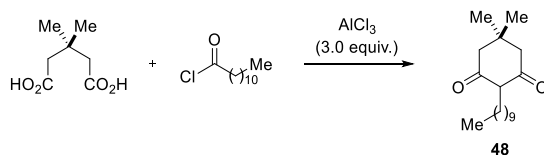
3-pentylbicyclo[3.3.1]nonane-2,4-dione (45) was obtained as a white solid (0.446 g, 67% yield in MeNO₂). ¹H NMR (400 MHz, CD₃OD) δ 12.99 (s, 2H), 3.46 (s, 2H), 2.33 (dd, *J* = 18.2, 11.4 Hz, 3H), 1.94 (d, *J* = 12.0 Hz, 2H), 1.75 – 1.64 (m, 3H), 1.48 – 1.33 (m, 3H), 1.30 – 1.22 (m, 4H), 0.85 (t, *J* = 6.9 Hz, 3H); ¹³C NMR (100 MHz, CD₃OD) δ 200.2, 119.3, 36.5, 33.5, 31.8, 27.8, 25.2, 22.5, 21.5, 17.7, 14.1; IR (Neat): ν 2935, 1710, 1705, 1305 cm⁻¹; HRMS-ESI (*m/z*) [M+H] calcd for C₁₀H₁₄O₂, 223.1693; found: 223.1694.



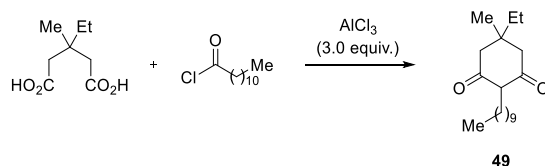
2-decylcyclohexane-1,3-dione (46) was heated for 5h and obtained as a white solid (0.536 g, 71% yield in MeNO₂). ¹H NMR (400 MHz, CD₃OD) δ 2.76 (dt, *J* = 28.7, 6.2 Hz, 1H), 2.46 – 2.19 (m, 5H), 1.99 – 1.80 (m, 2H), 1.56 (s, 1H), 1.28 (s, 16H), 0.89 (d, *J* = 6.3 Hz, 3H); ¹³C NMR (100 MHz, CD₃OD) δ 200.6, 200.1, 176.9, 117.2, 36.6, 35.9, 33.8, 33.09, 33.06, 30.80, 30.77, 30.72, 30.61, 30.54, 30.49, 30.45, 30.3, 29.7, 24.1, 23.7, 22.7, 22.1, 19.5, 14.5; IR (Neat): ν 2916, 2848, 1711, 1560, 1360, 1267, 1198, 1116, 943 cm⁻¹; HRMS-ESI (*m/z*) [M+H] calcd for C₁₆H₂₈O₂, 253.2162; found: 253.2166.



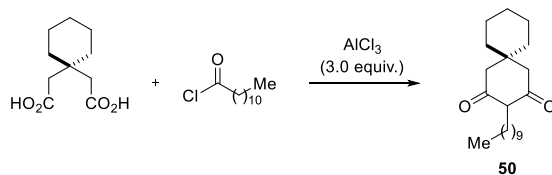
2-decyl-5-methylcyclohexane-1,3-dione (47) was heated for 5h and obtained as a white solid (0.327 g, 45% yield in MeNO₂). ¹H NMR (400 MHz, CD₃OD) δ 2.40 (d, *J* = 12.5 Hz, 2H), 2.16 (dt, *J* = 25.9, 8.8 Hz, 5H), 1.28 (d, *J* = 17.0 Hz, 16H), 1.04 (d, *J* = 4.6 Hz, 3H), 0.87 (dd, *J* = 6.8, 6.1 Hz, 3H); ¹³C NMR (100 MHz, CD₃OD) δ 115.3, 40.5, 31.7, 29.38, 29.34, 29.3, 29.1, 28.4, 28.3, 22.3, 21.2, 19.8, 13.1; IR (Neat): ν 2920, 2851, 1709, 1561, 1375, 1327, 1245, 1118cm⁻¹; HRMS-ESI (*m/z*) [M+H] calcd for C₁₇H₃₀O₂, 267.2319; found: 267.2317.



2-decyl-5,5-dimethylcyclohexane-1,3-dione (48) was heated for 5h and obtained as a white solid (0.379 g, 45% yield in MeNO₂). ¹H NMR (400 MHz, CD₃OD) δ 2.64 (s, 2H), 2.22 (dd, *J* = 15.8, 9.0 Hz, 2H), 1.28 (d, *J* = 16.1 Hz, 16H), 1.08 (s, 3H), 1.03 (s, 3H), 0.87 (t, *J* = 6.7 Hz, 1H); ¹³C NMR (100 MHz, CD₃OD) δ 167.1, 114.5, 42.6, 31.7, 31.5, 29.4, 29.31, 29.27, 29.25, 29.1, 28.8, 28.3, 27.1, 26.09, 22.3, 21.1, 13.04; IR (Neat): ν 2920, 2851, 1709, 1561, 1375, 1327, 1245, 1118 cm⁻¹; HRMS-ESI (*m/z*) [M+H] calcd for C₁₈H₃₂O₂, 281.2475; found: 281.2478.



2-decyl-5,5-dimethylcyclohexane-1,3-dione (49) was heated for 5h and obtained as a white solid (0.379 g, 43% yield in MeNO₂). ¹H NMR (400 MHz, CD₃OD) δ 2.61 (qd, *J* = 16.8, 3.1 Hz, 3H), 2.32 – 2.12 (m, 3H), 1.55 (s, 2H), 1.38 (dt, *J* = 7.2, 5.6 Hz, 2H), 1.25 (s, 16H), 0.98 (dd, *J* = 19.7, 3.1 Hz, 3H), 0.86 (d, *J* = 6.9 Hz, 6H); ¹³C NMR (100 MHz, CD₃OD) δ 177.6, 168.7, 116.0, 42.2, 35.7, 34.9, 34.7, 33.9, 33.14, 33.06, 30.7, 30.6, 30.5, 30.4, 30.2, 29.7, 26.1, 24.7, 24.2, 23.7, 22.5, 14.5, 8.4, 8.2; IR (Neat): ν 2916, 1812, 1763, 1382, 1186, 1073 cm⁻¹; HRMS-ESI (*m/z*) [M+H] calcd for C₁₉H₃₄O₂, 295.2632; found: 295.2636.

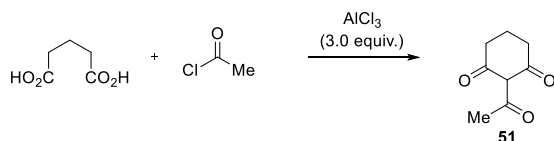


3-decylspiro[5.5]undecane-2,4-dione (50) was obtained as a white solid (0.422 g, 44% yield in MeNO₂). ¹H NMR (400 MHz, CD₃OD) δ 2.73 (s, 3H), 2.30 (dd, *J* = 22.1, 14.7 Hz, 2H), 1.65 – 1.42 (m, 11H), 1.31 (s, 16H), 0.91 (t, *J* = 6.4 Hz, 3H); ¹³C NMR (100 MHz, CD₃OD) δ 176.2, 167.1, 114.6, 40.4, 36.2, 35.4, 33.5, 31.8, 31.7, 29.3, 29.2, 29.1, 29.0, 28.8, 25.1, 24.7, 22.3, 21.3, 21.0, 13.1; IR (Neat): ν 2934, 1807, 1752, 1183, 1059, 950 cm⁻¹; HRMS-ESI (*m/z*) [M+H] calcd for C₂₁H₃₆O₂, 321.2788; found: 321.2790.

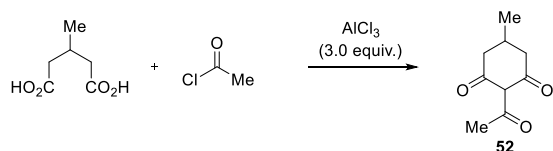
2.5.5 Synthesis of 2-acetyl-1,3-diones

General procedure for the synthesis of 2-acetyl-1,3-alkanediones: To a round bottom flask equipped with magnetic stir bar and reflux condenser was added AlCl₃ (9 mmol, 3 equiv) and MeNO₂ (0.25 M). Once AlCl₃ had dissolved, diacarboxylic acid (3 mmol, 1 equiv) was added and the solution was left to stir at room temperature for one hour. Then acetyl chloride (9 mmol, 3

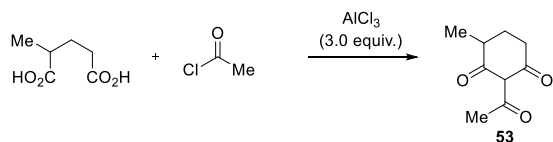
equiv) was introduced at room temperature. Flask was heated to 80 °C in an aluminum heating block for two hours. After cooling to room temperature, the reaction was poured into and Erlenmeyer flask containing 1:1 mixture saturated solution of Rochelle's salt and DCM (100 mL). After stirring for one hour, the layers were separated. The organic layer was dried over sodium sulfate, filtered, and concentrated to give the crude product, which was purified by flash chromatography (EtOAc/hexanes).



2-acetylcyclohexane-1,3-dione (51) was obtained as a white solid (338 mg, 73% yield). **¹H NMR** (400 MHz, CDCl₃) δ 18.13 (s, 1H), 2.66 (t, *J* = 6.4 Hz, 2H), 2.60 (s, 3H), 2.51 – 2.45 (m, 2H), 2.01 – 1.95 (m, 2H); **¹³C NMR** (100 MHz, CDCl₃) δ 203.2, 198.8, 195.5, 113.5, 77.5, 77.2, 76.8, 38.7, 33.4, 29.0, 19.1; **IR** (Neat): ν 2956, 1659, 1547, 1407, 1156, 1180, 1008, 841 cm⁻¹; **HRMS-ESI** (*m/z*) [M+H] calcd for C₈H₁₀O₃, 155.0702; found: 155.0703.

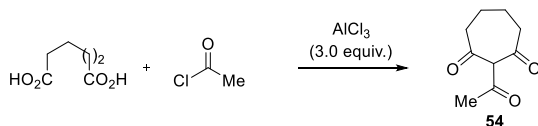


2-acetyl-5-methylcyclohexane-1,3-dione (52) was obtained as a white solid (328 mg, 65% yield). **¹H NMR** (400 MHz, CDCl₃) δ 17.91 (s, 1H), 2.67 (t, *J* = 6.4 Hz, 2H), 2.60 (t, *J* = 6.2 Hz, 2H), 2.37 (s, 3H), 1.88 – 1.83 (m, 4H); **¹³C NMR** (100 MHz, CDCl₃) δ 202.4, 198.9, 198.6, 116.8, 41.9, 36.8, 26.2, 22.0, 21.6; **IR** (Neat): ν 2940, 1664, 1558, 1418, 1216 cm⁻¹; **HRMS-ESI** (*m/z*) [M+H] calcd for C₉H₁₂O₃, 169.0865; found: 169.0864.

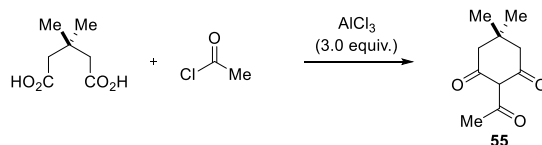


2-acetyl-4-methylcyclohexane-1,3-dione (53) was obtained as a white solid (328mg, 65% yield). **¹H NMR** (400 MHz, CDCl₃) δ 18.39 (s, 1H), 18.02 (s, 1H), 2.72 – 2.61 (m, 3H), 2.55 (d, *J* = 2.4 Hz, 6H), 2.45 – 2.29 (m, 2H), 2.09 – 1.96 (m, 2H), 1.73 – 1.61 (m, 2H), 1.27 (dd, *J* = 7.0, 2.2 Hz, 3H), 1.15 (dd, *J* = 6.8, 2.3 Hz, 3H); **¹³C NMR** (100 MHz, CDCl₃) δ 203.3, 202.8, 202.0, 198.0, 197.8, 195.6, 113.0, 112.6, 41.7, 37.7, 37.4, 32.4, 29.0, 28.6, 27.2, 27.0, 16.1, 15.6; **IR** (Neat): ν

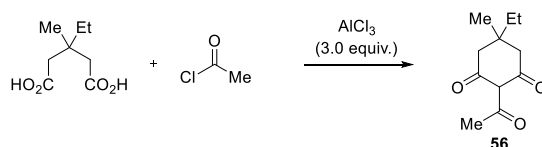
2932, 1664, 1548, 1438, 1222, 1027 cm^{-1} ; **HRMS**-ESI (m/z) [$M+H$] calcd for $\text{C}_9\text{H}_{12}\text{O}_3$, 169.0859; found: 169.0857.



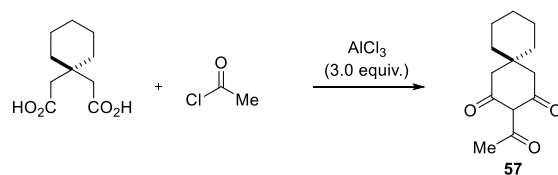
2-acetylcycloheptane-1,3-dione (54) was obtained as a white solid (319 mg, 63% yield). **^1H NMR** (400 MHz, CDCl_3) δ 18.39 (s, 1H), 18.02 (s, 1H), 2.72 – 2.61 (m, 3H), 2.55 (d, $J = 2.4$ Hz, 6H), 2.45 – 2.29 (m, 2H), 2.09 – 1.96 (m, 2H), 1.73 – 1.61 (m, 2H), 1.27 (dd, $J = 7.0, 2.2$ Hz, 3H), 1.15 (dd, $J = 6.8, 2.3$ Hz, 3H); **^{13}C NMR** (100 MHz, CDCl_3) δ 203.3, 202.8, 202.0, 198.0, 197.8, 195.6, 113.0, 112.6, 41.7, 37.7, 37.4, 32.4, 29.0, 28.6, 27.2, 27.0, 16.1, 15.6; **IR** (Neat): ν 2932, 1664, 1548, 1438, 1222, 1027 cm^{-1} ; **HRMS**-ESI (m/z) [$M+H$] calcd for $\text{C}_9\text{H}_{12}\text{O}_3$, 169.0859; found: 169.0857.



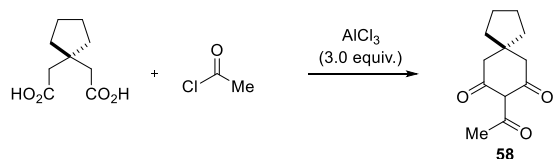
2-acetyl-5,5-dimethylcyclohexane-1,3-dione (55) was obtained as a white solid (361 mg, 66% yield). **^1H NMR** (400 MHz, CDCl_3) δ 18.06 (s, 1H), 2.56 (d, $J = 1.6$ Hz, 3H), 2.49 (s, 2H), 2.32 (s, 2H), 1.04 (s, 6H); **^{13}C NMR** (100 MHz, CDCl_3) δ 202.3, 197.8, 195.1, 112.3, 52.4, 46.8, 30.6, 28.5, 28.1; **IR** (Neat): ν 2958, 1664, 1553, 1442, 1048, 1046, 918 cm^{-1} ; **HRMS**-ESI (m/z) [$M+H$] calcd for $\text{C}_{10}\text{H}_{14}\text{O}_3$, 83.1016; found: 83.1015.



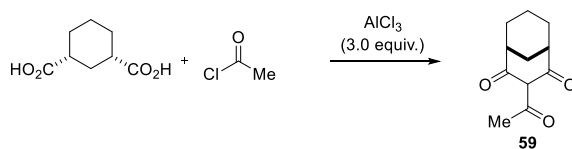
2-acetyl-5,5-ethylmethylcyclohexane-1,3-dione (56) was obtained as a white solid (377 mg, 64% yield). **^1H NMR** (400 MHz, CDCl_3) δ 18.09 (s, 1H), 2.59 (d, $J = 1.2$ Hz, 3H), 2.56 – 2.24 (m, 4H), 1.39 (q, $J = 7.5$ Hz, 2H), 1.00 (s, 3H), 0.87 (t, $J = 7.5$ Hz, 3H); **^{13}C NMR** (100 MHz, CDCl_3) δ 202.4, 198.2, 195.5, 112.7, 50.7, 45.2, 33.9, 33.5, 33.1, 28.6, 24.5, 8.1; **IR** (Neat): ν 2967, 1764, 1665, 1565, 1440, 1073, 943 cm^{-1} ; **HRMS**-ESI (m/z) [$M+H$] calcd for $\text{C}_{11}\text{H}_{16}\text{O}_3$, 197.1172; found: 197.1172.



3-acetylspiro[5.5]undecane-2,4-dione (57) was obtained as a white solid (367 mg, 55% yield). $^1\text{H NMR}$ (400 MHz, CDCl_3) δ 18.02 (s, 1H), 2.53 (s, 5H), 2.37 (s, 2H), 1.50 – 1.33 (m, 10H); $^{13}\text{C NMR}$ (100 MHz, CDCl_3) δ 202.1, 197.8, 195.1, 112.6, 50.3, 44.8, 36.5, 33.4, 28.4, 25.9, 21.5; **IR** (Neat): ν 2926, 2853, 1663, 1552, 1438, 1360, 1047, 942 cm^{-1} ; **HRMS-ESI** (m/z) [$\text{M}+\text{H}$] calcd for $\text{C}_{13}\text{H}_{18}\text{O}_3$, 223.1329; found: 223.1331.

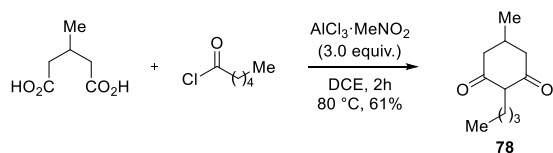


8-acetylspiro[4.5]decane-7,9-dione (58) was obtained as a white solid (344 mg, 55% yield). $^1\text{H NMR}$ (400 MHz, CDCl_3) δ 18.10 (s, 1H), 2.62 (s, 2H), 2.60 (s, 3H), 2.45 (s, 2H), 1.72 – 1.66 (m, 4H), 1.50 (td, $J = 6.7, 3.8$ Hz, 4H); $^{13}\text{C NMR}$ (100 MHz, CDCl_3) δ 202.7, 198.4, 195.5, 112.9, 51.0, 45.7, 42.3, 41.3, 38.2, 37.7, 28.7, 24.3; **IR** (Neat): ν 2951, 2876, 1767, 1664, 1558, 1441, 1044, 952 cm^{-1} ; **HRMS-ESI** (m/z) [$\text{M}+\text{H}$] calcd for $\text{C}_{12}\text{H}_{16}\text{O}_3$, 209.1172; found: 209.1170.



3-acetylbicyclo[3.3.1]nonane-2,4-dione (59) was obtained as a white solid (355 mg, 61% yield). $^1\text{H NMR}$ (400 MHz, CDCl_3) δ 18.09 (s, 1H), 2.75 (s, 1H), 2.61 (s, 3H), 2.57 (s, 1H), 2.19 (d, $J = 13.0$ Hz, 1H), 1.89 (t, $J = 12.4$ Hz, 2H), 1.73 (dd, $J = 16.9, 8.7$ Hz, 2H), 1.65 – 1.55 (m, 2H), 1.43 (ddd, $J = 14.0, 10.0, 4.9$ Hz, 1H); $^{13}\text{C NMR}$ (100 MHz, CDCl_3) δ 202.4, 201.4, 198.8, 115.3, 43.3, 38.9, 30.4, 28.9, 28.6, 27.8, 19.0; **IR** (Neat): ν 2932, 1663, 1548, 1434, 1253, 1008, 861 cm^{-1} ; **HRMS-ESI** (m/z) [$\text{M}+\text{H}$] calcd for $\text{C}_{11}\text{H}_{14}\text{O}_3$, 195.1016; found: 195.1013.

2.5.6 Synthesis of Chiloglottone 3 (78)



To a 25 mL round bottom flask equipped with magnetic stir bar and reflux condenser was added AlCl_3 (9 mmol, 3 eq.), MeNO_2 (9 mmol, 3 eq.) and 1,2-DCE (0.25 M). To this solution was then added diacarboxylic acid (3 mmol, 1 eq.) and left to stir at room temperature for one hour. Then propionyl chloride (9 mmol, 3 eq.) was introduced at room temperature. Flask was heated to 80 °C in an aluminum heating block for three hours. After cooling to room temperature, the reaction was poured into an Erlenmeyer flask containing 1:1 mixture saturated solution of Rochelle's salt and DCM (100 mL). After stirring for one hour, the layers were separated. The organic layer was dried over sodium sulfate, filtered, and concentrated to give the crude product, which was purified by flash chromatography (EtOAc/hexanes) to provide **78** (0.333 g, 61%) as a white solid. **^1H NMR** (400 MHz, CD_3OD) δ 2.39-2.36 (d, $J = 12$, 2H), 2.20-2.16 (t, $J = 8$, 2H), 2.10-2.08 (m, 3H), 1.24-1.23 (m, 4H), 1.02-1.01 (m, 3H), 0.86-0.83 (t, $J = 8$ Hz, 3H). **^{13}C NMR** (100 MHz, CD_3OD) δ 116.7, 42.0, 32.0, 29.8, 23.8, 22.4, 21.2, 14.5. **IR** (Neat): ν 2956, 1705, 1562, 1376, 1242, 1115, 1000, 1072, 884 cm^{-1} ; **HRMS-ESI** (m/z) $[\text{M}+\text{H}]$ calcd for $\text{C}_{12}\text{H}_{18}\text{O}_2$, 183.1383; found: 183.1384.

2.6 References

- (1) a) Thompson, R.B. *Org. Synth.* **1947**, *27*, 21; b) Orchin, M.; Butz, L.W. *J. Am. Chem. Soc.* **1943**, *65*, 2296; c) Grenda, V.J.; Lindberg, G.W.; Wendler, N.L.; Pines, S.H. *J. Org. Chem.* **1967**, *32*, 1236; d) John, J.P.; Swaminathan, S.; Venkataramani, P.S. *Org. Synth.* **1967**, *47*, 83; e) Hengartner, U.; Chu, V. *Org. Synth. Coll.* **1978**, *58*, 83.
- (2) Ramachary, D.B.; Reddy, Y.V.; Kishor, M. *Org. Biomol. Chem.*, **2008**, *6*, 477.
- (3) a) Schick, H.; Lehmann, G.; Hilgetag, G. *Chem. Ber.* **1969**, *102*, 3238; b) Schick, H.; Lehmann, G.; Hilgetag, G. *Angew. Chem. Int. Ed.* **1967**, *6*, 371; c) Schick, H.; Lehmann, G.; Hilgetag, G. *Angew. Chem. Int. Ed.* **1967**, *6*, 80; d) Schick, H.; Lehmann, G.; Hilgetag, G. *Chem. Ber.* **1967**, *100*, 2973; For a review of the synthesis of 2-alkyl-1,3-diones from dicarboxylic acids and their derivatives, see: Schick, H.; Eichhorn, I. *Synthesis* **1989**, 477.
- (4) Matoba, K.; Tachi, M.; Itooka, T.; Yamazaki, T. *Chem. Pharm.Bull.* **1986**, *34*, 2007.
- (5) a) Hanessian, S.; Auzzas, L. *Org. Lett.* **2008**, *10*, 261; b) Chow, S.; Kreß, C.; Albæk, N.; Jessen, C.; Williams, C.M. *Org. Lett.* **2011**, *13*, 5286; c) Lopchuk, J.M.; Green, I.L.; Badenock, J.C.; Gribble, G.W. *Org. Lett.* **2013**, *15*, 4485; d) Kita, Y.; Futamura, J.; Ohba, Y.; Sawama, Y.; Ganesh, J.K.; Fujioka, H. *J. Org. Chem.* **2003**, *68*, 5917; e) Jhuo, D.-H.; Hong, B.-C.; Chang, C.-W.; Lee, G.-H. *Org. Lett.* **2014**, *16*, 2724; f) Andrä, M.S.; Tzschucke, C.C. *Eur. J. Org. Chem.* **2014**, 7265.
- (6) Sekhar, B.C. *J. Heterocyclic Chem.* **2004**, *41*, 807.
- (7) Wieland, P.; Miescher, K. *Helv. Chim. Acta* **1950**, *33*, 2215.
- (8) Hajos, Z.G.; Parrish, D.R. *J. Org. Chem.* **1974**, *39*, 1615-1621.
- (9) a) Paquette, L.A.; Wang, T.-Z.; Philippo, C.M.G.; Wang, S. *J. Am. Chem. Soc.* **1994**, *116*, 3367; b) Smith, A.B.; Kingery-Wood, J.; Leenay, T.L.; Nolen, E.G.; Sunazuka, T. *J. Am. Chem. Soc.* **1992**, *114*, 1438; c) Stahl, P.; Kissau, L.; Mazitschek, R.; Huwe, A.; Furet, P.; Giannis, A.; Waldmann, H. *J. Am. Chem. Soc.* **2001**, *123*, 11586; d) Waters, S.P.; Tian, Y.; Li, Y.-M.; Danishefsky, S.J. *J. Am. Chem. Soc.* **2005**, *127*, 13514; e) Lee, H.M.; Nieto-Oberhuber, C.; Shair, M.D. *J. Am. Chem. Soc.* **2008**, *130*, 16864. f) Hajos, Z.G. Parrish, D.R. *J. Org. Chem.* **1973**, *38*, 3239.
- (10) a) Sharpe, R.J.; Johnson, J.S. *J. Am. Chem. Soc.* **2015**, *137*, 4968; b) Breitler, S.; Carreira, E.M. *Angew. Chem. Int. Ed.* **2013**, *52*, 11168; c) Liu, L.L.; Chiu, P. *Chem. Commun.* **2011**, *47*, 3416; d) Yeung, Y.-Y.; Chein, R.-J.; Corey, E.J. *J. Am. Chem. Soc.* **2007**, *129*, 10346; e)

- Watannabe, H.; Iwamoto, M.; Nakada, M. *J. Org. Chem.* **2005**, *70*, 4652; f) Katoh, T.; Mizumoto, S.; Fudesaka, M.; Nakashima, Y.; Kajimoto, T.; Node, M. *Synlett* **2006**, 2176; g) Fujieda, S.; Tomita, M.; Fuhshuku, K.; Ohba, S.; Nishiyama, S.; Sugai, T. *Adv. Synth. Catal.* **2005**, *347*, 1099; h) Katoh, T.; Mizumoto, S.; Fudesaka, M.; Takeo, M.; Kajimoto, T.; Node, M. *Tetrahedron: Asymmetry* **2006**, *17*, 1655.
- (11) Olah, G.A.; Kobayashi, S.; Tashiro, M. *J. Am. Chem. Soc.* **1972**, *94*, 7448.
- (12) Sartori, G.; Bigi, F.; Baraldi, D.; Maggi, R.; Casnati, G.; Tao, X. *Synthesis* **1993**, 851-852.
- (13) a) Pines, S.H.; Douglas, A.W. *J. Org. Chem.* **1978**, *43*, 3126; b) Olah, G.A.; Kuhn, S.J.; Flood, S.H. *J. Am. Chem. Soc.* **1962**, *84*, 1688-1695; c) Schmerling, L. *Ind. Eng. Chem.* **1948**, *40*, 2072-2077
- (14) a) Potapovich, M.V.; Eremin, A.N.; Rubinov, D.B.; Metelitz, D.I. *Appl. Biochem. Microbiol.* **2008**, *44*, 19-27. b) Chabbert, T.A.; Scavizzi, M.R. *Antimicrob. Agents Chemother.* **1976**, *9*, 36-41. c) Chu, D.T.W.; Bernstein, E.; Huckin, S.N. *Can. J. Chem.* **1978**, *56*, 1059-1062. d) Safak, B.; Ciftci, I.H.; Ozedemir, M.; Kiyildi, N.; Cetinkaya, Z.; Aktepe, O.C.; Altindis, M. *Phytother. Res.* **2009**, *23*, 955-957. e) For a review, see: Rubinov, D.B.; Rubinova, I.L.; Akhrem, A.A. *Chem. Rev.* **1999**, *99*, 1047-1066.
- (15) a) Lim, S.; Min, Y.; Choi, B.; Kim, D.; Lee, S.S.; Lee, I.M. *Tet. Lett.* **2001**, *42*, 7645-7649. b) Skarzewski, J. *Tetrahedron* **1989**, *45*, 4593-4598. c) Jung, J.C.; Watkins, E.B.; Avery, M.A. *Synth. Comm.* **2002**, *32*, 3767-3777.
- (16) a) Tabuchi, H.; Hamamoto, T.; Ichihara, A. *Synlett* **1993**, 651-652. b) Isobe, T. *J. Org. Chem.* **1999**, *64*, 6984-6988. c) Shen, Q.; Huang, W.; Wang, J.; Zhou, X. *Org. Lett.* **2007**, *9*, 4491-4494.
- (17) Schiestl, F.P.; Peakall, R.; Mant, J.G.; Ibarra, F.; Schulz, C.; Franke, S.; Francke, W. *Science* **2003**, *302*, 437.
- (18) Poldy, J.; Peakall, R.; Barrow, R.A. *Tetrahedron Lett.* **2008**, *49*, 2446.
- a) Franke, S.; Ibarra, F.; Schulz, C.M.; Twele, R.; Poldy, J.; Barrow, R.A.; Peakall, R.; Schiestl, F.P.; Francke, W. *P. Natl. Acad. Sci. USA* **2009**, *106*, 8877; b) Poldy, J.; Peakall, R.; Barrow, R.A. *Org. Biomol. Chem.* **2009**, *7*, 4296; c) Madhavachary, R.; Ramachary, D.B. *Eur. J. Org. Chem.* **2014**, 7317.

*Adapted with permission from Ahlam M. Armaly, Sukanta Bar, Corinna S. Schindler, *Org.*

Lett. **2017**, *19*, 3958-3961. Copyright 2017 American Chemical Society.

Chapter 3 Acid Chlorides as Formal Carbon Dianion Linchpin Reagents in the Aluminum Chloride-Mediated Dieckmann Cyclization of Dicarboxylic Acids

3.1 Introduction

During our investigations of the aluminum chloride-mediated Dieckmann cyclization of dicarboxylic acids we found that an $\text{AlCl}_3 \cdot \text{MeNO}_2$ complex was better suited for more complex dicarboxylic acid and higher order acid chloride substrates.¹ Using this method, we could access 2-alkyl-1,3-diones (**1**) from readily available dicarboxylic acid and acid chloride substrates (**2**). We also extended this method to the synthesis of 2-acyl-1,3-diones (**5**) when acetyl chloride (**4**) was used as the acid chloride of choice. This dichotomous reactivity is summarized in Figure 3.1.

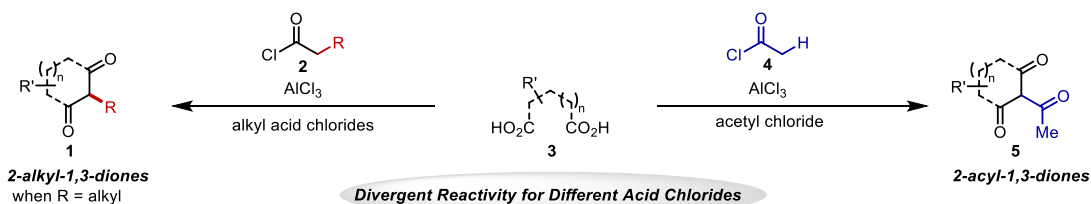


Figure 3.14 Divergent reactivity leading to 2-alkyl-1,3-diones or 2-acyl-1,3-diones based on choice of acid chloride

In order to assess the viability of this approach for the synthesis of atropurpuran and the arcutines, we investigated the viability of β -substituted acid chloride **7** in this transformation (Figure 3.2). Not only were these substrates poorly tolerated in the reaction, but they gave an unexpected result; rather than providing the desired 2-alkyl-1,3-dione **8** we isolated a 2-acyl-1,3-dione **9**. Unlike the case of acetyl chloride **4** (Figure 3.1), it was unclear how these compounds were forming due to what seemed to be an extra carbon at 2-position. We could not discern whether or not the enhanced steric bulk in these substrates prohibited the desired reactivity required to form 2-alkyl-1,3-diones **8** and led to an alternate mode of reactivity to provide 2-acyl-1,3-dione **9**.

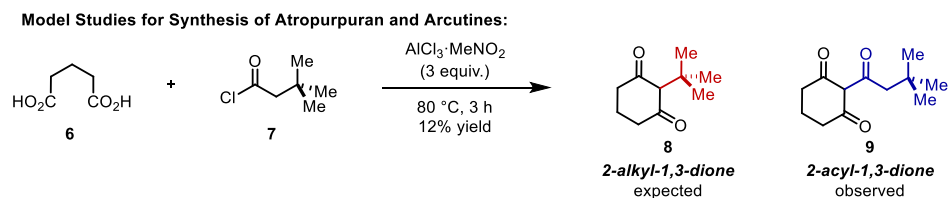


Figure 15 Unexpected isolation of 2-acyl-1,3-dione with 3,3-dimethyl butyryl chloride (**7**)

3.2 Results and Discussion

Shick et al. had previously proposed a mechanism² for the Dieckmann cyclization of dicarboxylic acids and acid chlorides that was further explained by Ivanov et al. (Figure 3.3). The mechanism proceeds via initial Friedel-Crafts-like acylation of the dicarboxylic acid **10** with the acid chloride to provide β -ketoacid **11**. Decarboxylation of **11** results in loss of the carbonyl of the original dicarboxylic acid **10** to ultimately provide **12**. The new ketoacid **12** can then undergo Lewis acid-mediated Dieckmann cyclization via intermediate enol **13** to give **14**. However, this was only a proposed mechanism and no mechanistic investigations regarding this transformation had been conducted. As such, we initiated ^{13}C -labelling studies in order to elucidate the controlling features of this transformation and assess its viability in our synthesis of atropurpuran and the arcutines.

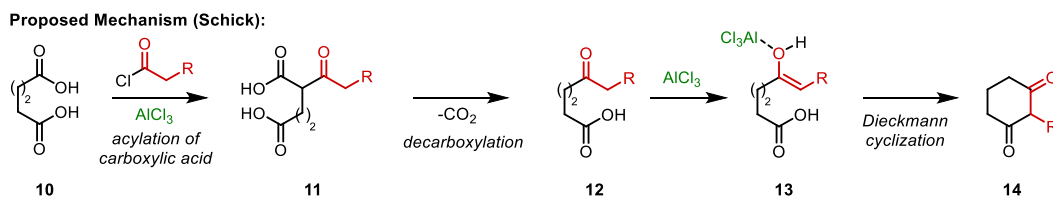


Figure 3.16 Previously proposed mechanism by Schick et al.

3.3 Mechanistic Investigations

In order to gain experimental support for this mechanism, we conducted ^{13}C -labeling experiments (Figure 3.4). When ^{13}C -labeled propionyl chloride **16** was subjected to the reaction conditions with glutaric acid **15**, we obtained dione **17** that did not contain an ^{13}C -incorporation. The lack of incorporation of the ^{13}C -labeled carbonyl of propionyl chloride implies that the mechanism of the reaction differs from what was previously proposed by Schick et al. Specifically, the previously reported mechanistic hypothesis suggested decarboxylation of one of the acid moieties of the dicarboxylic acid to allow for complete inclusion of the acid chloride fragment in the final product, which would result in **18** as the expected product. We then evaluated a fully ^{13}C -labeled propionyl chloride **19** with glutaric acid **15** and found that the product **20** again maintained

both carbonyls of glutaric acid **15** and only incorporated ^{13}C at the 2- and 3'-positions. The sole incorporation of the alkyl component of the ^{13}C -labeled acid chloride (and no carbonyl incorporation) suggested that the acid chloride was serving as carbon dianion linchpin reagent in the AlCl_3 -mediated Dieckmann cyclization of dicarboxylic acids. Linchpin reagents present two sites of reactivity that enable the formation of two new C–C bonds.^{4,5} Furthermore, these studies establish acid chloride linchpin reagents to previously developed linchpin strategies towards carbonyls.⁶

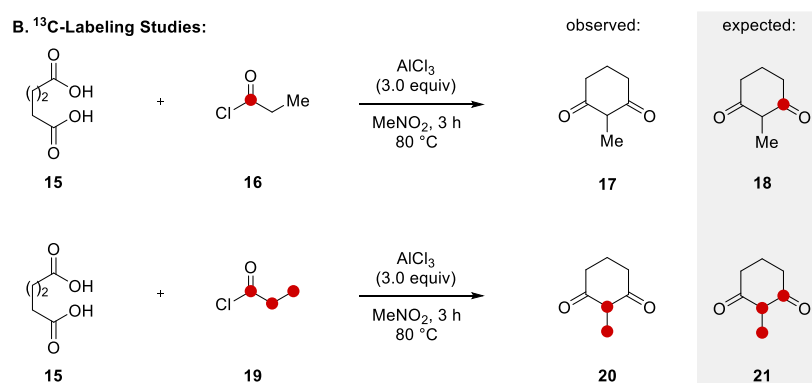


Figure 3.17 ^{13}C -labelling studies of 2-alkyl-1,3-diones

We also conducted ^{13}C -labelling studies with acetyl chloride to determine mechanism for the formation of the 2-acetyl-1,3-diones proceeded in a similar fashion to the 2-alkyl-1,3-diones (Figure 3.5). We were particularly interested in determining the origin of the carbon at the 2-position. If the 2-acetyl-1,3-diones resulted from an alternative mechanism, we suspected that the carbon from the nitromethane could get incorporated into the final products (**9** in Figure 3.2 and **24** in Figure 3.5). When we subjected glutaric acid **15** with ^{13}C -labelled MeNO_2 we found no ^{13}C -incorporation in the isolated product **23**. We then turned to ^{13}C -labelled acetyl chloride substrates **25** and **28** to help elucidate the mechanism. When ^{13}C -labelled acetyl chloride **25** was subjected to the reaction conditions with glutaric acid **15** we only observed ^{13}C -incorporation at the 3'-position and did not observe any ^{13}C -incorporation at the carbonyls of the cyclic 1,3-dione in **26**. The use of ^{13}C -labelled substrates also allowed us to determine the origin of the carbon at the 2-position by using ^{13}C -labelled acetyl chloride **28**. Altogether these studies revealed that the

formation of 2-acetyl- and 2-alkyl-1,3-diones proceed via a similar mechanism as in the case of propionyl chloride (Figure 3.5) and that the previously proposed mechanism by Shick et al.² does not account for the mechanistic observations (Figure 3.5).

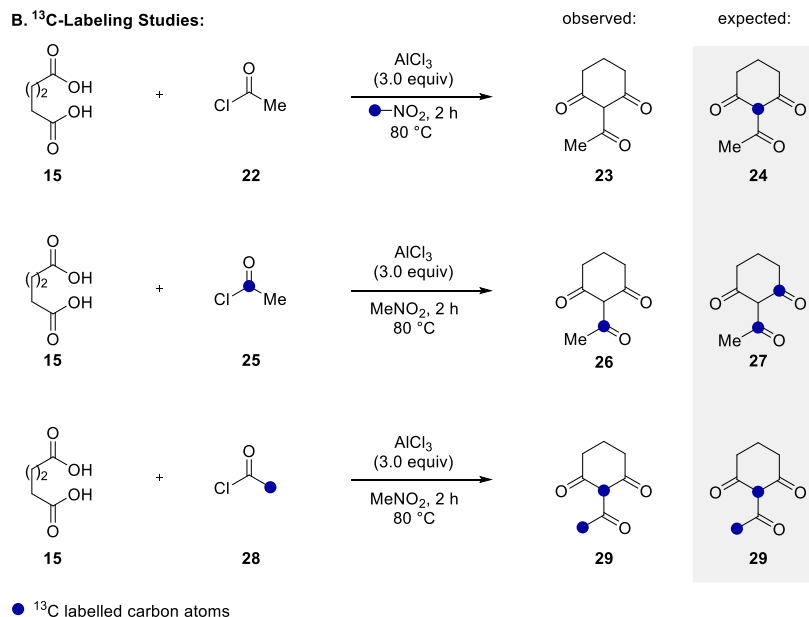


Figure 3.5 ¹³C-labelling studies of 2-acetyl-1,3-diones

Based on our ¹³C-labelling studies, we propose an alternative mechanistic hypothesis for the AlCl₃-mediated Dieckmann cyclization of dicarboxylic acids (Figure 3.6). Our proposal is primarily guided by mechanistic observations where the carbonyl of the acid chloride is not observed in the final product, suggesting that it must be lost during a decarboxylation event. As such, our proposed mechanism starts with acylation of the dicarboxylic acid **15** with one equivalent of acid chloride **30** to provide the corresponding-mixed anhydride **31**. This mixed anhydride **31** undergoes Lewis acid-mediated condensation to the symmetrical anhydride **33** upon the extrusion of **32**. The activated enol **32** subsequently cleaves anhydride **33**, which results in the formation of keto acid **34** that can then undergo decarboxylation to form enol **35**. Activation of **35** with either the Lewis acid or an equivalent of acid chloride **30** induces final condensation to yield Dieckmann cyclization product **36**. Importantly, this revised reaction mechanism accounts for both carbonyl subunits of the dicarboxylic acid being transferred to the corresponding cyclization products and confirms the role of acid chlorides as formal carbon dianion linchpin reagents.

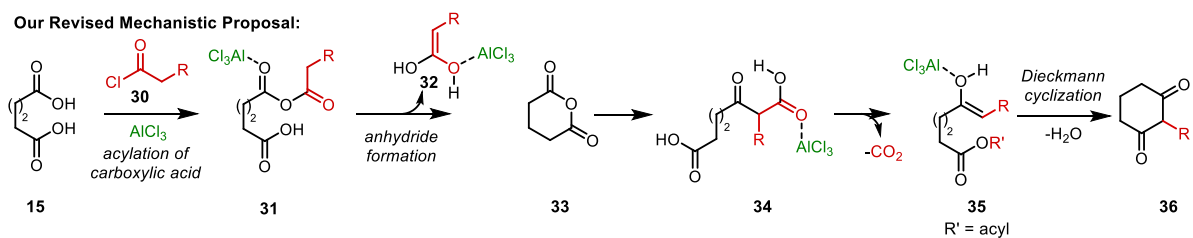


Figure 3.6 Our revised reaction mechanism for the AlCl_3 -mediated Dieckmann cyclization of dicarboxylic acids

Our revised mechanistic proposal explains the requirement of super-stoichiometric amounts of acid chloride that ultimately serves as a linchpin reagent and also demonstrates two distinct roles of the acid chloride – only one equivalent is ultimately incorporated in the final product **40** and serves as a linchpin **37** whereas the other two equivalents **39** are required to induce cyclization (Figure 3.6A). In order to gain further support for our mechanistic proposal, we investigated the use of a sacrificial acylating agent to help promote the cyclization of intermediate keto acid **38** (Figure 3.6B). Specifically, when one equivalent of propionyl chloride **42** was used in the Dieckmann cyclization of *cis*-1,3-cyclohexanedicarboxylic acid **41** followed by two equivalents of acetyl chloride as a sacrificial acylating agent, the corresponding 1,3-dione **43** is formed in 58% yield. Alternatively, when this same transformation is conducted without the addition of 2 equivalents of acetyl chloride the desired 2-alkyl-1,3-dione **43** is produced in diminished yields (28% yield). These studies provide additional support for our revised mechanistic hypothesis for the AlCl_3 -mediated Dieckmann cyclization of dicarboxylic acids and justify the requirements of super-stoichiometric amounts of acid chloride in the transformation.

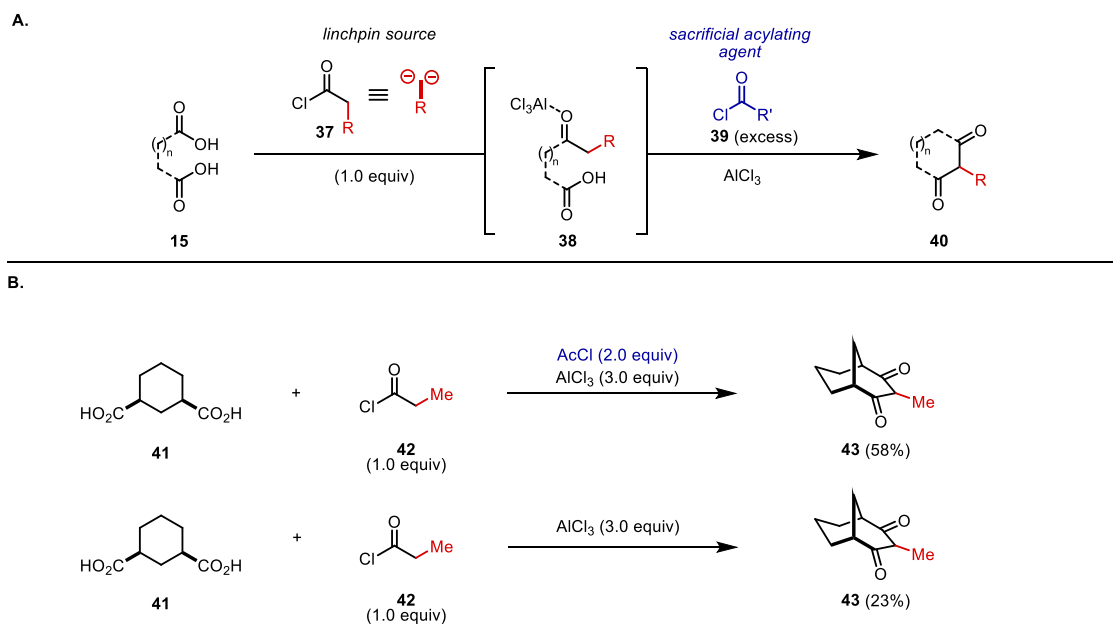


Figure 3.6 A) The use of a sacrificial acylating agent to induce cyclization after linchpin incorporation; B) Experimental probe of dual role of acid chlorides as linchpin reagents and acylating agents

Importantly, our mechanistic investigations provided us with a reasonable explanation for the unexpected formation of 2-acyl-1,3-dione **9** with β -substituted acid chloride **7** (Figure 3.7). Because we did not observe any incorporation of the solvent in the final products, we suspected that all of the 2-acyl-1,3-dione products **45** arose from a similar mechanism – through acylation of an unsubstituted 1,3-dione **44**. In the case of acetyl chloride, the AlCl_3 -Dieckmann cyclization of dicarboxylic acids would provide the unsubstituted 1,3-cyclohexane dione **44** as the product. However, this product **44** rapidly undergoes a subsequent acylation under the superstoichiometric amounts of Lewis acid and acetyl chloride to provide the 2-acyl-1,3-dione **45** ($\text{R} = \text{H}$). In a similar fashion, β -substituted acid chlorides should readily undergo AlCl_3 -mediated Dieckmann cyclization to give rise to 2-alkyl-1,3-diones such as **46**. However, dione **46** as well as any 2-alkyl-1,3-dione bearing any substitution at the β -position succumb to Lewis acid-mediated retro-ene cleavage to give rise to unsubstituted dione **44**. Dione **44** similarly undergoes a second acylation to provide the 2-acyl-1,3-dione **45** ($\text{R} = \text{tbutyl}$). It is important to note that this alternative mode of reactivity is only observed for acetyl chloride and β -substituted acid chlorides that are capable of forming unsubstituted cyclic 1,3-diones under the reaction conditions. Dieckmann cyclization

products arising from *n*-alkyl acid chlorides do not undergo the Lewis acid-mediated fragmentation pathway to unsubstituted 1,3-diones due to lack of carbocation stabilization.

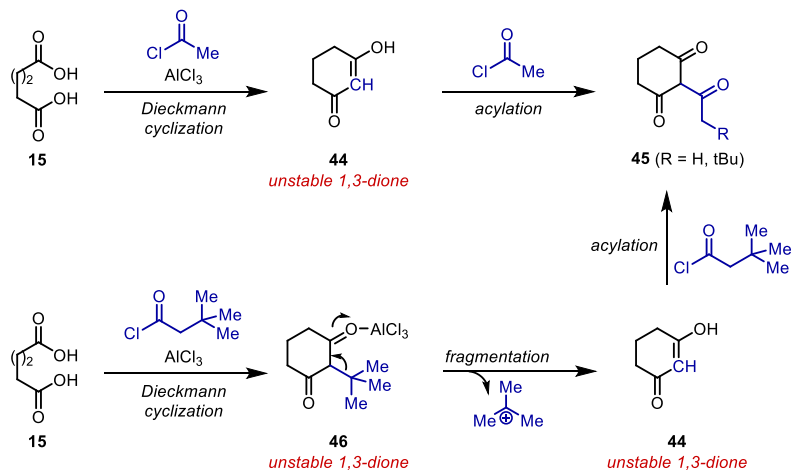


Figure 3.718 Our mechanistic hypothesis that accounts for the formation of 2-acyl-1,3-diones with β -substituted acid chlorides

3.4 Conclusion

Based on mechanistic investigations relying on ^{13}C -labeling experiments, we propose a revised reaction mechanism for the aluminum(III)-mediated Dieckmann-cyclization of dicarboxylic acids with acid chlorides. Our revised mechanistic hypothesis establishes acid chlorides as formal carbon dianion linchpin reagents. These linchpin reagents present two sites of reactivity that enable the formation of two new C–C bonds and ultimately are responsible for the one-step approach to cyclic 2-alkyl-1,3-diones from acyclic starting materials. Experiments based on sacrificial acylating reagents provide additional support for this revised reaction mechanism that affirm the requirement for super-stoichiometric amounts of acid chloride despite incorporation of only one equivalent of acid chloride into the corresponding products.

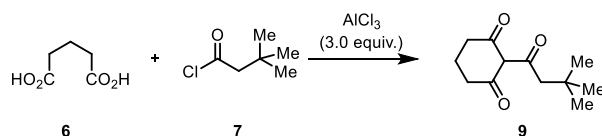
3.5 Experimental Details

3.5.1 General Information

Unless otherwise noted, all reactions were performed in oven-dried glassware under an atmosphere of nitrogen. All chemicals were purchased from commercial suppliers and were used without further purification. Anhydrous nitromethane (MeNO_2) and anhydrous 1,2-dichloroethane (DCE) were obtained from Acros Organics and were used as received. Flash chromatography was performed using Biotage Isolera One ACI™ Accelerated Chromatography Isolation system on

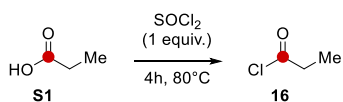
Silicycle Silia Flash[®] 40-63 micron (230-400 mesh). Proton Nuclear Magnetic Resonance NMR (¹H NMR) spectra and carbon nuclear magnetic resonance (¹³C NMR) spectra were recorded on a Varian Unity Plus 400, Varian MR400, Varian vnmrs 500, Varian Inova 500, Varian Mercury 500, and Varian vnmrs 700 spectrometers. Chemical shifts for protons are reported in parts per million and are referenced to the NMR solvent peak (CDCl₃: δ 7.26; CD₃OD: δ 4.87). Chemical shifts for carbons are reported in parts per million and are referenced to the carbon resonances of the NMR solvent (CDCl₃: δ 77.16; CD₃OD: δ 49.00). Data are represented as follows: chemical shift, integration, multiplicity (br = broad, s = singlet, d = doublet, t = triplet, q = quartet, p = pentet, m = multiplet), and coupling constants in Hertz (Hz). Mass spectroscopic (MS) data was recorded at the Mass Spectrometry Facility at the Department of Chemistry of the University of Michigan in Ann Arbor, MI on an Agilent Q-TOF HPLC-MS with ESI high resolution mass spectrometer. Infrared (IR) spectra were obtained using either an Avatar 360 FT-IR or Perkin Elmer Spectrum BX FT-IR spectrometer. IR data are represented as frequency of absorption (cm⁻¹).

3.5.2 Isolation of 2-(3,3-dimethylbutanoyl)cyclohexane-1,3-dione (**9**)

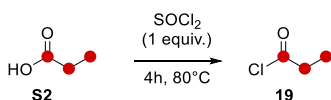


2-(3,3-dimethylbutanoyl)cyclohexane-1,3-dione (9**):** To a round bottom flask equipped with magnetic stir bar and reflux condenser was added AlCl₃ (9 mmol, 3 equiv) and MeNO₂ (0.25 M). Once AlCl₃ had dissolved, glutaric acid **6** (3 mmol, 1 equiv) was added and the solution was left to stir at room temperature for one hour. Then 3,3-dimethyl butyryl chloride **7** (9 mmol, 3 equiv) was introduced at room temperature. Flask was heated to 80 °C in an aluminum heating block for two hours. After cooling to room temperature, the reaction was poured into and Erlenmeyer flask containing 1:1 mixture saturated solution of Rochelle's salt and DCM (100 mL). After stirring for one hour, the layers were separated. The organic layer was dried over sodium sulfate, filtered, and concentrated to give the crude product, which was purified by flash chromatography (EtOAc/hexanes) to provide **9** as a brown oil (76 mg, 12% yield). ¹H NMR (400 MHz, CDCl₃) δ 18.49 (s, 1H), 3.05 (s, 2H), 2.65 (t, *J* = 6.4 Hz, 2H), 2.47 (t, *J* = 6.9 Hz, 2H), 1.96 (m, 2H), 1.03 (s, 9H); ¹³C NMR (126 MHz, CDCl₃) δ 205.2, 199.4, 195.5, 114.5, 50.3, 39.3, 34.0, 32.8, 30.1, 19.0; IR (Neat): ν 2953m 1664, 1544, 1462, 1410, 1364, 1221, 1072, 1012; HRMS-ESI (*m/z*) [M+H] calcd for C₁₂H₁₈O₃, 211.1329; found: 211.1311.

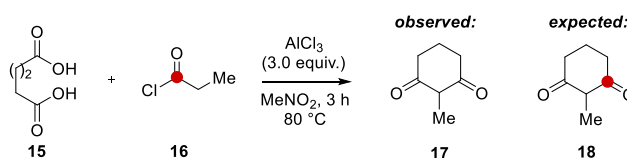
3.5.3 ¹³C-Labeling Experiments



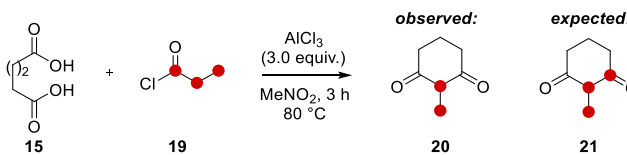
Propionyl Chloride-1-¹³C (18): To a 10 mL round bottom flask equipped with reflux condenser and magnetic stir bar was added **S1** (13.5 mmol, 1 eq.) and SOCl₂ (13.5 mmol, 1 eq). Flask was heated to 80 °C in an aluminum heating block for four hours. Once reaction had cooled, acid chloride **18** was instantly employed in the Dieckmann cyclization reaction.



Propionyl Chloride-¹³C₃ (21): To a 10 mL round bottom flask equipped with reflux condenser and magnetic stir bar was added **S2** (13.5 mmol, 1 eq.) and SOCl₂ (13.5 mmol, 1 eq). Flask was heated to 80 °C in an aluminum heating block for four hours. Once reaction had cooled, acid chloride **21** was instantly employed in the Dieckmann cyclization reaction.

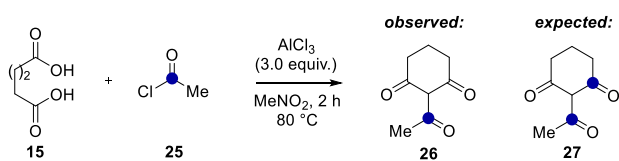


2-methylcyclohexane-1,3-dione (19): In an oven dried round bottomed flask equipped with reflux condenser and stir bar was added AlCl₃ (11.35 mmol, 3 equiv) and MeNO₂ (15 mL, 0.25 M). Once AlCl₃ had dissolved, **10** (3.79 mmol, 1 equiv) was added and the solution was left to stir at room temperature for one hour. Then **18** (11.35 mmol, 3 equiv) was added and flask was heated to 80 °C in an aluminum heating block for two hours. The solution was then poured into an Erlenmeyer flask containing a 1:1 mixture saturated solution of Rochelle's salt and DCM (100 mL). After stirring for one hour, the layers were separated. The organic layer was dried over sodium sulfate, filtered, and concentrated to give the crude product **19**, which was purified by flash chromatography (EtOAc/hexanes).

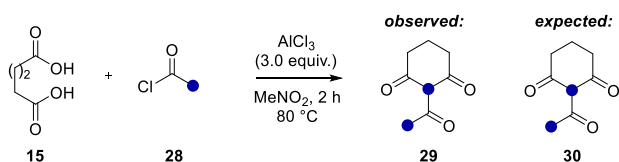


2-methyl-¹³C-cyclohexane-1,3-dione-1-¹³C (20): In an oven dried round bottomed flask equipped with reflux condenser and stir bar was added AlCl₃ (11.35 mmol, 3 equiv) and MeNO₂ (15 mL,

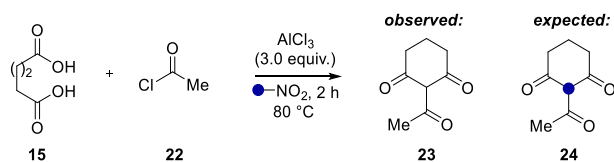
0.25 M). Once AlCl_3 had dissolved, **10** (3.79 mmol, 1 equiv) was added and the solution was left to stir at room temperature for one hour. Then **21** (11.35 mmol, 3 equiv) was added and flask was heated to 80 °C in an aluminum heating block for two hours. The solution was then poured into an Erlenmeyer flask containing 1:1 mixture saturated solution of Rochelle's salt and DCM (100 mL). After stirring for one hour, the layers were separated. The organic layer was dried over sodium sulfate, filtered, and concentrated to give the crude product **20**, which was purified by flash chromatography (EtOAc/hexanes). $^1\text{H NMR}$ (500 MHz, CD_3OD) δ 2.36 (t, $J = 5.0$ Hz, 4H), 1.89 (p, $J = 5.0$ Hz, 2H), 1.74 – 1.47 (dd, $J = 130, 5.0$ Hz, 3H); $^{13}\text{C NMR}$ (125 MHz, CD_3OD) δ 112.1 (d, $J = 135$), 22.0, 7.31 (d, $J = 185$); **HRMS-ESI** (m/z) [$\text{M}+\text{H}$] calcd for $\text{C}_5^{13}\text{C}_2\text{H}_9\text{O}_2$, 127.0670; found: 127.0671.



2-(acetyl-1- ^{13}C)cyclohexane-1,3-dione (26): In an oven dried round bottomed flask equipped with reflux condenser and stir bar was added AlCl_3 (11.35 mmol, 3 equiv) and MeNO_2 (15 mL, 0.25 M). Once AlCl_3 had dissolved, **15** (3.79 mmol, 1 equiv) was added and the solution was left to stir at room temperature for one hour. Then **25** (11.35 mmol, 3 equiv) was added and flask was heated to 80 °C in an aluminum heating block for two hours. The solution was then poured into an Erlenmeyer flask containing 1:1 mixture saturated solution of Rochelle's salt and DCM (100 mL). After stirring for one hour, the layers were separated. The organic layer was dried over sodium sulfate, filtered, and concentrated to give the crude product **26**, which was purified by flash chromatography (EtOAc/hexanes). $^1\text{H NMR}$ (400 MHz, CDCl_3) δ 18.17 – 17.90 (m, 1H), 2.64 (dd, $J = 12.0, 5.7$ Hz, 2H), 2.59 – 2.53 (m, 3H), 2.46 (dd, $J = 12.8, 5.9$ Hz, 2H), 1.99 – 1.90 (m, 2H); $^{13}\text{C NMR}$ (100 MHz, CDCl_3) δ 203.5, 203.4, 203.2, 203.0, 202.9, 198.8, 195.5, 195.4, 113.8, 113.2, 77.5, 77.2, 76.9, 38.7, 38.7, 33.3, 29.1, 28.7, 19.1; **IR** (Neat): ν 2956, 1659, 1547, 1407, 1156, 1180, 1008, 841cm^{-1} ; **HRMS-ESI** (m/z) [$\text{M}+\text{H}$] calcd for $\text{C}_7^{13}\text{CH}_{11}\text{O}_3$, 156.0736; found: 156.0734.

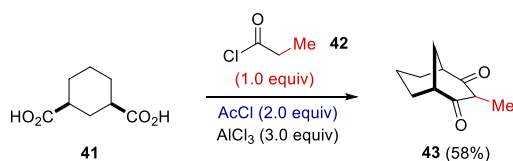


2-¹³C-(acetyl-1-¹³C)cyclohexane-1,3-dione (29): In an oven dried round bottomed flask equipped with reflux condenser and stir bar was added AlCl₃ (11.35 mmol, 3 equiv) and MeNO₂ (15 mL, 0.25 M). Once AlCl₃ had dissolved, **15** (3.79 mmol, 1 equiv) was added and the solution was left to stir at room temperature for one hour. Then **28** (11.35 mmol, 3 equiv) was added and flask was heated to 80 °C in an aluminum heating block for two hours. The solution was then poured into and Erlenmeyer flask containing 1:1 mixture saturated solution of Rochelle's salt and DCM (100 mL). After stirring for one hour, the layers were separated. The organic layer was dried over sodium sulfate, filtered, and concentrated to give the crude product **29**, which was purified by flash chromatography (EtOAc/hexanes). ¹H NMR (400 MHz, CDCl₃) δ 18.14 – 17.97 (m, 1H), 2.69 (s, 1.5H), 2.66 – 2.56 (m, 2H), 2.47 – 2.39 (m, 2H), 2.37 (s, 1.5H), 1.96 – 1.87 (m, 2H); ¹³C NMR (100 MHz, CDCl₃) δ 203.5, 203.1, 202.9, 202.5, 198.9, 198.3, 195.6, 195.0, 114.6, 113.4, 113.3, 38.6, 38.5, 33.2, 33.1, 29.0, 28.9, 28.8, 28.7, 28.6, 28.5, 18.9; IR (Neat): ν 2956, 1659, 1547, 1407, 1156, 1180, 1008, 841cm⁻¹; HRMS-ESI (*m/z*) [M+H] calcd for C₆¹³C₂H₁₁O₃, 157.0770; found: 156.0771.



2-acetylcyclohexane-1,3-dione (12): In an oven dried round bottomed flask equipped with reflux condenser and stir bar was added AlCl₃ (11.35 mmol, 3 equiv) and MeNO₂-¹³C **S15** (15 mL, 0.25 M). Once AlCl₃ had dissolved, **10** (3.79 mmol, 1 equiv) was added and the solution was left to stir at room temperature for one hour. Then **9** (11.35 mmol, 3 equiv) was added and flask was heated to 80 °C in an aluminum heating block for two hours. The solution was then poured into and Erlenmeyer flask containing 1:1 mixture saturated solution of Rochelle's salt and DCM (100 mL). After stirring for one hour, the layers were separated. The organic layer was dried over sodium sulfate, filtered, and concentrated to give the crude product **12**, which was purified by flash chromatography (EtOAc/hexanes).

3.5.4 Sacrificial Acylating Agent



AlCl₃ (1.74 mmol, 3.0 equiv) and dicarboxylic acid **41** (0.58 mmol, 1.0 equiv) in MeNO₂ (0.25 M) were stirred at rt for 1.5 h then propionyl chloride **42** (0.58 mmol, 3.0 equiv) was added and reaction was heated at 80 °C for 1 h. Then, acetyl chloride (1.16 mmol, 2.0 equiv) was added and reaction was heated for another 1.5 h at 80 °C. Yields were determined using dodecane (0.58 mmol, 1 equiv) was added as an internal standard for quantitative GC analysis. The GC yield was determined based on a linear calibration curve (minimum 5 points) with dodecane.

3.6 References

- (1) Armaly, A.M.; Bar, S.; Schindler, C.S.; *Org. Lett.* **2017**, *19*, 3958-3961.
- (2) a) Schick, H.; Lehmann, G. *J. Prakt. Chem.* **1968**, 391-396.
- (3) Dziomko, V.M.; Ivanov, O.V. *Zh. Org. Khim.* **1967**, *3*, 712-717.
- (4) a) Adachi, S.; Liew, S.K.; Lee, C.F.; Lough, A.; He, Z.; St. Denis J.D.; Poda, G.; Yudin, A.K. *Org. Lett.* **2015**, *17*, 5504-5507. b) Rolfe, A.; Lushington, G.H.; Hanson, P.R. *Org. Biomol. Chem.* **2010**, *8*, 2198-2203. c) Amaotre, M.; Beeson, T.D.; Brown, S.P.; MacMillan, D.W.C. *Angew. Chem. Int. Ed.* **2009**, *48*, 5121-5124. d) Shi, S.; Szostak, M. *Chem. Eur. J.* **2016**, *22*, 10420-10424.
- (5) For reviews, see: a) Kirschning, A.; Kujat, C.; Schaumann, E. *Eur. J. Org. Chem.* **2007**, *15*, 2387. b) Rentner, J.; Kljajic, M.; Offner, L.; Breinbauer, R. *Tetrahedron* **2014**, *70*, 8983-9027.
- (6) a) Smith, A.B.; Boldi, A.M. *J. Am. Chem. Soc.* **1997**, *119*, 6925-6929. b) Smith, A.B.; Pitram, S.M.; Boldi, A.M.; Gaunt, M.J.; Sfougataki, C.; Moser, W.H. *J. Am. Chem. Soc.* **2003**, *125*, 14435-14445. c) Tietze, L.F.; Geissler, H.; Gewert, J.A.; Jakobi, U. *Synlett* **1994**, 511-512. d) Wu, X.-F.; Neumann, H.; Beller, M. *Chem. Soc. Rev.* **2011**, *40*, 4986. e) Heller, S.T.; Newton, J.N.; Fu, T.; Sarpong, R. *Angew. Chem. Int. Ed.* **2015**, *54*, 9839.

*Adapted with permission from Ahlam M. Armaly, Sukanta Bar, Corinna S. Schindler, *Org. Lett.* **2017**, *19*, 3962-3965. Copyright 2017 American Chemical Society.

Chapter 4 Enantioselective Total Synthesis of Atropurpuran and the Arcutines

4.1 Introduction

In 2009, Wang et al. isolated an intriguing compound from *Aconitum hemsleyanum* var. *atropurpureum*, which they called atropurpuran (Figure 4.1).¹ Atropurpuran (**1**) bears an unprecedented pentacyclic carbon skeleton which incorporates two fused bicyclo[2.2.2]octane units and poses a significant synthetic challenge, including 8 stereocenters with 3 of them being all-carbon quaternary centers. Atropurpuran **1** was isolated in a total of 12 mg from 2.4 kg and is characterized by a unique tetracyclo[5.3.3.0^{4,9}.0^{4,12}]tridecane core that was only observed in three other compounds – arcutine (**2**), arcutinine (**3**), and arcutinidine (**4**) – that were isolated from *Aconitum arcuatum* Maxim. (Figure 4.1).² The isolation of atropurpuran, a non-alkaloid diterpene, from an *Aconitum* plant fascinated researchers. Only two other non-alkaloid diterpenes, atisenol and Guan fu diterpenoid A, had been isolated from these plants that produce a vast array of structurally complex natural products.³ More importantly, the stark resemblance of atropurpuran (**1**) to arcutine (**2**), arcutinine (**3**), and arcutinidine (**4**) may serve as proof for the hypothesis that the biogenesis of the diterpene alkaloids arises from their diterpene precursors.

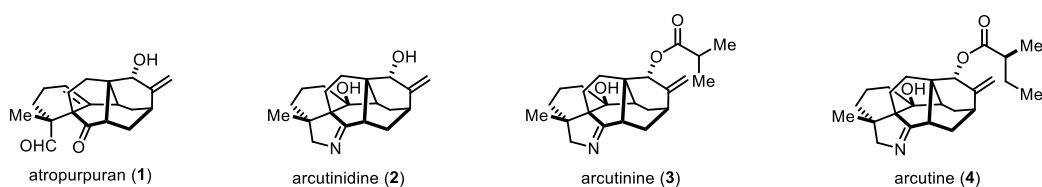


Figure 4.1 The diterpene atropurpuran (**1**) and related diterpene alkaloids the arcutines (**2-4**)

Beyond the interest in the biosynthetic origin of the diterpene alkaloids, the isolation of atropurpuran (**1**) and the related diterpene alkaloid analogs (**2-4**) further captivated researchers because they did not easily fit into any established classification of the diterpene alkaloids (Figure 4.2).⁴ The C₂₀-diterpenes can be broken down into four different classes –kauranes, atisanes, rearranged, and bisditerpenoid – that can then be further classified based on type.⁴ For example, the atisane class consists of the atisine type (**5-6**), hetidine type (**7-8**), and hetisine type (**9-10**).⁴

Each of these is structurally related. For example, formation of bond between C14-C20 in the atisines creates the hetidines. Formation of an additional bond between C6-N in the hetidines creates the hetisine type, which represented the most complex type of C₂₀-diterpene alkaloids. Upon the isolation of the C₂₀-diterpene atropurpuran (**1**) and the C₂₀-diterpene alkaloids, the arcutines (**2-4**), they appeared to resemble the different types within the atisane class. However, their skeletal structure consists of a C5-C20 bond instead of the commonly observed C10-C20 bond. As such, they were classified in the rearranged class.⁴ Together, these four compounds comprise a new type of C₂₀-diterpenes; the arcutanes refers to the diterpene members of this class, atropurpuran (**1**), whereas the arcutines refers to the diterpene alkaloids (**2-4**).⁴

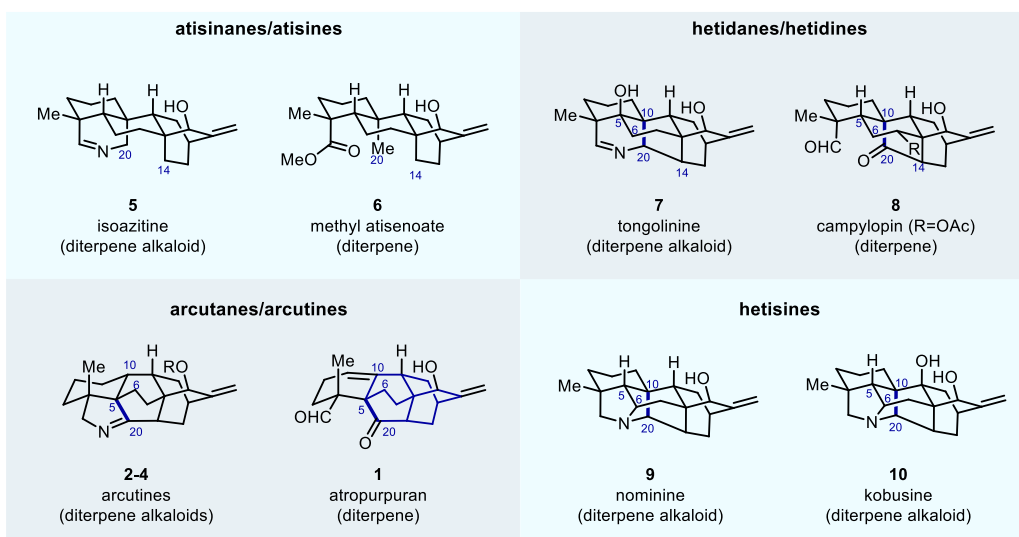


Figure 4.2 Members of the atisane class of diterpene alkaloids and atropurpuran and the arcutines

4.2 Proposed Biogenesis

Several biosynthetic hypotheses are proposed regarding atropurpuran (**1**) and its arcutine analogs (**2-4**). Atropurpuran (**1**) was first isolated by Wang et al., who had recently isolated another rare, non-alkaloid diterpene, campylopin (**8**), from the *Delphinium* genus.⁵ As such, Wang et al. proposed that the hetidane skeleton **11** may serve as a biosynthetic precursor to the arcutane, atropurpuran (Figure 4.3).¹ Starting from the hetidane **11**, fragmentation of the C13-C14 bond would yield a dialdehyde **12** that could give hemiquinone **13** after loss of ethylene. Michael addition and subsequent reintroduction of ethylene via a Diels-Alder yields the cycloadduct **15**. Dehydration and subsequent Aldol reaction forms the tetracyclo[5.3.3.0^{4,9}.0^{4,12}]tridecane carbon core in **17**. A reduction/oxidation series gives rise to atropurpuran (**1**).

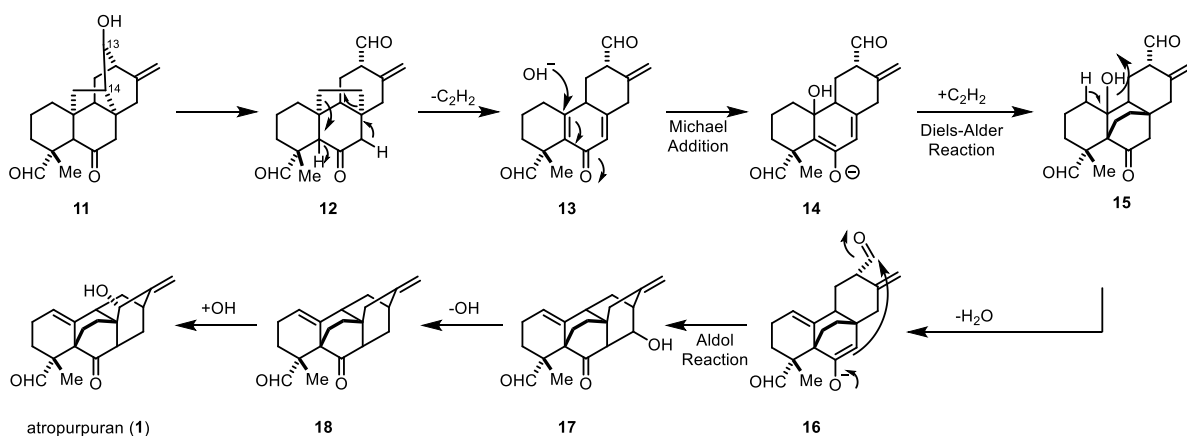


Figure 4.3 Wang's proposed biosynthesis of atropurpuran from hetidane (**11**)

Two alternative biosynthetic proposals are suggested by Sarpong et al. relying on either *ent*-atisir-16-ene (**19**) or the hetidine core (**25**).⁶ Both routes rely on the generation of carbocation intermediates and 1,2-alkyl and 1,2-acyl shifts that are energetically supported by computational analysis. *Ent*-atisir-16-ene is a well-studied and widely accepted intermediate in the diterpene biosynthesis and is thought to be a precursor to the hetidines. Relying on this established route to *ent*-atisir-16-ene, Sarpong et al. propose that atropurpuran (**1**) may be a shunt product *en route* to the arcutines (**2-4**, Figure 4.4). Specifically, oxidation of *ent*-atisir-16-ene **19** would enable formation of the C14-C20 bond to give **20**. Generation of a carbocation intermediate **21** upon loss of water would induce a 1,2-alkyl shift in **21** to forge a new C20-C5 bond in **22** and forms the key the tetracyclo[5.3.3.0^{4,9}.0^{4,12}]tridecane motif. From this common intermediate **22**, elimination and oxidation would yield atropurpuran **1**. Alternatively, capture of the carbocation in **22** with water could give dialdehyde **23**. Introduction of a nitrogen source and subsequent oxidation would provide the arcutines (**2-4**).

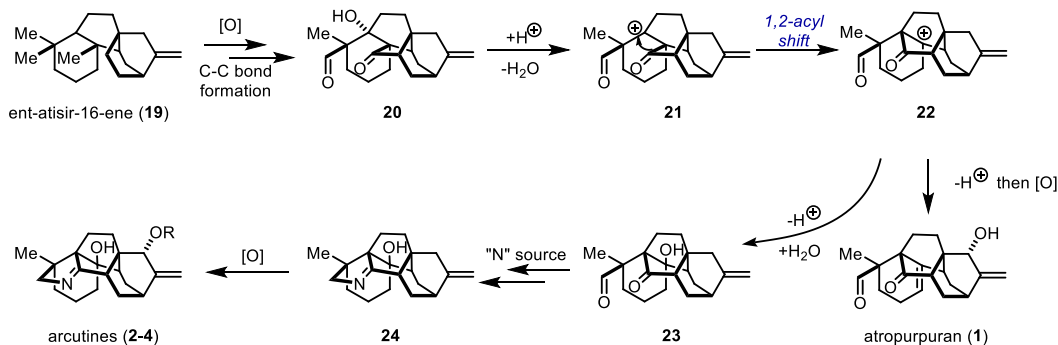


Figure 4.4 Sarpong's proposed biosynthesis of atropurpuran (**1**) and arcutines (**2-4**) from terpene precursor *ent*-atisir-16-ene (**19**)

An alternative proposal by Sarpong et al.⁶ suggests that atropurpuran and the arcutines are derived from the hetidines **25** (Figure 4.5). Oxidation of hetidine core **25** gives the tertiary alcohol **26**. Loss of the alcohol generates the carbocation **27** that can undergo a 1,2-alkyl shift to provide a new tertiary carbocation **28** bearing the tetracyclo[5.3.3.0^{4,9}.0^{4,12}]tridecane core. Addition of water to **28** and subsequent oxidation provides arcutinidine **2**. An alternative pathway from the hetidine core **25** to arcutinidine **2** is proposed relying on the same steps but in a different order. From the arcutinidine **2**, oxidation and hydrolysis would give atropurpuran.

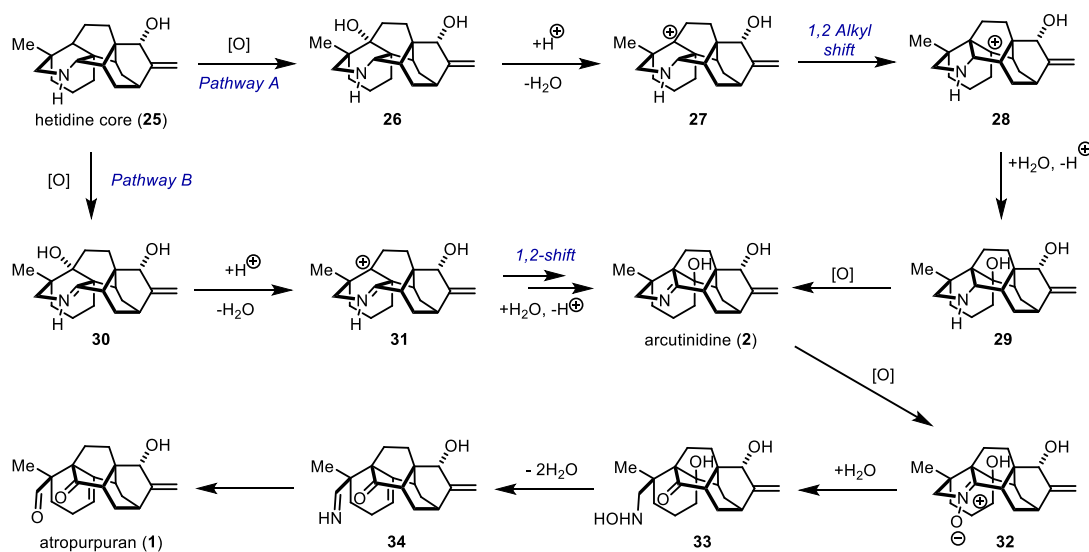


Figure 4.5 Sarpong's proposed biosynthesis of atropurpuran (**1**) and arcutines (**2-4**) from hetidine core (**25**)

4.3 Previous Synthetic Approaches

The unique biological activity associated with *Aconitum*-derived diterpene alkaloids^{4,7} coupled with the unprecedented carbon framework of the arcutin analogs has inspired numerous synthetic approaches. When we initiated our studies towards the synthesis of atropurpuran and the arcutines, there had been no reported syntheses to date. Many other efforts towards this class of compounds was later reported relying on *reverse-electron-demand Diels-Alder reactions*,^{8,9} *6π-electrocyclizations*,¹⁰ *intramolecular Michael additions*^{11,12} and *oxidative dearomatization reactions*.¹³ One of the first reports towards atropurpuran was reported by Kobayashi et al. in 2011 (Figure 4.6).⁸ This impressive effort from Kobayashi et al. represented the first successful synthesis of the tetracyclo[5.3.3.0^{4,9}.0^{4,12}]tridecane core of atropurpuran and the arcutines via an oxidative dearomatization and subsequent reverse-electron-demand Diels-Alder reaction sequence

of **35**. Although Kobayashi et al. could not elaborate **38** to the natural products, their efforts demonstrated the power of the oxidative dearomatization and subsequent Diels-Alder cycloaddition strategy¹⁴ to the core of atropurpuran (**1**) and the arcutines (**2-4**).

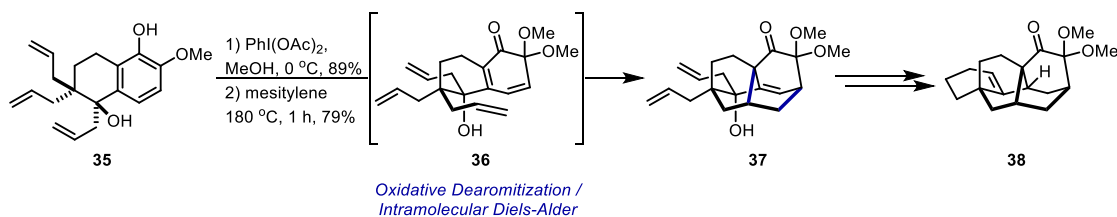


Figure 4.6 Key step in Kobayashi's synthesis of core of atropurpuran

It was not until 2016 that the first racemic total synthesis of atropurpuran (**1**) was accomplished by the Qin group (Figure 4.7).¹⁵ They employed an oxidative dearomatization and subsequent Diels-Alder cycloaddition strategy to construct a key tricyclic lactone **41**. The TBS-protected enol ether **42** was introduced via a Knoevenagel condensation, which ultimately enabled an Aldol reaction to provide tetracyclic intermediate **43**. This intermediate was posed for a SmI₂-mediated ketyl-olefin cyclization to forge the final bond in the pentacyclic core structure **44** that was elaborated to atropurpuran (**1**) in 11 synthetic steps.

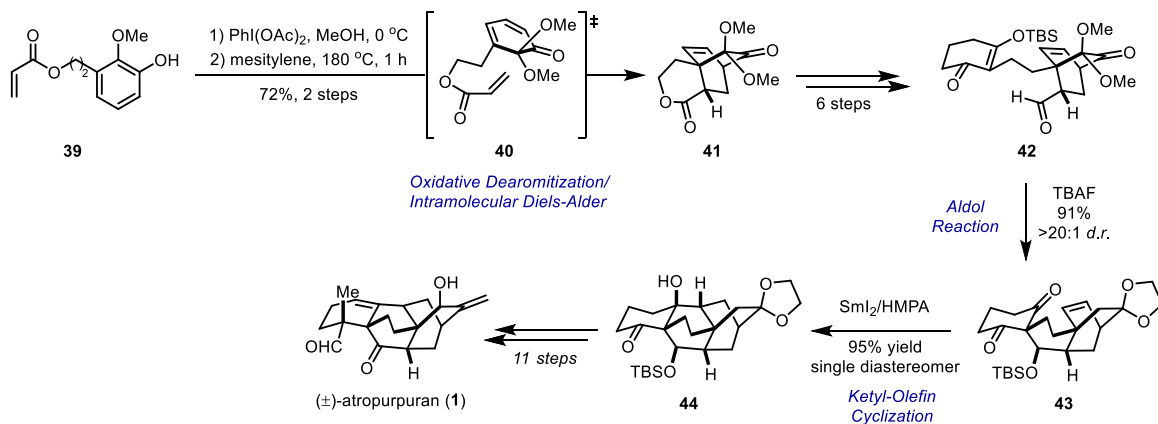


Figure 4.7 Key steps in Qin's total synthesis of atropurpuran (**1**)

In 2019, the Xu group¹⁶ reported a concise approach to racemic atropurpuran. Their strategy also took advantage of an oxidative dearomatization and subsequent Diels-Alder cycloaddition approach (Figure 4.8). They were able to construct their key spirocyclic substrate **46** via enyne metathesis of **45**. Subjection of spirocycle **46** to PhI(OAc)₂ allowed for the key oxidative dearomatization and subsequent Diels-Alder cycloaddition to furnish the pentacyclic core of atropurpuran **47**. Pentacycle **47** was converted to atropurpuran (**1**) in 9 synthetic steps.

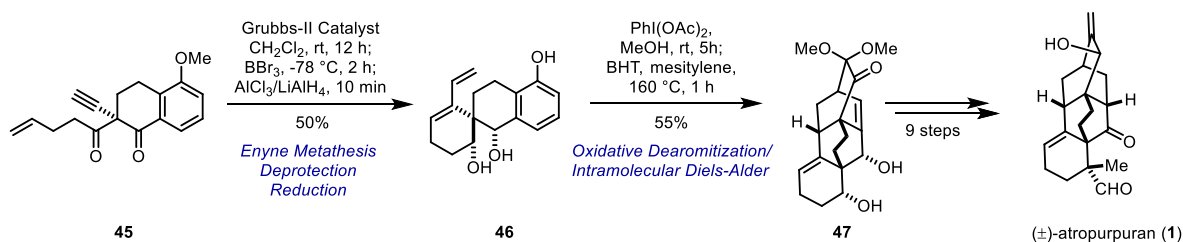


Figure 4.8 Key steps in Xu's total synthesis of atropurpuran (**1**)

Despite the successful syntheses of atropurpuran, it was not until 2019 that an approach to the arcutines (**2-4**) was reported nearly simultaneously by the Qin,¹⁷ Sarpong,¹⁸ and Li groups.¹⁹ The Qin group's pioneering efforts with the first total synthesis of atropurpuran (**1**) allowed them to investigate the proposed biosynthetic link between the diterpene atropurpuran (**1**) to the its diterpene alkaloid analogs, the arcutines (**2-4**). However, despite attempts to convert atropurpuran as well as other late stage intermediates to nitrogen-containing analogs failed.¹⁷ The Qin group was able to develop an enantioselective approach to the arcutines by pre-installing the pyrroline early in the synthesis using an aza-wacker oxidation of **48** (Figure 4.9).¹⁷ Subjection of pyrroline **49** to oxidative dearomatization and subsequent Diels-Alder cycloaddition conditions provide the tetracycle **50**. The final ring could be formed using SmI₂-mediated ketyl-olefin cyclization to give the pentacyclic intermediate **51**, which was converted to arcutinidine (**2**) in 5 synthetic steps.

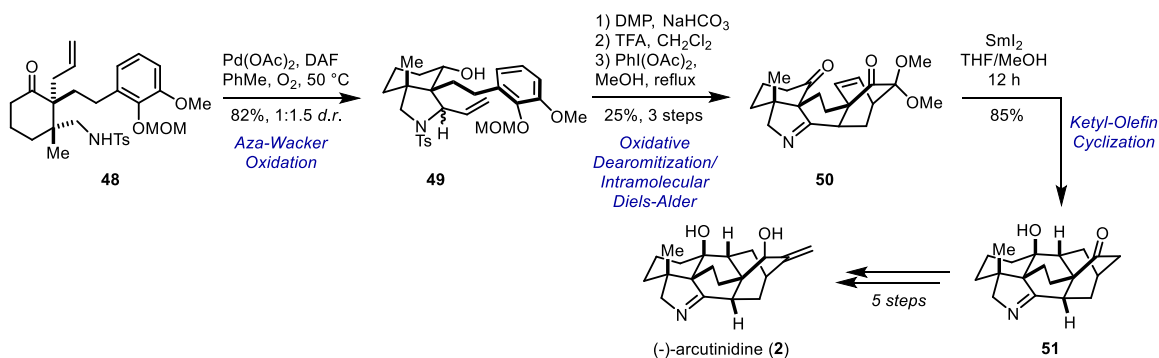


Figure 4.9 Key steps in Qin's total synthesis of arcutinidine (**2**)

The Sarpong group¹⁸ relied on chemical network analysis to reduce the synthetic complexity by initially accessing fused tetracycle **52** (Figure 4.10). Initial acylation of **52** and subjection to oxidative dearomatization and subsequent Diels-Alder cycloaddition reaction gave **54**. The cycloadduct **54** was converted to the pinacol coupling substrate **55** over three steps. Subjection of **55** to SmI₂ forged the final ring in **56** that is observed in the arcutines. With the carbocyclic framework formed in **56**, it was then converted to arcutinidine (**2**) in 8 synthetic steps.

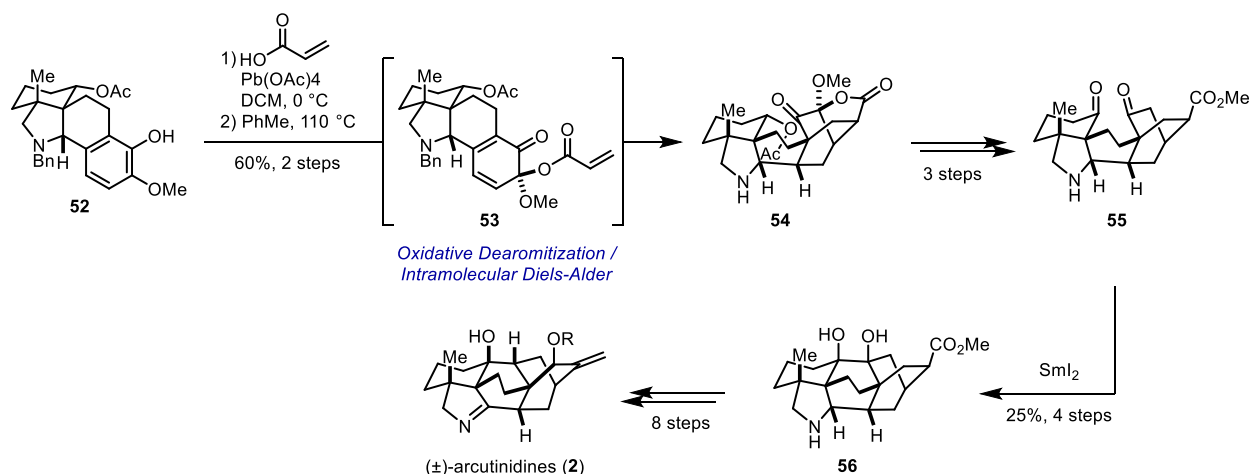


Figure 4.10 Key steps in Sarpong's total synthesis of arctunidine (**2**) relying on network guided analysis

A distinct synthetic approach towards the arcutines was reported by the Li group (Figure 4.11).¹⁹ Starting from chiral alcohol **57**, they could rapidly construct the pentacycle **58** bearing a MOM-protected alcohol. Subjection of **58** to SnCl₄ enabled a biomimetic cascade sequence to construct the hexacyclic core structure **59**. This was converted to arctunidine (**2**) in an additional 9 steps.

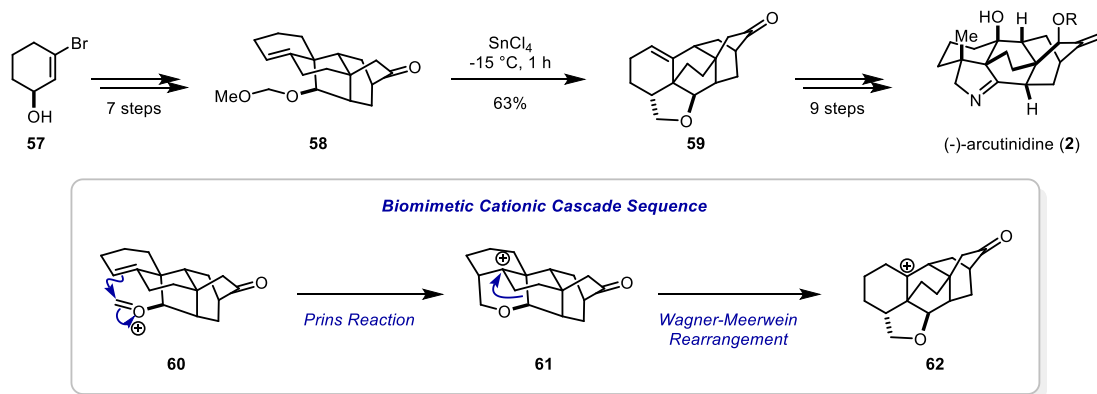


Figure 4.1119 Key steps in Li's total synthesis of arctunidine (**2**) via biomimetic cation cascade

4.4 Results and Discussion

Our distinct approach to atropurpuran (**1**) and the arcutines (**2-4**) takes advantage of the inherent symmetry present in the molecule in a unified enantioselective synthesis (Figure 4.12). Specifically, access to a common intermediate **63** would enable divergence to atropurpuran (**1**) and the arcutines (**2-4**). This common intermediate would come from iodination and subsequent Barbier reaction of acetal **64**. Importantly, DFT energy calculations (Q-Chem, B3LYP [6-31G**])

suggest that intermediate acetal **64** is energetically favored over all other possible regio- and diastereoisomer by >6 kcal/mol upon ozonolysis and reduction of pseudo-symmetric dione **65**. This key pseudo-symmetric intermediate **65** can be accessed from cyclic 2-alkyl-1,3-dione **66**, which is the product of a Dieckmann cyclization reaction. As such, our synthesis of atropurpuran and the arcutines hinges on accessing this key pseudo-symmetric intermediate **65** and, ultimately, the viability of our proposed Dieckmann cyclization. Importantly, our approach relies on a single chiral center in pseudo-symmetric dione **65** that will set all subsequent stereocenters in the synthesis; the selective formation of acetal **64** will enable diastereoselective carbon-carbon bond formation in **63**, giving providing the stereochemical configuration observed in atropurpuran (**1**) and the arcutines (**2-4**).

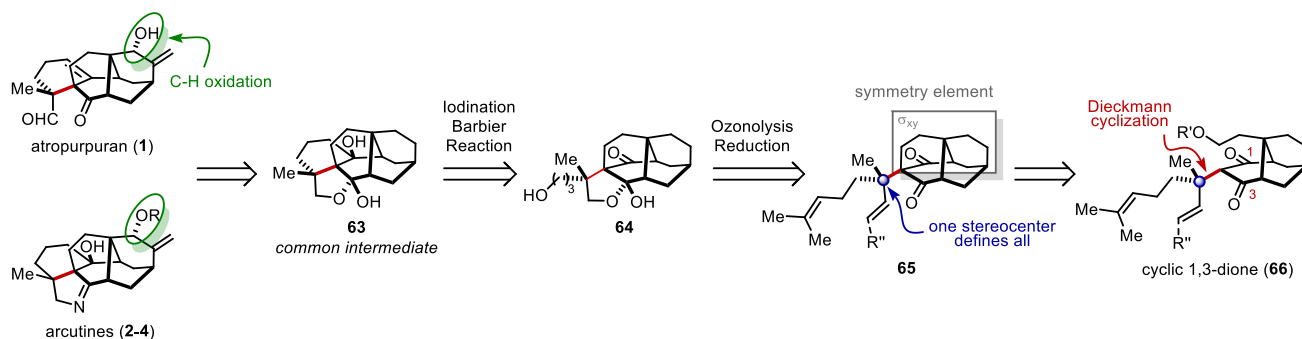


Figure 4.12 Our unique strategy towards atropurpuran (**1**) and the arcutines (**2-4**) that takes advantage of their inherent symmetry and relies on a key cyclic 1,3-dione (**66**)

We initially intended using our AlCl_3 -mediated Dieckmann cyclization of dicarboxylic acid **67** and enantioenriched acid chloride **68** to gain access to the cyclic 1,3-dione **66** required for our synthesis (see chapter 1).²⁰ However, we had found that β -substituted acid chlorides such as **68** are not tolerated in the reaction (see chapter 2).²¹ As such, we turned to a more traditional base-mediated Dieckmann cyclization strategy from lactone **69** (Figure 4.13). Dieckmann cyclization of the lactone **69** would forge the 1,3-dione in **66** and generate a free alcohol that was required for the final annulation of **66** to the tetracycle **65**. We thought that we could efficiently access this Dieckmann substrate **69** via a Diels-Alder cycloaddition of diene **70** and enantioenriched vinyl ketone **71**.

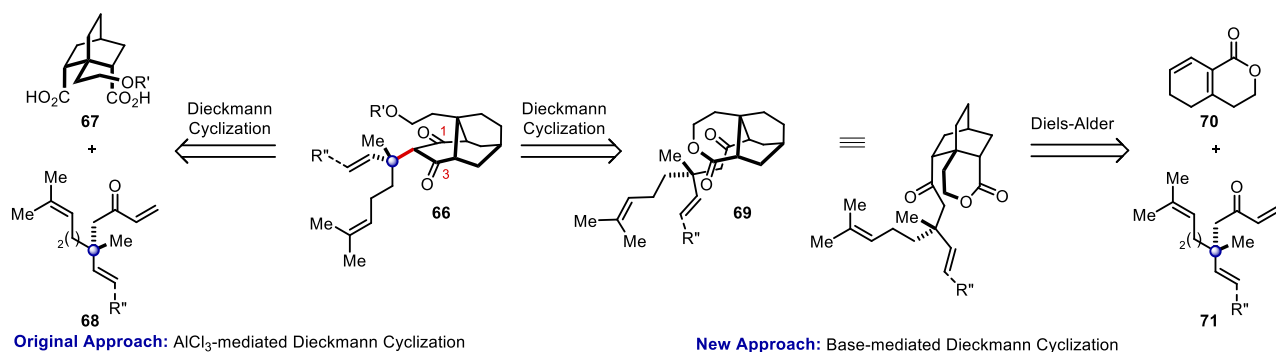


Figure 4.13 Our original approach to the key cyclic 1,3-dione **66** via the AlCl_3 -mediated Dieckmann cyclization (left) and our revised strategy relying on a base-mediated Dieckmann cyclization approach (right)

We initially investigated the viability of this approach in a racemic model system with racemic vinyl ketone **74** (Figure 4.14). We developed a highly scalable three-step synthesis of a racemic vinyl ketone **74** for our model studies. Starting with commercially available geraniol, a Johnson-Claisen reaction provides the desired quaternary carbon center in ethyl ester **72**. Conversion of ethyl ester **72** to the Weinreb amide **73** and subsequent addition of vinylmagnesium bromide provides racemic vinyl ketone **74** (88% over three steps). Importantly, the sequence to the vinyl ketone **74** is not only high yielding, but it is also highly scalable. Access to the diene **70** is provided by Birch reduction of commercially available isochromanone after in situ isomerization. Subjection of the diene **70** and racemic vinyl ketone **74** to Diels-Alder cycloaddition conditions gave a mixture of regio- and diastereoisomers, affording the desired diastereoisomer **75** in 28% yield. Conjugate reduction of the enoate **75** provided the Dieckmann substrate **76** in quantitative yield. Unfortunately, despite extensive evaluation of cyclization conditions, we could not obtain the desired Dieckmann cyclization product **77**.

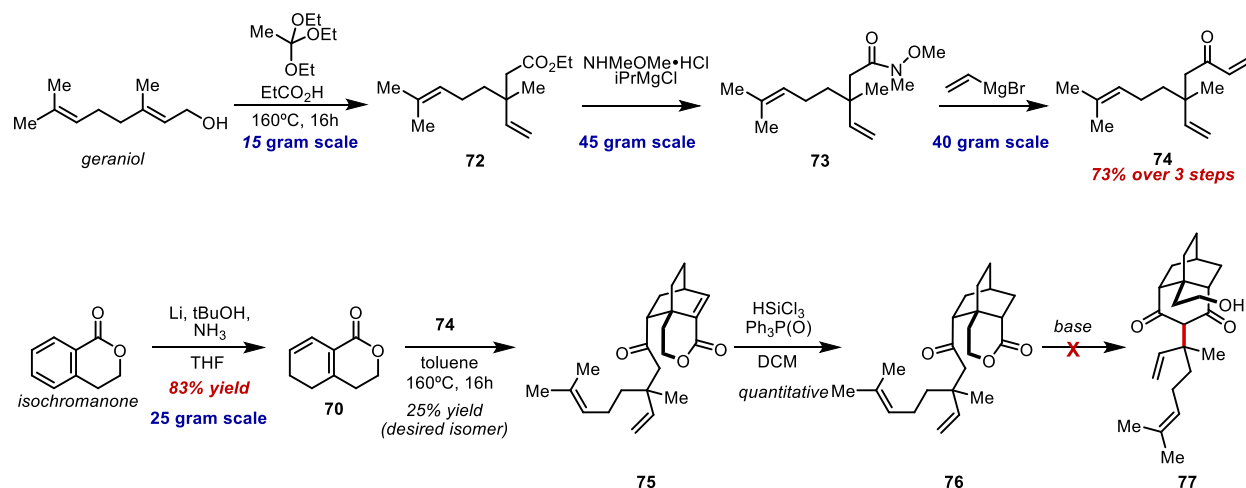


Figure 4.14 Investigation of key base-mediated Dieckmann cyclization in reacemic model system

We recognized the challenge posed by the Dieckmann cyclization of this complex substrate **76** (Figure 4.14). Specifically, the substrate **76** consists of a neopentyl ketone and lactone moieties. As such, we turned to model systems to assess the controlling features of this approach. We first analyzed a substrate bearing a neopentyl ketone **78** to determine whether enolate formation is viable in such a sterically constrained ketone (Figure 4.15). We found that the substrate **78** bearing a neopentyl ketone and methyl ester readily underwent Dieckmann cyclization to provide the desired Dieckman cyclization product **79** in very good yield. We then turned to substrate **80** bearing a lactone moiety. When this was subjected to base-mediated cyclization we isolated some 1,3-dione **81** but the major product was primarily the lactol **82**. When we evaluated substrate **83** comprised of both lactone and neopentyl units. Unfortunately, we did not observe any formation of 1,3-dione **84** or lactol **85** products but solely isolated epimerized starting material. Together, these results suggested that the lactone was the limiting feature in our proposed Dieckmann cyclization of **76**. However, the result with the substrate **78** bearing a neopentyl ketone and methyl ester suggested that a system that resembled this substrate may be more feasible.

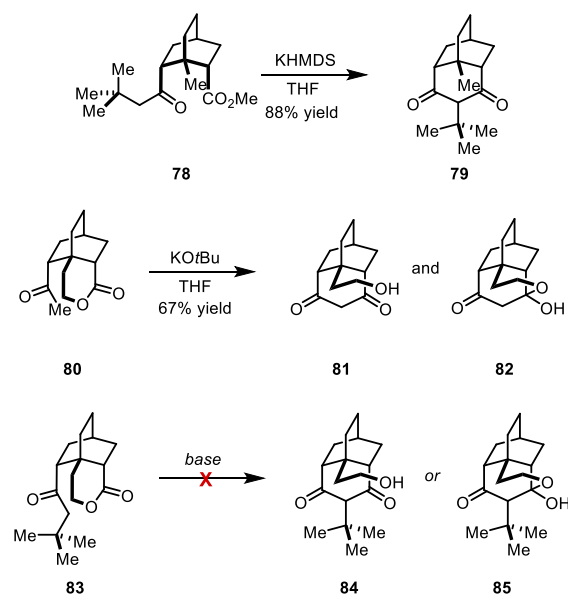


Figure 4.15 Model studies of base-mediated Dieckmann cyclization

Our revised base-mediated Dieckmann cyclization strategy was based on a methyl ester **87** bearing some sort of alcohol protecting group (Figure 4.16). Again, the Dieckmann substrate **87** is readily accessible from a Diels-Alder cycloaddition with diene **88** and enantioenriched vinyl ketone **89**. First, we had to identify a suitable protecting group for diene **88**. We developed a modular synthetic strategy relying on previously developed Birch reduction protocol (Figure 4.16). Hydrolysis of the lactone **70** with NaOH and subsequent esterification allowed for differential protection of the alcohol to give various methyl esters **90**. Diels-Alder cycloaddition with neopentyl vinyl ketone **91** gave the desired cycloadduct **92**, which was hydrogenated to provide the Dieckmann cyclization substrate **93**.

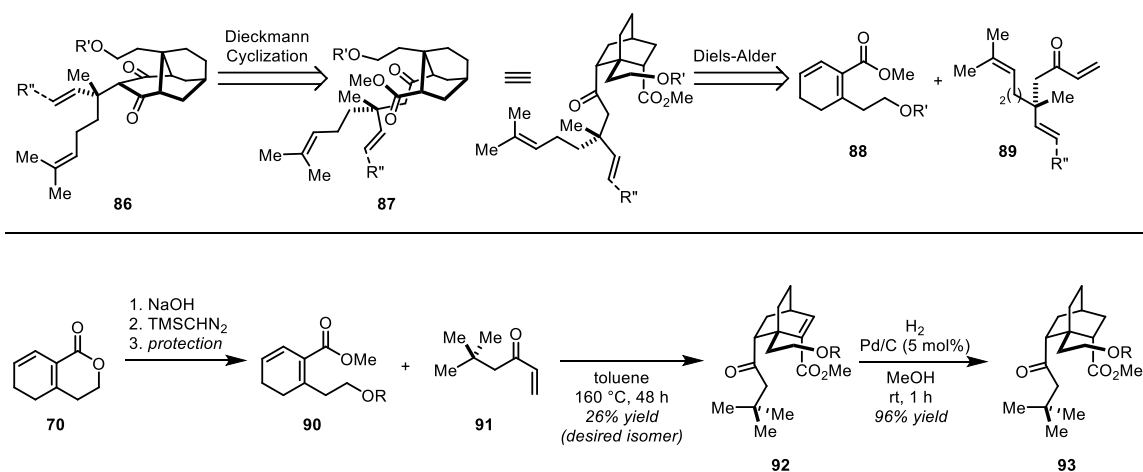


Figure 4.16 Our revised strategy for the base-mediated Dieckmann cyclization (top) and synthesis of a model substrate for preliminary investigations (bottom)

Using this approach, we first investigated the base-mediated Dieckmann cyclization of acetate-protected **94** (Figure 4.17A). Subjecting the Dieckmann substrate **94** did not afford the Dieckmann cyclization product **95** but rather the major product observed was a mixture of lactone epimers **96**. We suspected that this lactone was a result of acetate cleavage. However, the acetate could get cleaved one of two ways. In the first option, the base can directly cleave the acetate group in **94** to give the free alkoxide **97** (Figure 4.17B). This free alkoxide **97** can then lactonize onto the methyl ester to give lactone **96**, which can epimerize under the reaction conditions. The second option (Figure 4.17C) is based on the Dieckmann cyclization taking place with substrate **94**, which would give the Dieckmann product **98** and a free methoxide that would result from the cyclization on to the methyl ester. This methoxide could then be responsible for cleavage of the acetate in the Dieckmann cyclization product **98**, which would give the free alkoxide **99**. The alkoxide **99** can form a lactol **100** by cyclizing onto the 1,3-dione. The lactol **100** may not be stable and would ultimately undergo a retro-Dieckmann to give the lactone **96**. Differentiating these two acetate cleavage pathways would inform us if our revised base-mediated Dieckmann cyclization approach for our synthesis was viable.

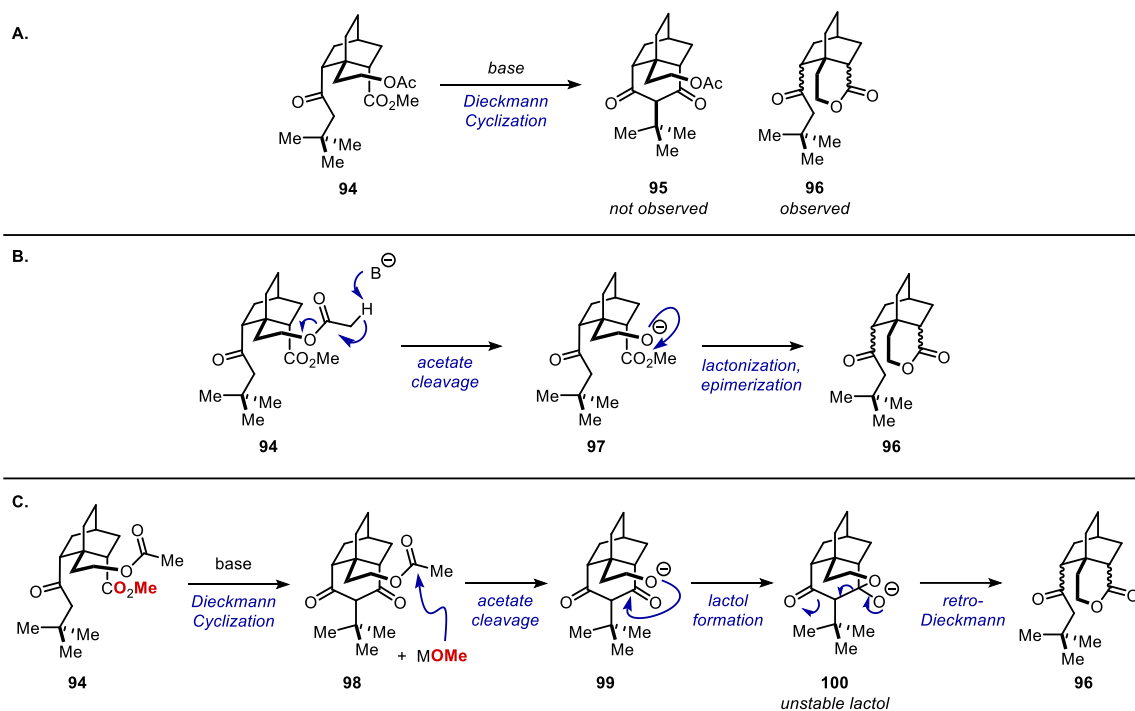


Figure 4.17 A) Preliminary investigations of base-mediated Dieckmann cyclization in acetate-protected substrate **94**; B) Possible path leading to acetate cleavage via direct deprotection; C) Alternative path for acetate cleavage that occurs after Dieckmann cyclization

We thought that we could differentiate these pathways and, most importantly, determine if the Dieckmann cyclization was taking place by switching the acetate to a pivalate in order to prevent direct acetate cleavage (Figure 4.18). We used our modular synthesis to access the pivalate **101**. However, we did not observe any the desired 1,3-dione **102** or any recovered lactones. These reactions solely returned epimerized starting material. We suspected that the pivalate was far too bulky due to the lack of reactivity. This led us to turn to a protecting group that was less sterically encumbering but more robust than an acetate – a methyl ether. We were able to gain access to the methyl ether substrate **103** and found that when this was subjected to KHMDS it readily underwent Dieckmann cyclization give the 1,3-dione **104** in 92% yield.

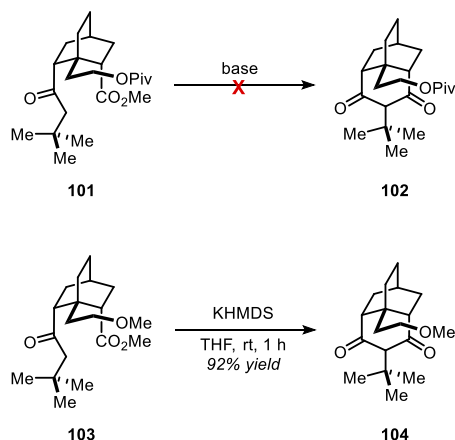


Figure 4.18 Evaluation of suitable protecting group for the Dieckmann cyclization

Having identified a promising alcohol protecting group in a model system **103** and **104**, we turned to the actual system to confirm the viability of this approach (Figure 4.19). Importantly, we first analyzed this approach in a racemic version of our actual system with racemic vinyl ketone **74**. We also developed a more efficient, higher-yielding approach to the methyl ether **107** via initial opening of isochromanone to give **105**. Birch reduction gave the 1,4-diene **106** that was subjected to DBU-mediated isomerization to provide the diene **107**. Diels-Alder cycloaddition of diene **107** with vinyl ketone **74** provided the desired cycloadduct **108**. Our previously employed conjugate reduction protocol gave very low yield and very low conversion. In order to assess the viability of this substrate as fast as possible, we proceeded with the fully saturated system **109** after hydrogenation.

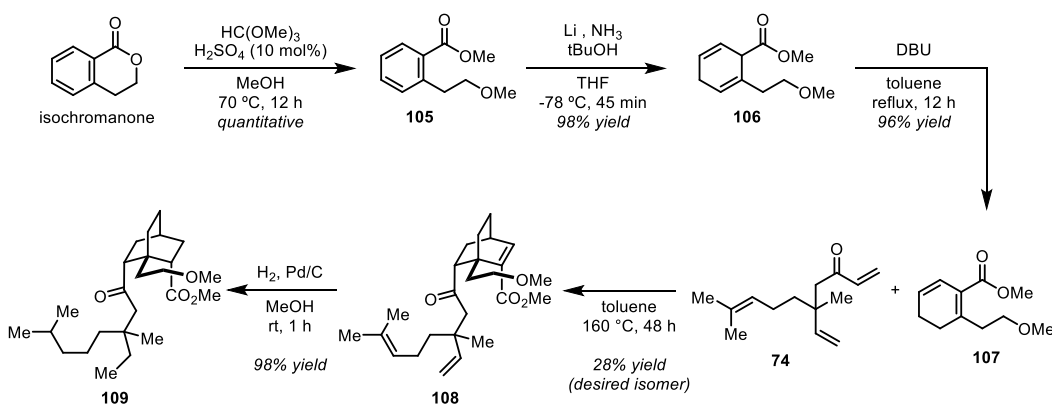
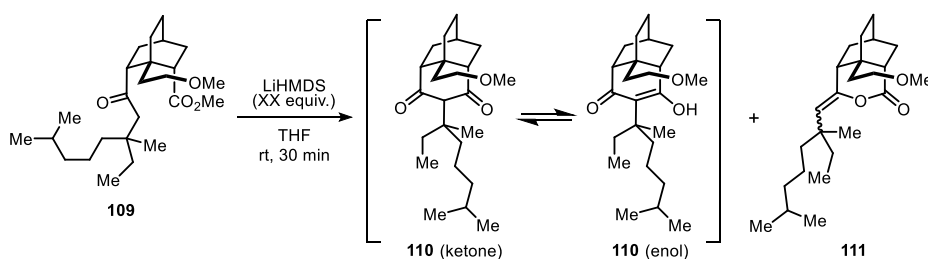


Figure 4.19 Synthesis of saturated substrate to evaluate the Dieckmann cyclization for the synthesis of atropurpuran and the arcutines

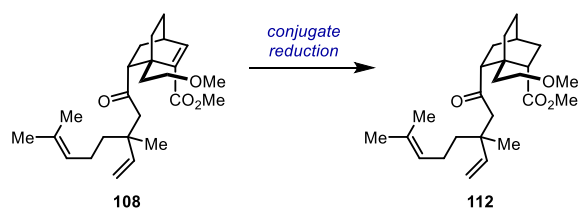
With the saturated Dieckmann substrate **109** in hand, we investigated the key Dieckmann cyclization reaction (Figure 4.20). We were very pleased to find that LiHMDS provided the desired Dieckmann cyclization product as a mixture of ketone and enol-tautomers (**110**). However, these C-cyclization products were the minor products that were obtained alongside a competing O-cyclization product **111**. However, we noticed that the ratio of O-cyclization to C-cyclization and conversion varied based on the equivalents of LiHMDS.



| Equivalents | Conversion | C-cyclization | O-cyclization |
|-------------|------------|---------------|---------------|
| 1.1 equiv. | 56% | 0% | 42% |
| 2.0 equiv. | 98% | 6% | 69% |
| 3.0 equiv. | 100% | 8% | 50% |
| 5.0 equiv. | 100% | 10% | 27% |

Figure 4.20 Evaluation of various bases for the Dieckmann cyclization of **109**

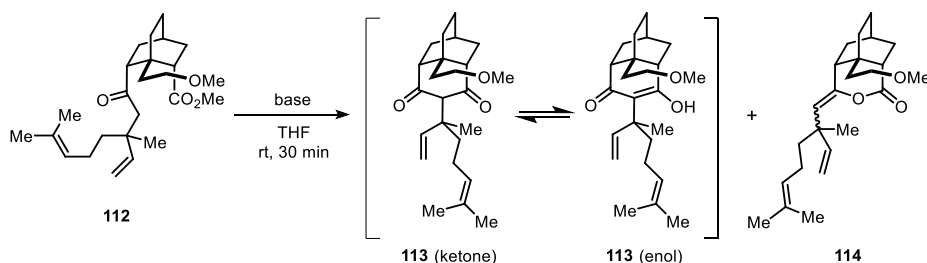
With this very promising result, we then focused on gaining sufficient quantities to investigate the Dieckmann cyclization in the Dieckmann substrate bearing the desired olefins **112** (Figure 4.21). We evaluated a variety of conditions for the conjugate reduction and found no conversion in systems based on Mg or Pd/C. Alternatively, B(C₆F₆) gave a complex mixture with only small amounts of the desired conjugate reduction product. Stryker's reagent provided the most promising result, giving 55% yield of **112** with 0.5 equivalents. We suspected that stoichiometric amounts would be required to get higher yields, however, to avoid stoichiometric amounts of this sensitive reagent we turned to an *in situ* protocol²² relying on Cu(OAc)₂ and PMHS. We found that these catalytic conditions gave 35% yield of **112** under dilute reaction conditions, which were optimized to 89% yield of **112** by employing more concentrated conditions.



| Conditions | Yield |
|---|-------|
| Mg (10 equiv.) in MeOH, rt, 12 h | 0% |
| Mg (10 equiv.) in MeOH, reflux, 5 h | 0% |
| 10% Pd/C (0.1 equiv.), NH ₄ CO ₂ H (4 equiv.) in MeOH, rt, 12 h | 0% |
| B(C ₆ F ₆) (2 mol%), 1,1,3,3-tetramethyldisiloxane (1 equiv.) | <5% |
| [Cu(PPh ₃)H] ₆ (0.5 equiv.) in toluene, rt, 12 h | 55% |
| Cu(OAc) ₂ ·H ₂ O (10 mol%), dppBz (1 mol%), tBuOH (3 equiv.), PMHS (3 equiv.) in toluene (0.05 M), rt, 12 h | 35% |
| Cu(OAc) ₂ ·H ₂ O (10 mol%), dppBz (1 mol%), tBuOH (3 equiv.), PMHS (3 equiv.) in toluene (0.29 M), rt, 12 h | 89% |

Figure 4.21 Optimization of conjugate reduction

Having developed a strategy to access the Dieckmann substrate **112** that resembles the one required for our synthesis, we turned to evaluate the key Dieckmann cyclization reaction of **112** (Figure 4.22). We first evaluated LiHMDS because we had previously obtained promising results in the saturated system. Using similar reaction conditions, we were surprised and very pleased to find that C-cyclization products **113** were the major products (74%, mixture of ketone and enol-automers) as well as 6% yield of the undesired O-cyclization product **114**. Diluting this reaction to 0.01 M THF provided exclusively C-cyclization, albeit, in 38% yield. We were pleased to find that slight adjustments to the reaction environment such as changing the counterion of the base gave drastically different results. In the case of KHMDS, full conversion was observed with only C-cyclization products isolated as the exclusive products in 34% yield. Switching to NaHMDS gave quantitative yield of the desired Dieckmann cyclization product **113**.



| Base | Equivalents | Concentration | Conversion | C-cyclization | O-cyclization |
|--------|-------------|---------------|------------|---------------|---------------|
| LiHMDS | 2 | 0.1 M | 100% | 74% | 6% |
| LiHMDS | 2 | 0.01 M | 40% | 38% | --- |
| KHMDS | 3 | 0.1 M | 100% | 34% | --- |
| NaHMDS | 3 | 0.1 M | 100% | 100% | --- |

Figure 4.22 Evaluation of various bases for the Dieckmann cyclization of **112**

With these very promising results for the Dieckmann cyclization, we applied this approach to in an enantioselective route (Figure 4.23). Importantly, we needed to access the vinyl ketone **118** in an enantioselective fashion. Our approach took advantage of the fact that the synthetic transformation that established the quaternary chiral center was a Johnson-Claisen reaction, which proceeds via a chair-like transition state. As such, we started from a reported enantioenriched secondary alcohol **115**. Using a previously reported literature procedure²³ relying on asymmetric diethyl zinc addition, we synthesized the chiral secondary alcohol **115**, which was reported to give 90-92 %ee (obtained after derivitization). We decided to proceed with the two other steps of the sequence and assess the %ee of the final vinyl ketone **118**. Doing so, we found a very poor result of 20 %ee. We determined that the elevated temperatures and acidic conditions required for the Johnson-Claisen reaction were detrimental to chiral allylic alcohol.

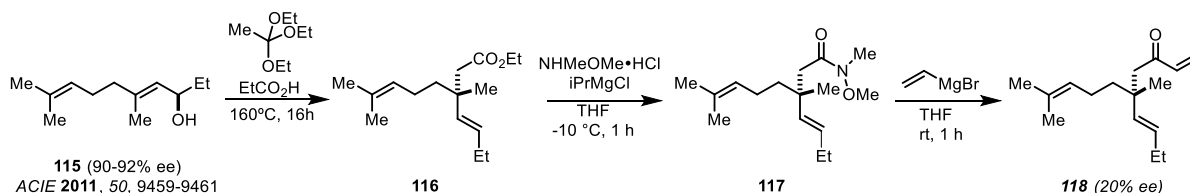


Figure 4.23 Asymmetric synthesis of chiral vinyl ketone **118** via a Johnson-Claisen strategy

We hypothesized that a milder approach relying on an Ireland-Claisen may be more conducive to our enantioselective route (Figure 4.24). Acylation of the enantioenriched secondary alcohol **115** provided the acetate **119**. Subjection to Ireland-Claisen reaction conditions using KHMDS and TMSCl gave the desired carboxylic acid **121** that was esterified to provide methyl ester **122**. Synthesis of the Weinreb amide **117** and subsequent addition of vinylmagnesium bromide provided the enantioenriched vinyl ketone **118** in 90% ee.

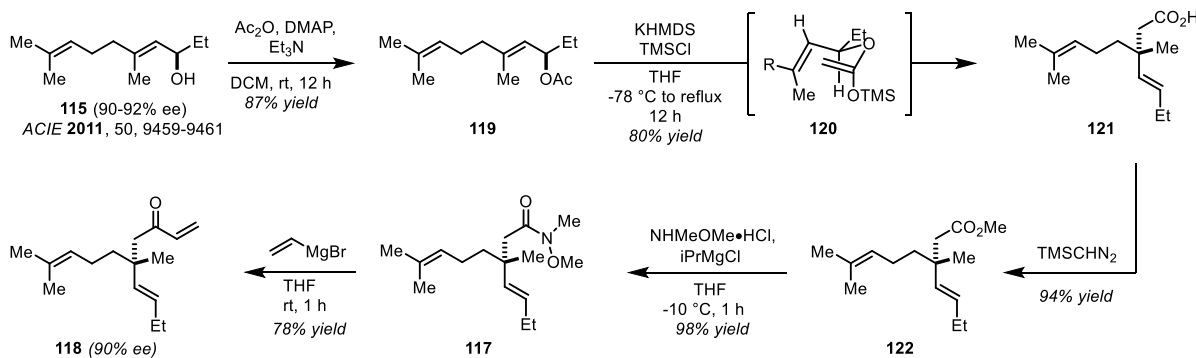


Figure 4.24 Asymmetric synthesis of chiral vinyl ketone **118** via an Ireland-Claisen strategy

The enantioenriched vinyl ketone **118** was subjected to Diels-Alder cycloaddition conditions to provide the desired cycloadduct **123** in 28% yield (Figure 4.25). Conjugate reduction of **123** gave the desired Dieckmann cyclization substrate **124** in 85% yield. Subjecting the enantioenriched Dieckmann substrate **124** gave the Dieckmann cyclization product **125** (ketone- and enol- tautomers) in 92% yield.

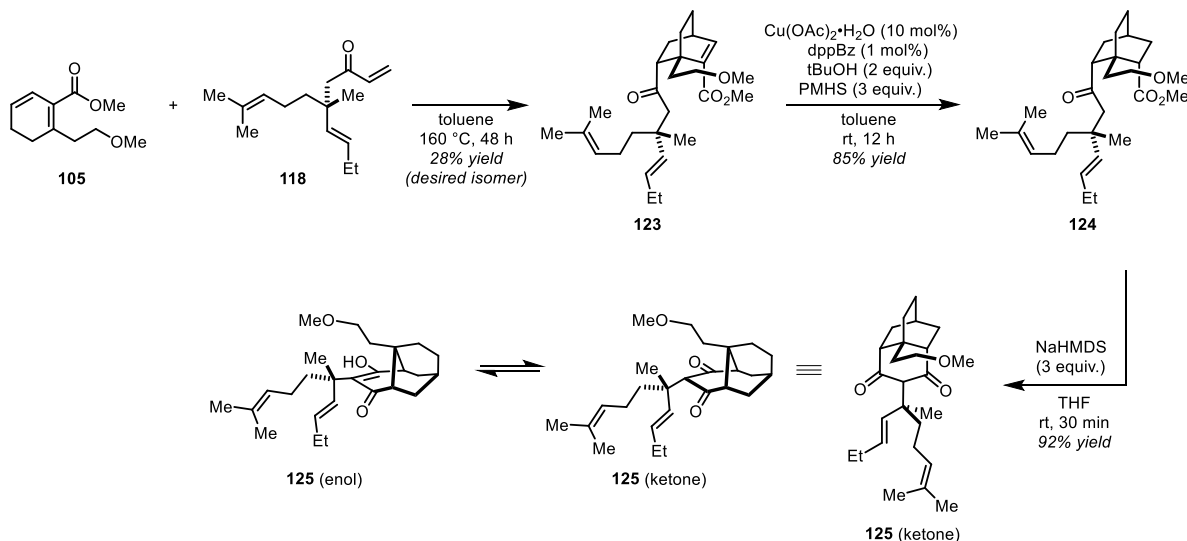


Figure 4.25 Synthesis of the key cyclic 1,3-dione **125** required for the synthesis of atropurpuran via NaHMDS-mediated Dieckmann cyclization

We then turned our focus to forming the tetracyclic core **126** (Figure 4.26). Although we recognized the challenging of conducting a substitution reaction with a methyl ether leaving group in **125**, we had developed a route to the 1,3-dione and thought it would be worth investigating with the material we had in hand. We initially attempted acidic conditions in hopes of activating the methyl ether in **125**. Unfortunately, we found that the use of Bronsted acids led to rapid decomposition even at low temperatures. We suspected that these decomposition pathways resulted from reactivity with the olefins or methyl ether deprotection. Turning to Lewis acids we found no reactivity even at elevated temperatures. Addition of DIPEA also did not promote the reaction.

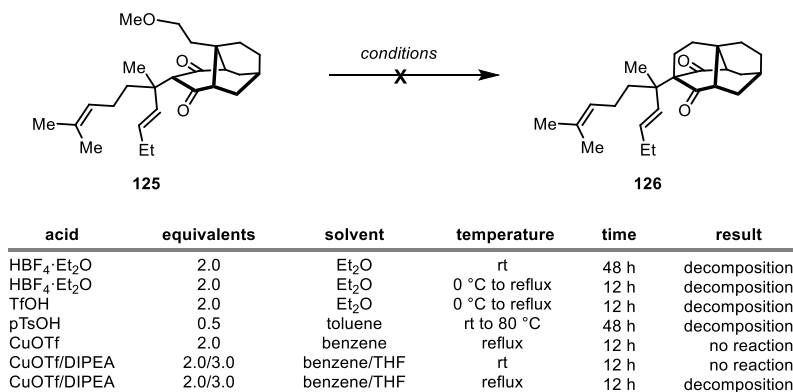


Figure 4.26 Acid-mediated approach to tetracycle formation

We then shifted our focus to basic conditions to enable the cyclization of **125** to the **126** (Figure 4.27). We attempted flooding the system with base but found no conversion of our starting material at room temperature or heating in benzene or THF. Switching to DMF as a solvent and heating led to decomposition of our material.

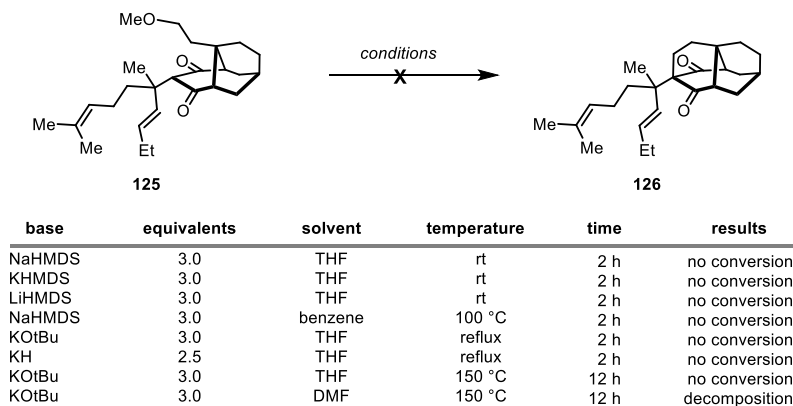


Figure 4.27 Base-mediated approach to tetracycle formation

Having observed no conversion of our starting material, we questioned whether the enolate could form in this complex, polycyclic system **125** (Figure 4.28). Such an experiment would elucidate if cyclization of this complex structure was at all viable. We conducted the experiment using KOtBu in d₈-THF. TLC analysis again showed no conversion of the starting material **125**, however, NMR showed that all the starting material had been consumed. This led us to propose that the enolate **127** did indeed form. To confirm this, we quenched the reaction with iodomethane and isolated the methyl enol ether **128**. This result suggested that enolate formation, which is the first step required for cyclization, was indeed possible.

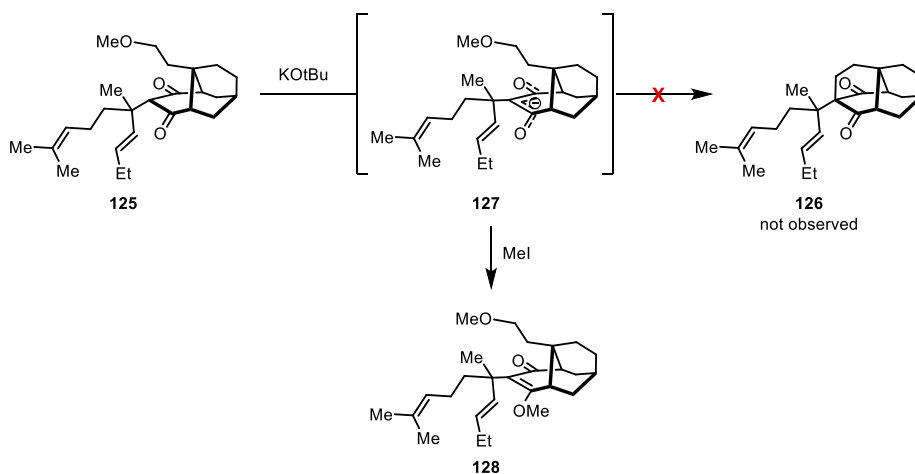


Figure 4.28 Study of enolate formation in base-mediated approach for tetracycle formation

Lastly, we considered dual activation of **125** using L-proline. We hoped that condensation of the proline to form enamine **129** would activate the 1,3-dione for cyclization while the carboxylic acid would protonate the methyl ether and activate it for substitution (Figure 4.29). Subjecting the 1,3-dione **125** to proline in DMF at elevated temperatures gave full conversion to a mixture of products, which were identified as the diastereomers **130** that arise from an alternative reaction pathway. After condensation of proline, the resultant enamine **131** activates the olefin for addition of water to give **132**. The alcohol in **132** recyclizes onto the enamine to give the furan **130** as a mixture of diastereomers. Similar results were obtained using toluene and benzene as the solvent. Attempts to capture the water by using rigorously anhydrous conditions (drying and distilling the solvents) as well as adding molecular sieves or sodium sulfate to capture exogenous water failed to prevent the hydration and cyclization event. As such, we suspect that the addition of water across the olefin must happen intramolecularly with the addition of the amine.

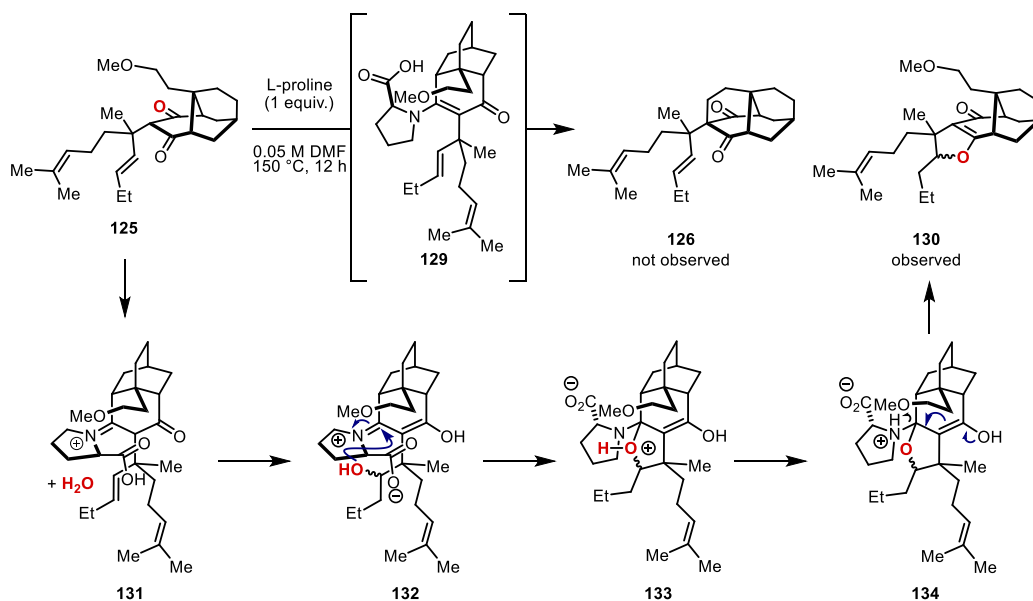


Figure 4.29 Organocatalytic approach to tetracycle formation

At this point it was apparent that the methyl ether protecting group was not the most optimal for a substitution reaction. We turned to our modular synthesis of the diene **90** to attempt to incorporate a good leaving group at that position (mesylate, tosylate, silyl, iodide in Figure 4.16). Unfortunately, these dienes did not survive the Diels-Alder cycloaddition. This led us to consider conducting a late-stage functional group conversion of the methyl ether in our 1,3-dione **125** to a suitable leaving group **135** (Figure 4.30). Conditions for methyl ether deprotection (pTsOH, HBF₄ Et₂O, I₂SiH₂, BBr₃, BI₃, Br-9-BBN, I-9-BBN) did not provide any of the desired deprotected methyl ether or derivatized alcohol **135**. Complex reaction mixtures led us to suspect that such reagents were conducive to react with the olefins and result in undesired products.

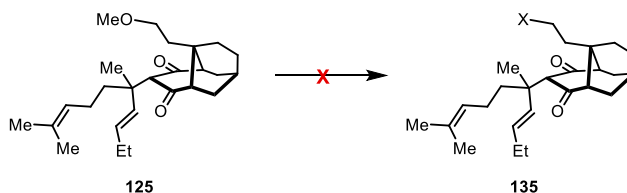


Figure 4.30 Functional group conversion of methyl ether into a good leaving group

We decided to turn to model systems to evaluate what reagent would be best-suited to deprotect and derivatize the methyl ether (Figure 4.31). Using a simple model system that is devoid of olefins we subjected the unsubstituted 1,3-dione bearing a methyl ether **136** to iodination conditions using TMSI/NaI as an alternative to TMSI.²⁴ We were very pleased to find that these conditions

provided the iodide **167** in 67% yield. Importantly, we found that this iodide **137** easily underwent substitution in the presence of KOtBu to give the tetracycle **138** in quantitative yield. Furthermore, we found that prolonged reaction time for the iodination of **136** allowed for tandem cyclization, giving rise to the tetracycle **138** in a single step. We then evaluated these conditions in a more representative model system bearing a *t*butyl group at the 2-position **139**. Subjection of **139** to TMSCl/NaI gave the desired iodide **140** in 17% yield. The major product observed was the lactone that resulted from alcohol deprotection and retro-Dieckmann. Despite this problematic side-reaction, we were able to access enough of the iodide **140** to evaluate whether or not cyclization would be viable with a system that bore substitution at the 2-position. Subjection of iodide **140** to KOtBu yielded the tetracycle **141** in 88% yield. However, when we attempted to access the iodide using these same conditions in the substrate for our synthesis **125**, we did not observe any iodide **142** or even lactone. We solely recovered a complex mixture of products. Again, we suspected that the olefins may be posing additional problems due to their high reactivity.

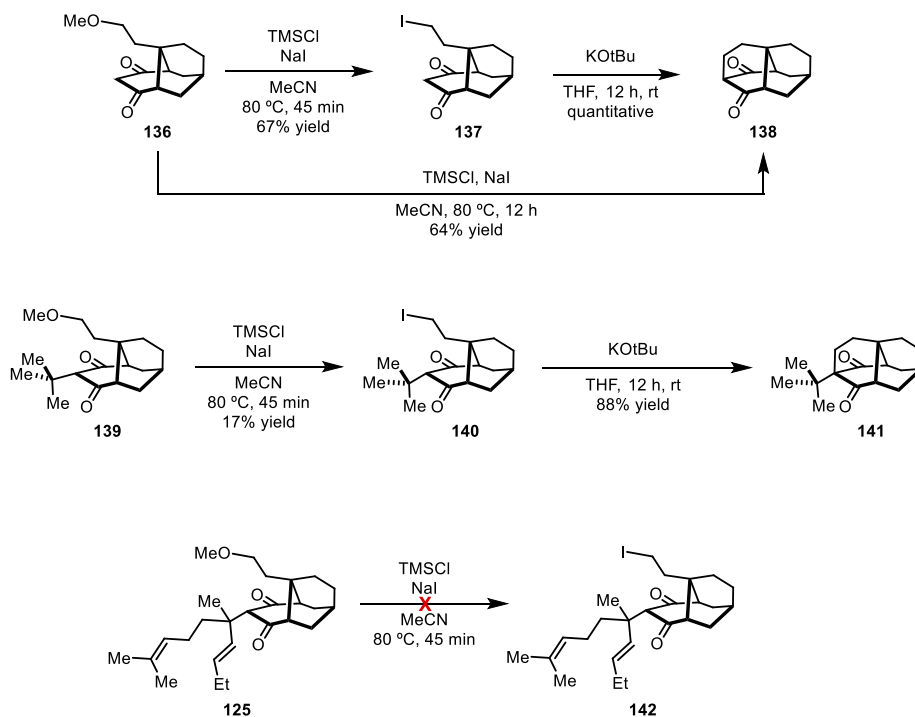


Figure 4.31 Conversion of methyl ether to iodide using TMSCl/NaI in model systems and actual system for the synthesis

At this point, we decided that we would turn away from the cyclization and focus on the ozonolysis as this would serve as a solution to our olefin problem (Figure 4.32). Ozonolysis of the 1,3-dione

125 did not give dialdehyde **143**, but aldehyde **144** and acetal **145** instead (both as mixtures of diastereomers). Importantly, both products are devoid of the problematic olefins and have also have pseudo-protected the 1,3-dione.

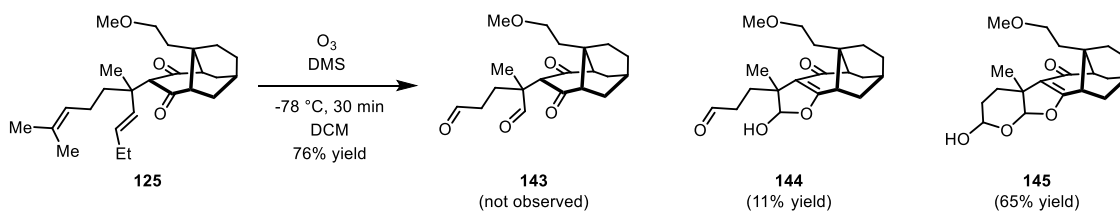


Figure 4.32 Ozonolysis of cyclic 1,3-dione

We decided to exploit the acetal **145** in a route towards our desired iodide by trapping it in the form of a lactone **146** (Figure 4.33). Subjection to our previously investigated iodination conditions (TMSCl/NaI) still yielded complex reaction mixtures, however, HRMS analysis of the crude reaction mixtures had peaks that were associated with the corresponding iodide and lactol that comes from the intermediate free alcohol produced. Evaluation of other iodination protocols for ethers allowed us access the iodide **147** using BI_3 in toluene at elevated temperatures. Reduction to the acetal **148** and subjection to $KOtBu$ gave the tetracycle **149**.

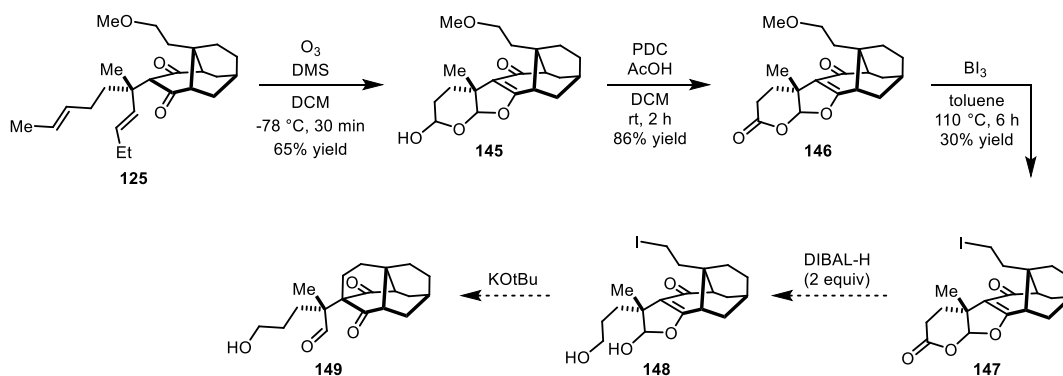


Figure 4.33 Strategy towards tetracycle formation relying on initial ozonolysis

Taking advantage of the promising reactivity of BI_3 , we also investigated an alternative route to the tetracycle directly from the Dieckmann product **125** (Figure 4.34). Subjection of the 1,3-dione **125** to the BI_3 gave a mixture of products that were observed by HRMS. While the desired iodide **150** did form, another bis-iodinated product **151** was also observed, presumably coming from hydroiodination of the olefin. Beyond the products that now bore an iodide instead of the methyl ether, lactones **152** and **153** that resulted from the intermediate alcohol were also observed. We hypothesized that subjection of this reaction mixture containing **150** and **151** to an excess of base

would enable cyclization and ultimately eliminate the iodide in **151** to return the olefin in **154**. Indeed, we found that subjection of this mixture of products provided small quantities of the desired tetracyclic **154**.

Preliminary Results: all products observed by HRMS

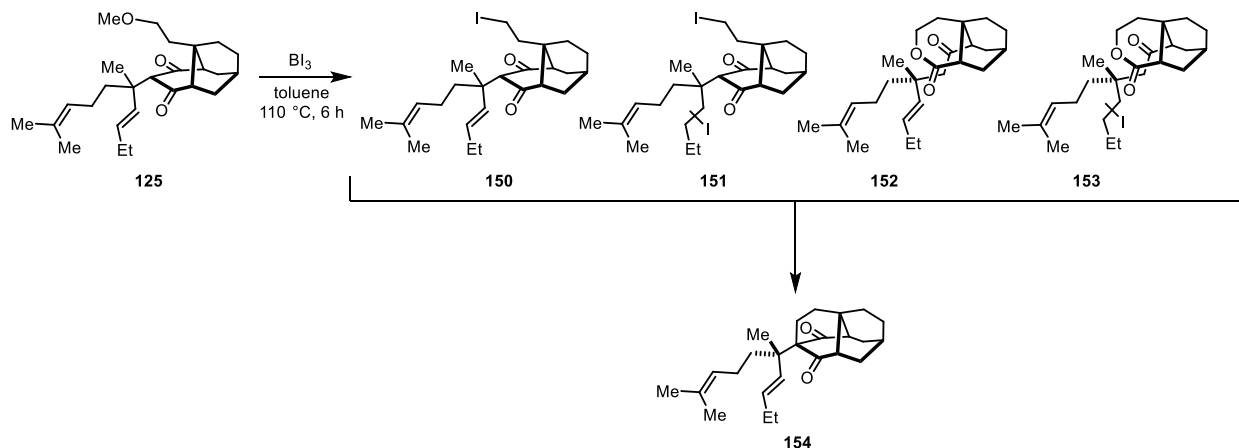


Figure 4.34 Alternative strategy for tetracycle formation

With two possible routes towards the tetracycle in hand, we have several options for the completion of the synthesis of atropurpuran and the arcutines (Figure 4.35). Starting from **149**, reduction and subsequent protection will give the protected diol **155**. Subjection of **155** to site-selective C-H oxidation condition is expected to oxidize the most electron-rich and sterically accessible C-H bond, providing ketone **156**. Olefination and oxidation will provide the enone **157**. Subsequent deprotection of both alcohols will provide the acetal **158a**, which the energetically favored regio- and diastereoisomer. Iodination of **158a** and subsequent SmI_2 -mediated Barbier reaction will provide **159**. Alternatively, if we proceed with tetracyclic **160**, ozonolysis will give the dialdehyde **161**. Reduction and protection will provide **155**, which intercepts the route previously described.

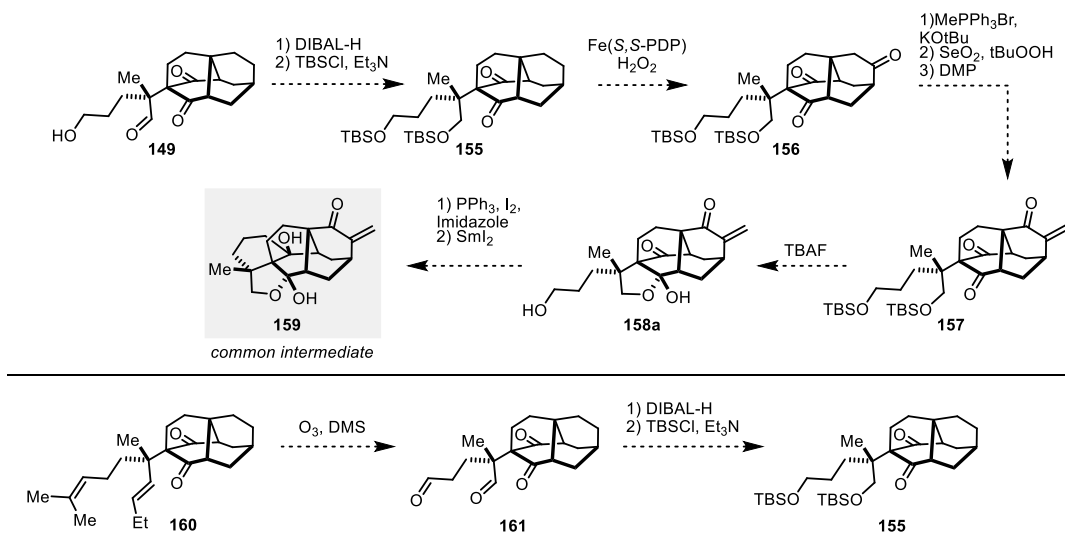


Figure 4.35 Synthesis of common intermediate (**159**) for the synthesis of atropurpuran and the arcutines

Preliminary investigations provide support for the selective C-H oxidation and diastereoselective acetal formation. The protocol described by White et al.²⁵ suggests that the most electron-rich and sterically-accessible C-H bond will preferentially be oxidized. Preliminary investigations in a model substrate **162** primarily gave two products that were oxidized at the bridgehead position of the bicyclo[2.2.2]octane, **163** and **164**, with the major product **163** bearing oxidation of the most distal methylene of the bridgehead (Figure 4.36). This selectivity can be attributed to the presence of two electron-withdrawing carbonyls of the ketone and lactone in **162**, of which the lactone also serves to deactivate the methylenes of the lactone ring. Similar functionalities are observed in our proposed substrate **155**. We expect that the two carbonyls of the 1,3-dione will deactivate the methylenes of the tetracycle that are in close proximity, favoring **156** in a similar fashion to what we observed in our model studies. This selectivity is also aided by the deactivation of the external alkyl chain by the protected alcohols in **155**.

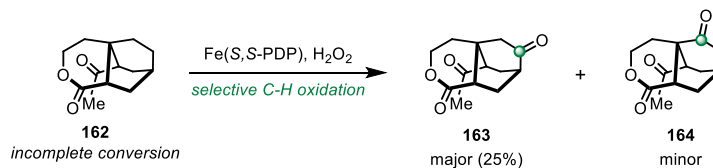


Figure 4.36 Preliminary investigations of selective C-H oxidation in model system

In terms of the selective formation of the acetal, DFT energy calculations (Q-Chem, B3LYP [6-31G**]) suggest that the diol **165** will preferentially form the acetal **157a** over all other regio- and diastereoisomers (favored by >6 kcal/mol over **157b-d**, Figure 4.37). The energetic preference for **157a** over **157b** is due to the chiral center as the steric interactions between the tetracycle and the methyl group in **157a** are more tolerated than they are with the longer alkyl chain in **157b**. The other two possible diastereoisomers, **157c** and **157d**, are far higher in energy, which is attributed to the eclipsing interaction along the carbon-carbon bond between the 2-carbon and 3'-carbon. Altogether, these results demonstrate how the single chiral center in **165** will enable the enantioselective synthesis of atropurpuran and the arcutines once the tetracycle is in place. Although these calculations were conducted for the substrate **165** that is devoid of functionality along the bridgehead, the same results are expected in **157** due to the fact that the two key components – the chiral center and the tetracycle – are in place.

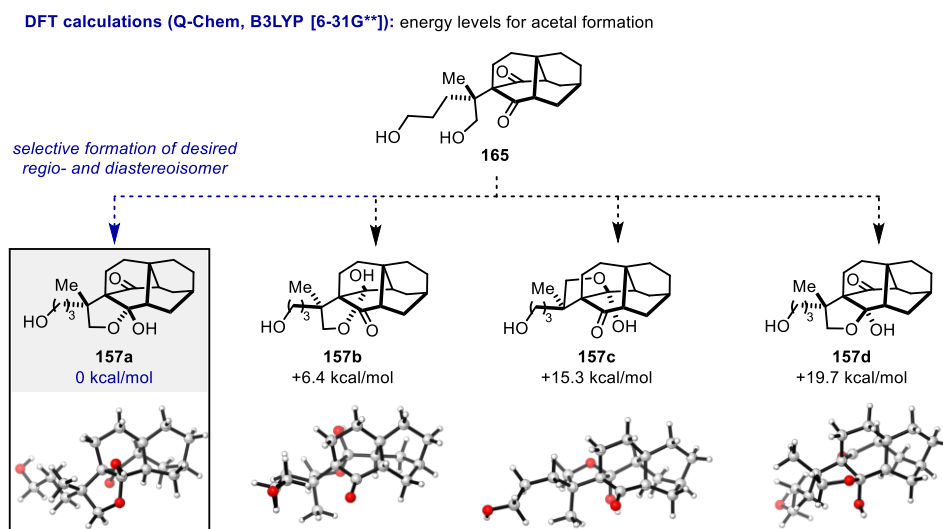


Figure 4.37 DFT energy calculations for selective acetal formation

The final stages of the synthesis are based on the common intermediate **159** and are well-established in this complex setting (Figure 4.38). Oxidation of **159** and dehydration will give **166**, which is preceded to undergo a diastereoselective reduction with $\text{NaBH}(\text{OMe})_3$ to give atropurpuran (**1**).^{15,16} Alternatively, a two-step protocol conducted by Li^{19} will give arcutinidine (**2**), which can be used to access arcutine and arcutinine.

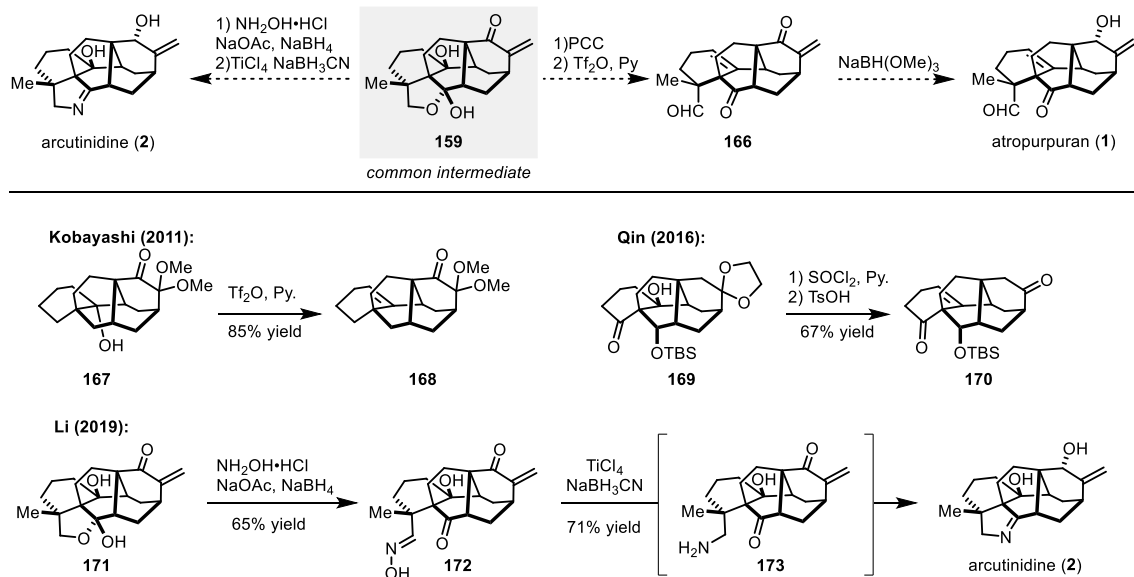


Figure 4.38 Synthesis of atropurpuran (1) and the arcutines (2-4) from the common intermediate 159

4.5 Conclusion

Our unique approach to atropurpuran (1) and the arcutines (2-4) takes advantage of their inherent symmetry and reactivity by relying on a key Dieckmann cyclization product (66, Figure 4.12). Our evaluation of various Dieckmann cyclization strategies has resulted in a route towards the key Dieckmann cyclization product 66. Importantly, we have developed a concise route to the enantioenriched vinyl ketone 118, which is the only chiral substrate required for the synthesis and is predicted to then enable diastereoselective bond formation in subsequent steps. There are four major challenges that remain for these natural products – tetracycle formation, ozonolysis, and selective C-H oxidation. Preliminary investigations of these steps suggest that they should be conducted in an alternate order than what was proposed in our original retrosynthetic analysis (Figure 4.12). A path forward will most likely rely on initial ozonolytic cleavage prior to tetracycle formation in order to eliminate the side-reactivity posed by the olefins as well as the competing retro-Dieckmann reaction of 1,3-dione moiety in 66. Furthermore, we found that the inherent

reactivity of the substrate is inclined to undergo site-selective C-H oxidation of the desired bridgehead carbon. More importantly, the single chiral center in dione **66** is predicted to enable subsequent diastereoselective C-C bond formation to provide an enantioselective total synthesis.

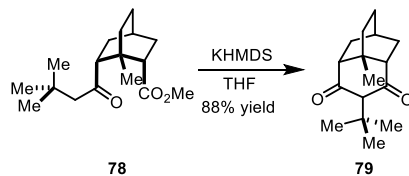
4.6 Experimental Details

4.6.1 General Information

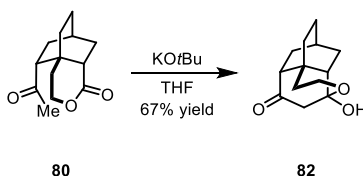
Unless otherwise noted, all reactions were performed in oven-dried glassware under an atmosphere of nitrogen. All chemicals were purchased from commercial suppliers and were used without further purification. Anhydrous nitromethane (MeNO₂) and anhydrous 1,2-dichloroethane (DCE) were obtained from Acros Organics and were used as received. Flash chromatography was performed using Biotage Isolera One ACI™ Accelerated Chromatography Isolation system on Silicycle Silia Flash® 40-63 micron (230-400 mesh). Proton Nuclear Magnetic Resonance NMR (¹H NMR) spectra and carbon nuclear magnetic resonance (¹³C NMR) spectra were recorded on a Varian Unity Plus 400, Varian MR400, Varian vnmrs 500, Varian Inova 500, Varian Mercury 500, and Varian vnmrs 700 spectrometers. Chemical shifts for protons are reported in parts per million and are referenced to the NMR solvent peak (CDCl₃: δ 7.26; CD₃OD: δ 4.87). Chemical shifts for carbons are reported in parts per million and are referenced to the carbon resonances of the NMR solvent (CDCl₃: δ 77.16; CD₃OD: δ 49.00). Data are represented as follows: chemical shift, integration, multiplicity (br = broad, s = singlet, d = doublet, t = triplet, q = quartet, p = pentet, m = multiplet), and coupling constants in Hertz (Hz). Mass spectroscopic (MS) data was recorded at the Mass Spectrometry Facility at the Department of Chemistry of the University of Michigan in Ann Arbor, MI on an Agilent Q-TOF HPLC-MS with ESI high resolution mass spectrometer. Infrared (IR) spectra were obtained using either an Avatar 360 FT-IR or Perkin Elmer Spectrum BX FT-IR spectrometer. IR data are represented as frequency of absorption (cm⁻¹).

4.6.2. Base-Mediated Dieckmann Cyclization in Model Systems

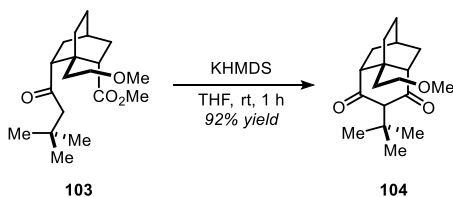
General Procedure for the base-mediated Dieckmann cyclization: To a solution of the substrate in THF (0.1 M) was added base (1.5-2 equiv.) Let reaction stir at room temperature for one hour and then quenched with 1M HCl and extracted with ethyl acetate (3x). Washed with brine, dried over sodium sulfate, filtered, and concentrated. Purified using ethyl acetate:hexanes.



3-(tert-butyl)-8a-methylhexahydro-1,6-methanonaphthalene-2,4(1H,3H)-dione (79) was obtained using 2 equivalents of KHMDS. $^1\text{H NMR}$ (400 MHz, cdCl_3) δ 4.04 (s, 1H), 2.41 (dd, $J = 11.4, 1.7$ Hz, 2H), 2.03 – 1.82 (m, 5H), 1.71 – 1.60 (m, 2H), 1.53 (dd, $J = 12.8, 4.8$ Hz, 3H), 1.16 (s, 9H), 1.01 (dd, $J = 7.2, 5.4$ Hz, 2H), 0.67 (s, 3H); $^{13}\text{C NMR}$ (176 MHz, cdCl_3) δ 207.07, 63.89, 54.19, 31.31, 30.99, 29.72, 27.85, 27.59, 26.92, 24.82, 23.44.

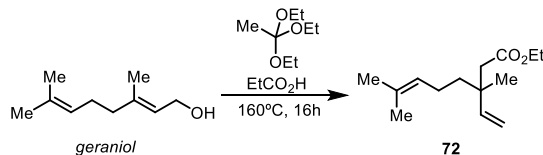


(10aR)-4-hydroxyoctahydro-4,10a,8-(epiethane[1,1,2]triy)benzo[d]oxocin-6(6aH)-one (82) was obtained in 67% yield using 1.5 equivalents of KOtBu. $^1\text{H NMR}$ (700 MHz, cdCl_3) δ 4.04 (s, 1H), 3.33 (t, $J = 7.0$ Hz, 2H), 3.23 (s, 3H), 2.54 (d, $J = 10.0$ Hz, 2H), 1.97 (t, $J = 12.8$ Hz, 2H), 1.90 – 1.81 (m, 3H), 1.65 – 1.58 (m, 3H), 1.19 (t, $J = 6.1$ Hz, 3H), 1.14 (s, 9H). $^{13}\text{C NMR}$ (100 MHz, cdCl_3) δ 212.46, 99.87, 61.84, 50.74, 44.31, 43.00, 36.78, 32.11, 31.89, 31.02, 28.33, 25.99, 24.06.

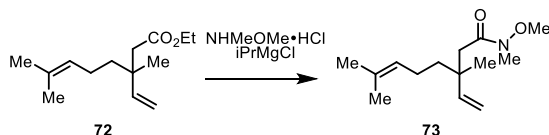


3-(tert-butyl)-8a-(2-methoxyethyl)hexahydro-1,6-methanonaphthalene-2,4(1H,3H)-dione (104) was obtained in 92% yield using 2.0 equivalents of KHMDS. $^1\text{H NMR}$ (700 MHz, cdCl_3) δ 4.04 (s, 1H), 3.33 (t, $J = 7.0$ Hz, 2H), 3.23 (s, 3H), 2.54 (d, $J = 10.0$ Hz, 2H), 1.97 (t, $J = 12.8$ Hz, 1H), 1.90 – 1.81 (m, 1H), 1.61 (s, 1H), 1.19 (t, $J = 6.1$ Hz, 1H), 1.14 (s, 1H). $^{13}\text{C NMR}$ (176 MHz, cdCl_3) δ 206.51, 67.88, 63.89, 58.43, 52.41, 36.37, 31.17, 29.61, 29.58, 27.69, 26.88, 26.45, 23.10.

4.6.3. Synthesis of Racemic Vinyl Ketone

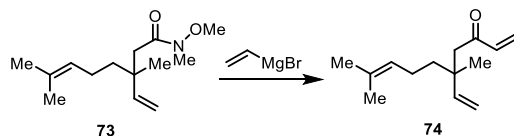


Ethyl 3,7-dimethyl-3-vinyloct-6-enoate (72): A pressure flask equipped with a magnetic stir bar was charged with geraniol (1 equiv.), triethyl orthoacetate (1 M) and propionic acid (10 mol%), sealed and heated at 160 °C in a oil bath during 16 h. The reaction mixture was then cooled down and poured over a mixture of ethyl acetate and 1 M solution of hydrochloric acid (1:1, 2mL/mmol). After stirring for 15 minutes the aqueous phase was extracted with ethyl acetate (3x) and the combined organic phases were washed with brine, dried over sodium sulfate and filtered. The solvents were evaporated in vacuo and the crude was purified via silica gel flash chromatography (hexanes:ethyl acetate 50:1 to 20:1) to give the ester **72** in 95% yield. $^1\text{H NMR}$ (400 MHz, CDCl_3) δ 5.82 (dd, $J = 17.5, 10.8$ Hz, 1H), 5.07 (dd, $J = 7.7, 6.5$ Hz, 1H), 4.99 (ddd, $J = 18.4, 14.2, 0.9$ Hz, 2H), 4.10 (q, $J = 7.1$ Hz, 2H), 2.31 (s, 2H), 1.96 – 1.86 (m, 2H), 1.67 (s, 2H), 1.58 (s, 2H), 1.45 – 1.37 (m, 2H), 1.24 (t, $J = 7.1$ Hz, 3H), 1.13 (s, 3H).



N-methoxy-N,3,7-trimethyl-3-vinyloct-6-enamide (73): A flame-dried round bottom flask equipped with an addition funnel and a magnetic stir bar was charged with ester **72** (1 equiv.) in THF (0.3 M) and N,O-dimethylhydroxylamine hydrochloride (1.55 equiv.). The reaction mixture was set at -10 °C and isopropylmagnesium bromide (2 M in THF, 3 equiv.) was added dropwise. After the addition was complete, the reaction was let to stir at -10 °C for 30 minutes and another additional 30 minutes at rt. Complete conversion was confirmed by TLC after this time. The reaction mixture was quenched with a saturated solution of ammonium chloride. The aqueous phase was extracted with ethyl acetate (x3) and the combined organic phases were washed with brine, dry over sodium sulfate and filtered. The solvents were evaporated in vacuo and the crude was purified via silica gel flash chromatography (hexanes:ethyl acetate 6:1) to give the Weinreb amide **73** in 91% yield. $^1\text{H NMR}$ (700 MHz, CDCl_3) δ 5.90 (dd, $J = 17.5, 10.8$ Hz, 1H), 5.09 (tt, $J = 7.1, 1.4$ Hz, 1H), 5.02 (dd, $J = 10.8, 1.2$ Hz, 1H), 4.96 (dd, $J = 17.5, 1.2$ Hz, 1H), 3.66 (s, 3H),

3.15 (s, 3H), 2.48 (d, J = 14.3 Hz, 1H), 2.42 (d, J = 14.2 Hz, 1H), 1.91 (q, J = 8.0 Hz, 2H), 1.66 (s, 1H), 1.58 (s, 1H), 1.54 – 1.43 (m, 2H), 1.16 (s, 3H); ¹³C NMR (100 MHz, CDCl₃) δ 146.34, 131.32, 124.84, 111.82, 61.13, 41.36, 40.93, 39.76, 25.83, 23.15, 23.06, 17.74.



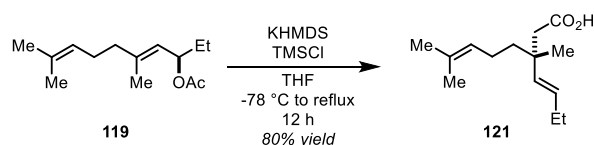
5,9-dimethyl-5-vinyldeca-1,8-dien-3-one (74): A flame-dried round bottom flask equipped with an addition funnel and a magnetic stir bar was charged with amide **73** (1 equiv.) in THF (0.3 M). This solution was set at 10 °C and vinylmagnesium bromide (0.7 M in THF, 2.5 equiv.) was added slowly. After 15 minutes complete conversion was confirmed by TLC. The mixture was cooled to 0 °C, diluted with diethyl ether (5 mL/mmol) and slowly quenched with a saturated solution of ammonium chloride (5mL/mmol). The salts formed during quenching were dissolved by slowly adding a 1 M solution of hydrochloric acid (2.5 mL/mmol) at 0 °C. The aqueous phase was extracted with diethyl ether (3x) and the combined organic phases were washed with brine, dry over sodium sulfate and filtered. The solvents were evaporated in vacuo and the crude was purified via silica gel flash chromatography (hexanes:ethyl acetate 6:1) to give the vinyl ketone **74** in 88% yield. ¹H NMR (700 MHz, CDCl₃) δ 6.34 (dd, J = 17.5, 10.6 Hz, 1H), 6.15 (dd, J = 17.6, 1.2 Hz, 1H), 5.83 (dd, J = 17.5, 10.8 Hz, 1H), 5.72 (dd, J = 10.6, 1.2 Hz, 1H), 5.07 (tt, J = 7.1, 1.5 Hz, 1H), 5.02 (dd, J = 10.8, 1.1 Hz, 1H), 4.93 (dd, J = 17.5, 1.1 Hz, 1H), 2.59 (d, J = 14.1 Hz, 1H), 2.55 (d, J = 14.1 Hz, 1H), 1.89 (q, J = 7.7 Hz, 2H), 1.66 (s, 2H), 1.58 (s, 3H), 1.50 – 1.37 (m, 2H), 1.12 (s, 3H); ¹³C NMR (100 MHz, CDCl₃) δ 199.83, 145.95, 137.90, 131.53, 127.71, 124.58, 112.25, 49.98, 40.91, 39.88, 25.82, 23.22, 23.02, 17.73.

4.6.4 Synthesis of Enantioenriched Vinyl Ketone

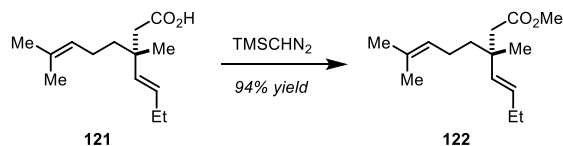


(R,E)-5,9-dimethyldeca-4,8-dien-3-yl acetate (119): To an oven-dried RBF containing substrate was added DCM (3 mL/mmol) and DMAP (0.1 equiv). Freshly distilled triethylamine (2.0 equiv) was then added. Let stir for 20 minutes then added acetic anhydride (2.0 equiv.). Let stir at room temperature overnight. Added water and extracted 3x with DCM. Washed with brine, dried over sodium sulfate, filtered, and concentrated. Purified using flash column chromatography (2%

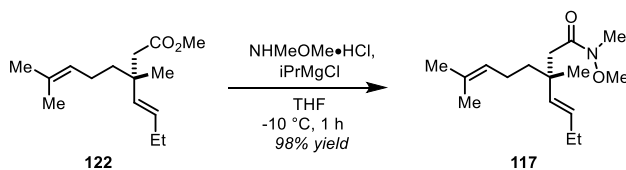
EtOAc/Hex) to give the acetate **119** in 87% yield. $^1\text{H NMR}$ (500 MHz, cdCl_3) δ 5.42 (dt, $J = 9.0$, 6.8 Hz, 1H), 5.12 – 5.02 (m, 2H), 2.14 – 2.06 (m, 2H), 2.02 (s, 3H), 1.71 (s, 3H), 1.67 (s, 3H), 1.60 (s, 1H), 1.55 – 1.47 (m, 1H), 0.89 – 0.82 (t, $J = 7.5$ Hz 3H).



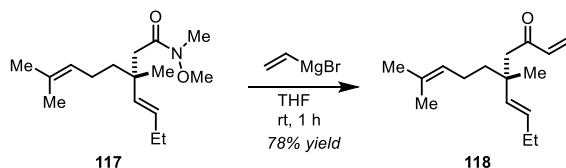
(R,E)-3-(but-1-en-1-yl)-3,7-dimethyloct-6-enoic acid (120): An oven-dried RBF was charged with the substrate and THF (0.1 M). A solution of KHMDS (1.39 equiv) in THF (6.97 M) was added to the solution at -78 °C. Let stir for 15 min then TMSCl (2 equiv) was added slowly. Let stir at -78 °C for 15 min and then let warm up to room temperature and then heated at reflux overnight. After stirring overnight, let cool to room temperature and then added 1M HCl and let stir for three hours. Then extracted with ethyl acetate. Washed with brine. Dried over magnesium sulfate, filtered, and concentrated. Purified by flash column chromatography (1:5 EtOAc:Hex) to give 80% yield of carboxylic acid **121**. $^1\text{H NMR}$ (500 MHz, cdCl_3) δ 5.46 – 5.36 (m, 2H), 5.08 (dd, $J = 8.3$, 5.9 Hz, 1H), 2.33 (s, 2H), 2.03 (qd, $J = 7.5$, 4.9 Hz, 2H), 1.91 (dd, $J = 16.7$, 7.2 Hz, 2H), 1.67 (s, 3H), 1.58 (s, 3H), 1.42 (td, $J = 7.3$, 3.6 Hz, 2H), 1.14 (s, 3H), 0.97 (t, $J = 7.5$ Hz, 3H).



methyl (R,E)-3-(but-1-en-1-yl)-3,7-dimethyloct-6-enoate (121): To an oven-dried RBF was added substrate and THF (1 ML) and MeOH (1 M). Flask was cooled to 0 °C and TMSdiazomethane (1.3 equiv, 2.0 M) was added drop wise. Removed from bath once addition was complete and let stir at room temperature for 15 min. Removed volatiles and then proceeded to next step without purification. $^1\text{H NMR}$ (500 MHz, cdCl_3) δ 5.39 – 5.35 (m, $J = 2.9$ Hz, 2H), 5.11 – 5.05 (m, $J = 6.6$ Hz, 1H), 2.05 – 1.98 (m, 2H), 1.94 – 1.85 (m, $J = 16.1$, 7.0 Hz, 2H), 1.67 (s, 3H), 1.57 (s, 3H), 1.38 (dd, $J = 11.1$, 6.0 Hz, 2H), 1.30 – 1.23 (m, $J = 11.3$ Hz, 2H), 1.11 (s, 3H), 0.96 (dd, $J = 10.1$, 4.8 Hz, 3H), 0.88 (t, $J = 6.1$ Hz, 2H).

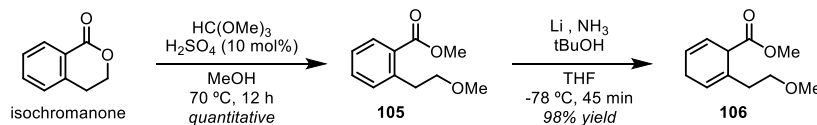


(R,E)-3-(but-1-en-1-yl)-N-methoxy-N,3,7-trimethyloct-6-enamide (117): A flame-dried round bottom flask equipped with an addition funnel and a magnetic stir bar was charged with ester **72** (1 equiv.) in THF (0.3 M) and N,O-dimethylhydroxylamine hydrochloride (1.55 equiv.). The reaction mixture was set at -10 °C and isopropylmagnesium bromide (2 M in THF, 3 equiv.) was added dropwise. After the addition was complete, the reaction was let to stir at -10 °C for 30 minutes and another additional 30 minutes at rt. Complete conversion was confirmed by TLC after this time. The reaction mixture was quenched with a saturated solution of ammonium chloride. The aqueous phase was extracted with ethyl acetate (3x) and the combined organic phases were washed with brine, dry over sodium sulfate and filtered. The solvents were evaporated in vacuo and the crude was purified via silica gel flash chromatography (hexanes:ethyl acetate 6:1) to give the Weinreb amide **117** in 98% yield. ¹H NMR (500 MHz, cdcl₃) δ 5.40 (ddd, *J* = 22.0, 15.7, 10.9 Hz, 2H), 5.10 (t, *J* = 6.7 Hz, 1H), 2.41 (dd, *J* = 46.4, 13.9 Hz, 2H), 2.03 (p, *J* = 7.3 Hz, 2H), 1.90 (dd, *J* = 15.9, 7.9 Hz, 2H), 1.66 (s, 3H), 1.58 (s, 3H), 1.51 – 1.42 (m, 2H), 1.14 (s, 3H), 0.97 (t, *J* = 7.5 Hz, 3H).

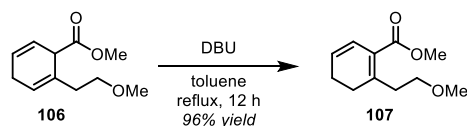


(R,E)-5-(but-1-en-1-yl)-5,9-dimethyldeca-1,8-dien-3-one (118): A flame-dried round bottom flask equipped with an addition funnel and a magnetic stir bar was charged with amide **117** (1 equiv.) in THF (0.3 M). This solution was set at 10 °C and vinylmagnesium bromide (0.7 M in THF, 2.5 equiv.) was added slowly. After 15 minutes complete conversion was confirmed by TLC. The mixture was cooled to 0 °C, diluted with diethyl ether (5 mL/mmol) and slowly quenched with a saturated solution of ammonium chloride (5mL/mmol). The salts formed during quenching were dissolved by slowly adding a 1 M solution of hydrochloric acid (2.5 mL/mmol) at 0 °C. The aqueous phase was extracted with diethyl ether (3x) and the combined organic phases were washed with brine, dry over sodium sulfate and filtered. The solvents were evaporated in vacuo and the crude was purified via silica gel flash chromatography (hexanes:ethyl acetate 6:1) to give the vinyl ketone **118** in 88% yield. ¹H NMR (500 MHz, cdcl₃) δ 6.34 (dd, *J* = 17.5, 10.5 Hz, 1H), 6.13 (d, *J* = 17.5 Hz, 1H), 5.70 (d, *J* = 10.6 Hz, 1H), 5.44 – 5.29 (m, 2H), 5.08 (t, *J* = 7.0 Hz, 1H), 2.54 (dd, *J* = 39.7, 13.6 Hz, 2H), 2.06 – 1.98 (m, 2H), 1.89 (dd, *J* = 15.7, 8.0 Hz, 2H), 1.66 (s, 3H), 1.58 (s, 3H), 1.44 – 1.37 (m, 2H), 1.09 (s, 3H), 0.96 (t, *J* = 7.5 Hz, 3H).

4.6.5. Synthesis of Key Dieckmann Cyclization Product in the Synthesis of Atropurpuran and the Arcutines

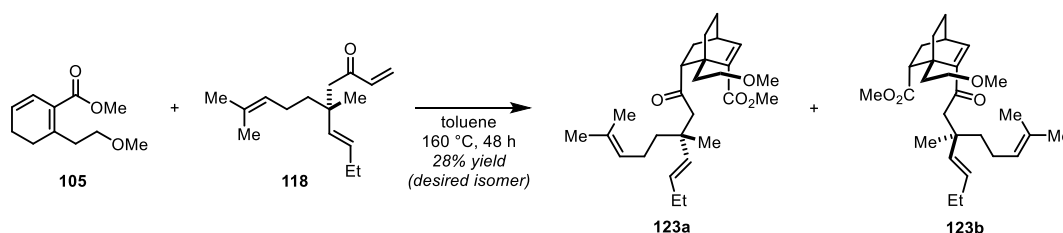


methyl 2-(2-methoxyethyl)cyclohexa-2,5-diene-1-carboxylate (**106**): Isochromanone was dissolved in MeOH (1M) and $\text{HC}(\text{OMe})_3$ (2 equivalents) and 10 mol% H_2SO_4 was added. Let stir at reflux for 12 h. Once cooled, added water and extracted with ethyl acetate (3x). The organic layers were combined and washed with brine, dried over sodium sulfate, filtered, and concentrated to quantitatively give **105**. A flask was charged with methyl ester **105** and tBuOH (1.09 equiv.) in THF (0.285 M). An oven-dried 3-neck round bottom flask was equipped with stir bar and two oven-dried condensers. These condensers were connected to an ammonia tank using a t-joint. The third next was capped with a septum. The glassware was cooled under nitrogen. Then the flask was submerged in an acetone/dry ice bath and ammonia was condensed (0.0515 M). Once condensation of ammonia was complete, the contents of the flask containing the ester **105** were added via a funnel. The reaction was left to stir for two minutes before Li (2.29 equiv) in a single portion. Reaction turned brown then blue within two minutes. The reaction remained blue for about 5min and then turned yellow. Let stir for an additional 40 min then quenched with solid NH_4Cl and saw yellow color dissipate to white. Removed from bath and removed the condensers and septum and let stir (in a secondary container) overnight with a nitrogen line inserted to help evaporate ammonia. Next day, dissolved solid white contents of flask in water and extracted with ethyl acetate (3x). The combined organic layers were washed with brine, dried over sodium sulfate, filtered, and concentrated. The crude product was purified using 4% ethyl acetate/hexanes to give 98% yield of the 1,4-diene **106**. $^1\text{H NMR}$ (500 MHz, CDCl_3) δ 5.95 – 5.85 (m, 1H), 5.73 (ddd, $J = 7.3, 3.7, 2.0$ Hz, 2H), 3.80 – 3.73 (m, 1H), 3.70 (s, 3H), 3.49 (t, $J = 6.8$ Hz, 2H), 3.33 (s, 3H), 2.84 – 2.64 (m, 2H), 2.40 – 2.24 (m, 2H).

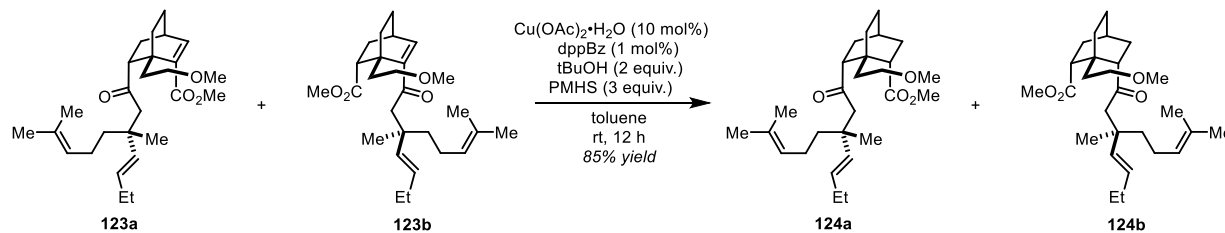


methyl 2-(2-methoxyethyl)cyclohexa-1,5-diene-1-carboxylate (**107**): To an oven-dried RBF was added the substrate **106**, DBU (2.06 equiv), and toluene (0.0635). The flask was sparged

with nitrogen for three hours and then it was equipped with a reflux condenser and let reflux for 12 hours. Once reaction had cooled, it was quenched with saturated NH_4Cl . The contents of the flask were transferred to a separatory funnel using ethyl acetate and then washed with saturated NH_4Cl (3x) and then brine. Dried over sodium sulfate, filtered, and concentrated. The crude product was purified using 4% ethyl acetate/hexanes to give 96% yield of the diene **107**. ^1H NMR (500 MHz, cdcl_3) δ 6.32 (d, $J = 9.8$ Hz, 1H), 5.85 – 5.79 (m, 1H), 3.75 (s, 3H), 3.56 (t, $J = 6.9$ Hz, 2H), 3.35 (s, 3H), 2.84 (t, $J = 6.9$ Hz, 2H), 2.32 (t, $J = 9.5$ Hz, 2H), 2.15 – 2.08 (m, 2H).

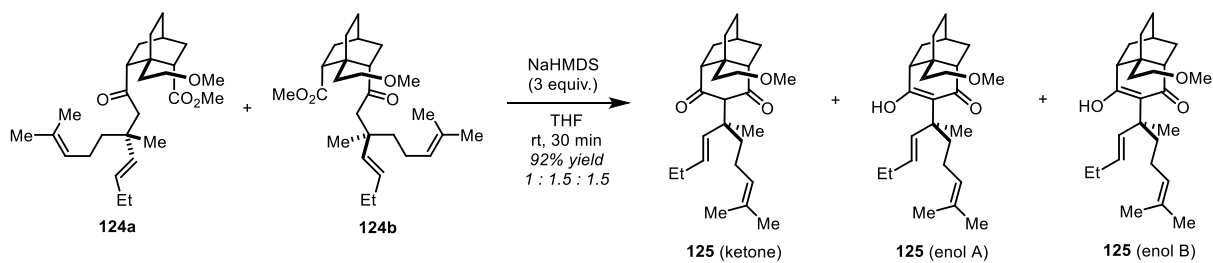


Methyl(1R,4R,6R)-6-((R)-3-((E)-but-1-en-1-yl)-3,7-dimethyloct-6-enoyl)-1-(2-methoxy ethyl) bicyclo[2.2.2]oct-2-ene-2-carboxylate (123a** and **123b**):** To an oven-dried pressure flask was added the diene **105** and vinyl ketone **118** in toluene (0.75 M). Flask was sealed and heated at 160 C in an oil bath for 48 h. The contents of the pressure flask were transferred to a round bottom flask and concentrated. The crude product was purified using 4% ethyl acetate:hexanes to give the desired diastereoisomers **123a** and **123b** as an inseparable mixture in 28% yield. ^1H NMR (500 MHz, CDCl_3) δ 7.29 (dd, 2H), 5.41 – 5.26 (m, 4H), 5.05 (s, 2H), 3.72 (s, 3H), 3.71 (s, 3H), 3.46 (tq, $J = 9.6, 6.1$ Hz, 5H), 3.29 (s, 6H), 2.80 – 2.75 (m, 2H), 2.75 – 2.67 (m, 2H), 2.62 (td, $J = 13.8, 6.0$ Hz, 2H), 2.39 (dd, $J = 85.0, 14.4$ Hz, 2H), 2.04 – 1.97 (m, 4H), 1.88 – 1.72 (m, 9H), 1.65 (s, 3H), 1.65 (s, 3H), 1.56 (s, 3H), 1.55 (s, 3H), 1.53 – 1.44 (m, 3H), 1.37 – 1.33 (m, 4H), 1.32 – 1.26 (m, 2H), 1.26 – 1.20 (m, 4H), 1.05 (s, 3H), 1.00 (s, 3H), 0.96 (t, $J = 7.5$ Hz, 6H).



methyl(1R,2S,4R,6R)-6-((R)-3-((E)-but-1-en-1-yl)-3,7-dimethyloct-6-enoyl)-1-(2-methoxy ethyl) bicyclo[2.2.2]octane-2-carboxylate (124a** and **124b**):** The cycloadducts **123a** and **123b** were added to a flask and dried under vacuo while the reagent was being prepared in a separate flask. To an oven-dried RBF was added $\text{Cu}(\text{OAc})_2 \cdot \text{H}_2\text{O}$ (10 mol%) and dppBz (1 mol%) in the

glovebox. The flask was removed from the glovebox, wrapped in foil and added toluene (1.06 M, freshly distilled from solvent system) and of tBuOH (2 equiv., freshly degassed). Let stir for 40 min and then added PMHS (3 equiv). Saw color turn from blue to green to brown - let stir for another 40 min. The contents of this flask were added to a flask containing the cycloadducts **123a** and **123b**, which was also wrapped in foil. Then used toluene (0.21 M) to rinse contents of flask into the reaction. Let stir for 12 h (prolonged reaction time gave epimerization of products). The reactions were transferred to a separatory funnel using ethyl acetate. They were washed with 1 M NaOH, then 1 M HCl, then brine. Re-extracted the aqueous layers, washed with brine, and combined with organic layers and dried over sodium sulfate. Filtered and concentrated to give the crude product, which was purified using silica gel flash chromatography using 4% ethyl acetate/hexanes to give **124a** and **124b** as an inseparable mixture of diastereoisomers in 85% yield.

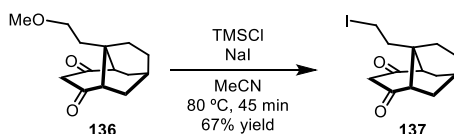


3-((S,E)-5,9-dimethyldeca-3,8-dien-5-yl)-8a-(2-methoxyethyl)hexahydro-1,6-

methanonaphthalene-2,4(1H,3H)-dione (125-ketone): To an oven-dried round bottom flask as added NaHMDS (3 equiv.) in the glovebox. This flask was removed from the glovebox and THF (0.2 M, freshly distilled from the solvent system) was added. To this flask was added the substrate in THF (0.2 M, freshly distilled from the solvent system) at room temperature and let stir for 2 hours. Quenched with 1 M HCl and extracted with ethyl acetate (3x). The combined organic layers were washed with brine, dried over sodium sulfate, filtered, and concentrated. The residue was filtered over a florisil plug eluting with diethyl ether then ethyl acetate to give 92% yield of the desired Dieckmann cyclization product as 1:1.5:1.5 mixture of **125** (ketone:enol A:enol B). **¹H NMR** (400 MHz, C₆D₆) δ 7.78 (s, 1H), 7.75 (s, 1H), 6.02 – 5.87 (m, 2H), 5.69 – 5.48 (m, 2H), 5.28 (t, *J* = 6.6 Hz, 2H), 4.21 (s, 1H), 3.29 (dd, *J* = 14.7, 7.7 Hz, 2H), 3.15 (t, *J* = 6.8 Hz, 2H), 3.07 (d, *J* = 2.3 Hz, 3H), 3.00 (s, 3H), 2.60 (dtd, *J* = 25.0, 12.7, 5.0 Hz, 1H), 2.46 – 2.38 (m, 2H), 2.33 (dt, *J* = 14.8, 5.6 Hz, 2H), 2.26 – 2.15 (m, 2H), 2.09 (m, *J* = 26.4, 13.5, 7.3 Hz, 3H), 1.86 – 1.71 (m, 4H), 1.68 – 1.45 (m, 6H), 1.40 – 1.17 (m, 6H), 1.16 – 1.08 (m, 1H), 0.99 (t, *J* = 7.4 Hz, 3H), 0.81 (t, *J* = 7.4 Hz, 3H). **¹³C NMR** (176 MHz, C₆D₆) δ 205.53, 204.90, 201.15, 201.05, 139.04,

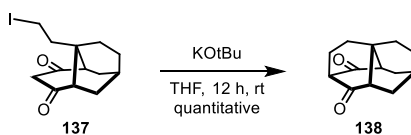
138.62, 137.27, 132.88, 132.27, 130.96, 130.85, 130.84, 129.32, 125.71, 125.68, 125.64, 111.50, 111.35, 69.18, 69.09, 68.11, 63.56, 58.36, 58.31, 58.24, 52.59, 52.37, 49.16, 48.65, 42.17, 42.08, 41.88, 41.82, 40.08, 39.99, 39.25, 38.81, 37.54, 37.17, 36.89, 33.09, 32.46, 31.66, 31.53, 30.51, 30.23, 29.95, 29.76, 29.47, 29.42, 29.30, 28.10, 28.03, 27.05, 26.80, 26.76, 26.48, 26.47, 26.02, 25.99, 25.92, 25.91, 25.90, 25.54, 25.38, 25.37, 24.76, 24.55, 24.49, 23.68, 23.53, 21.60, 17.79, 17.70, 14.57, 13.61, 13.58.

4.6.6 Investigation of Tetracycle Formation



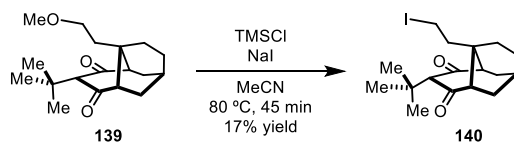
(1R,6R,8aR)-8a-(2-iodoethyl)hexahydro-1,6-methanonaphthalene-2,4(1H,3H)-dione (137):

An oven-dried round bottom flask was charge with the methyl ether **136** and NaI (5 equiv) and MeCN (0.1 M). TMSCl was then added dropwise and the solution was heated at 80 °C for 45 min. Once cooled, the reaction mixture was quenched with saturated Na₂S₂O₃. The layers were separated ad the aqueous layer was extracted with ethyl acetate (3x). The combined organic layers were washed with brine, dried over sodium sulfate, filtered, and concentrated. Analysis of the crude reaction mixture using mesitylene as an internal standard provided 67% yield of the iodide **137**, which was used in the subsequent reaction without further purification. ¹H NMR (500 MHz, CDCl₃) δ 3.92 (d, *J* = 19.0 Hz, 2H), 3.12 – 2.98 (m, 2H), 2.58 (d, *J* = 10.5 Hz, 2H), 1.91 – 1.88 (m, 1H), 1.68 (d, *J* = 6.3 Hz, 10H). ¹³C NMR (176 MHz, CDCl₃) δ 206.54, 60.54, 49.16, 49.07, 43.73, 29.56, 26.52, 25.45, 23.25, -3.45.

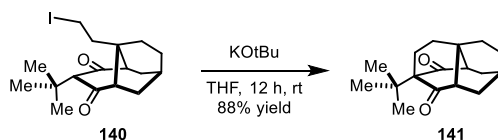


(2S,4R,4aR,7R)-tetrahydro-2H-2,4a-ethano-4,7-methanonaphthalene-1,3(4H,5H)-dione (138):

To a solution of the iodide **137** in THF (0.1 M) was added KOtBu (1.2 equiv) at room temperature. Let stir overnight and then quenched with saturated NH₄Cl. Extracted with EtOAc (3x), washed with brine, dried over sodium sulfate, filtered and concentrated. ¹H NMR (500 MHz, cdcl₃) δ 3.21 (t, *J* = 2.8 Hz, 1H), 2.32 (dd, *J* = 12.2, 3.5 Hz, 2H), 2.10 (td, *J* = 8.2, 3.0 Hz, 2H), 2.03 (td, *J* = 13.8 Hz, 3.0 Hz, 2H), 1.80 – 1.74 (m, 1H), 1.58 (m, 8H). ¹³C NMR (176 MHz, cdcl₃) δ 211.52, 63.68, 47.97, 33.63, 30.36, 28.82, 28.70, 24.80, 24.65, 22.48.



(1R,3R,6R,8aR)-3-(tert-butyl)-8a-(2-iodoethyl)hexahydro-1,6-methanonaphthalene-2,4(1H,3H)-dione (140): An oven-dried round bottom flask was charge with the methyl ether **136** and NaI (5 equiv) and MeCN (0.1 M). TMSCl was then added dropwise and the solution was heated at 80 °C for 45 min. Once cooled, the reaction mixture was quenched with saturated Na₂S₂O₃. The layers were separated ad the aqueous layer was extracted with ethyl acetate (3x). The combined organic layers were washed with brine, dried over sodium sulfate, filtered, and concentrated. Analysis of the crude reaction mixture using mesitylene as an internal standard provided 17% yield of the iodide **140**, which was used in the subsequent reaction without further purification.



(2R,4R,4aR,7R)-2-(tert-butyl)tetrahydro-2H-2,4a-ethano-4,7-methanonaphthalene-1,3(4H,5H)-dione (141): To a solution of the iodide **140** in THF (0.1 M) was added KOtBu (1.2 equiv) at room temperature. Let stir overnight and then quenched with saturated NH₄Cl. Extracted with EtOAc (3x), washed with brine, dried over sodium sulfate, filtered and concentrated. ¹H NMR (700 MHz, CDCl₃) δ 2.23 (d, *J* = 9.1 Hz, 2H), 2.13 – 2.08 (m, 2H), 1.94 (t, *J* = 12.8 Hz, 2H), 1.73 – 1.69 (m, 1H), 1.57 (dd, *J* = 11.0, 5.3 Hz, 2H), 1.50 (dd, *J* = 11.1, 5.9 Hz, 6H), 1.30 (s, 3H), 1.06 (s, 6H), 1.01 – 0.92 (m, 4H). ¹³C NMR (176 MHz, CDCl₃) δ 211.95, 49.38, 33.15, 31.86, 30.56, 29.65, 28.95, 27.15, 24.99, 24.86, 23.71.

4.7 References

- (1) P. Tang, Q.-H. Chen, F.-P. Wang, *Tet. Lett.* **2009**, *50*, 460-462.
- (2) B. Tashkhodzhaev, S. A. Saidkhodzhaeva, I. A. Bessonova, M. Y. Antipin, *Chem. Nat. Compd.* **2000**, *36*, 79–83; b) S.A. Saidkhodzhaeva, I. A. Bessonova, N. D. Abdullaev, *Chem. Nat. Compd.* **2001**, *37*, 466 – 469.
- (3) Yin, T.; Zhou, H; Cai, L.; Ding, Z. *RSC Adv.* **2019**, *9*, 10184-10194.
- (4) F.-P. Wang, X.-T. Liiang in *The Alkaloids, Chemistry and Biology, Vol 59* (Ed.: G. A. Cordell), Elsevier, Amsterdam, **2002**, pp. 1–280.
- (5) Wang, F.-P.; Yan, L.-P. *Tetrahedron* **2007**, *63*, 1417-1420.
- (6) Weber, M.; Owens, K.; Sarpong, R. *Tetrahedron Lett.* **2015**, *56*, 3600-3603.
- (7) Wang, F.-P.; Chen, Q.-H.; Liu, X.-Y. *Nat. Prod. Rep.* **2010**, *27*, 529-570.
- (8) Suzuki, T.; Sasaki, A.; Egashira, N.; Kobayashi, S. *Angew. Chem. Int. Ed.* **2011**, *50*, 9177-9179.
- (9) Suzuki, T.; Okuyama, H.; Takano, A.; Suzuki, S.; Shimizu, I.; Kobayashi, S. *J. Org. Chem.* **2014**, *79*, 2803-2808.
- (10) Hayashi, R.; Ma, Z.-X.; Hsung, R.P. *Org. Lett.* **2012**, *14*, 252-255.
- (11) Chen, H.; Zhang, D.; Xue, F.; Qin, Y. *Tetrahedron* **2013**, *69*, 3141-3148.
- (12) Chen, H.; Li, X.-H.; Gong, J.; Song, H.; Liu, X.-Y.; Qin, Y. *Tetrahedron* **2016**, *72*, 347-353.
- (13) Portalier, F.; Bourdreux, F.; Marrot, J.; Moreau, X.; Coeffard, V.; Greck, C. *Org. Lett.* **2013**, *15*, 5642-5645
- (14) Liu, X.-Y.; Qin, Y. *Nat. Prod. Rep.* **2017**, *34*, 1044-1050.
- (15) Gong, J.; Chen, H.; Liu, X.-Y.; Wang, Z.-X.; Nie, W.; Qin, Y. *Nat. Commun.* **2016**, *7*, 12183.
- (16) Xie, S.; Chen, G.; Yan, H.; Hou, J.; He, Y.; Zhao, T.; Xu, J. *J. Am. Chem. Soc.* **2019**, *141*, 3453-3439.
- (17) Nie, W.; Gong, J.; Chen, Z.; Liu, J.; Tian, D.; Song, H.; Liu, X.-Y.; Qin, Y. *J. Am. Chem. Soc.* **2019**, *141*, 9712-9718.
- (18) a) Owens, K.R.; McCowen, S.; Blackford, K. A.; Ueno, S.; Hirooka, Y.; Weber, M.; Sarpong, R. *ChemRxiv* **2019**, DOI: 10.26434/chemrxiv.8202380.v1; b) Owens, K.R.; McCowen, S.; Blackford, K. A.; Ueno, S.; Hirooka, Y.; Weber, M.; Sarpong, R. *J. Am. Chem. Soc.* **2019**, *Just Accepted*.

- (19) a) Zhou, S.; Xia, K. Leng, X.; Li, A. *ChemRxiv* **2019**, DOI; 10.26434/chemrxiv.8202242.v1; b) Zhou, S.; Xia, K. Leng, X.; Li, A. *J. Am. Chem. Soc.* **2019**, *Just Accepted*.
- (20) Armaly, A.M.; Bar, S.; Schindler, S. *Org. Lett.* **2017**, *19*, 3958-3961.
- (21) Armaly, A.M.; Bar, S.; Schindler, S. *Org. Lett.* **2017**, *19*, 3962-3965.
- (22) Baker, B.A.; Boskovic, Z.V.; Lipshutz, B.H. *Org. Lett.* **2008**, *10*, 289-292.
- (23) Das, P.P.; Lysenko, I.L.; Cha, J.K. *Angew. Chem. Int. Ed.* **2011**, *50*, 9459-9461.
- (24) Olah, G.A.; Narang, S.C.; Balaram Gupta, B.G.; Malhotra, R. *J. Org. Chem.* **1979**, *44*, 1247-1251.
- (25) Chen, M.S.; White, M.C. *Science*, **2007**, 783-787.